ALGORITHM BASED OPTIMIZATION OF FRACTIONAL PLL FOR COMMUNICATION BASED APPLICATIONS

Thesis Submitted for the Award of the Degree of

DOCTOR OF PHILOSOPHY

in

Electronics and Communication Engineering

By

Mohammad Abdul Muqueem

Registration Number: 41800742

Supervised By

Dr. Shanky Saxena (25061)

School of Electronics & Electrical Engineering, Assistant Professor

Lovely Professional University
Phagwara, Punjab, India

Co-Supervised by

Dr. Govind Singh Patel (100)

ECE Department, Professor

SITCOE, Ichalkaranji, MH,India

LOVELY PROFESSIONAL UNIVERSITY, PUNJAB

2024

DECLARATION

I hereby declare that the thesis entitled **"Algorithm based Optimization of Fractional PLL for Communication based Applications"** has been prepared and submitted by me under the guidance of Supervisor **Dr. Shanky Saxena,** Assistant Professor, School of Electronics & Electrical Engineering, Lovely Professional University, Phagwara, Punjab and Co-Supervisor **Dr. Govind Singh Patel**, Professor, Department of Electronics & Computer Engineering, SITCOE, Ichalkaranji, Maharashtra the requirement for the award of the degree of **Doctor of Philosophy (Ph.D.)** in **Electronics & Communication Engineering** is entirely my original work and ideas, references are duly acknowledged. It does not contain any work that has been submitted for the award of any other degree or diploma from any University.

Mr. Mohammad Abdul Muqueem
Reg.No-41800742
Lovely Professional University,
Phagwara, Punjab, India.

CERTIFICATE

This is to certify that **Md Abdul Muqueem** has completed his Doctor of Philosophy (Ph.D.) in Electronics & Communication Engineering thesis entitled **"Algorithm based Optimization of Fractional PLL for Communication based Applications"** is a bonafide work carried out by him under my supervision and guidance. To the best of my knowledge, the present work is the result of his original investigation and study. No part of the thesis has ever been submitted to any other University or Institute for the award of any degree or diploma.

	

Dr. Shanky Saxena

Supervisor

Assistant Professor,

School of Electrical & Electronics Engineering

Lovely Professional University

Phagwara,Punjab,India

Dr. Govind Singh Patel

Co-Supervisor

Professor,

ECE Department

SITCOE,

Ichalkaranji,MH,India

ABSTRACT

A Phase-Lock Loop (PLL) is a control system-equipped device that produces an output signal which stage is correlated with the stage of input signal. The fundamental electrical circuit consists of a phase detector and variable frequency oscillator with a feedback loop. The only difference between the fractional-N PLL and the integer-N PLL is the fractional outcome of the divider ratio is produced, and extra electric circuits must be included the feedback loop to keep the optimistic bandwidth and further decrease noise. The primary idea behind fractional-N PLL is to switch among two different divider ratios in order to obtain the appropriate fractional value. The pulse swallowing technique can be used to do this, which replaces the divider value for the first half of time period and then moves the value to next neighboring integer for the second half of the time period. A resolution multielement divider (fractional) is available and utilized to reduce noise that occurs in FNPLL and is known as quantization noise. Grouping of frequencies by a fraction of reference is possible using FNPLL. Both digital and analog PLLs can use it. It provides a higher frequency and a broader band width, which speed up the settling process. FNPLL has additional noise from the Delta Sigma modulator's quantization error that is used to produce the division ratio. With this suggested method, noise is systematically decreased across the full frequency range. It is difficult to simulate and Delta Sigma f-NPLL frequency synthesis. In order to create a quick simulation environment, MATLAB is used for Delta-Sigma based FNPLL frequency synthesis. In order to achieve improved reduction of noise, quick simulation environment, and various methods to lower phase noise in FNPLL, a FNPLL with a Delta-Sigma modulator is created in this study. And also The primary purpose of the PLL, which is a structural circuit design for a closed loop control system, is to make it easier for the supplied input signal to be phase and frequency synchronized. The frequency synthesizer, which takes the form of PLL, is one of the most crucial components of integrated transceivers. The explanation that follows provides an example of the 3rd order Delta-Sigma modulator design model. Changing your approach can help with this creating a new PLL architecture that is suitable for wireless applications and has low noise. The PLL overcomes several obstacles by reducing power, taking up less space, and increasing frequency. This comparison includes a diagram that illustrates various PLL. The fundamental loop transfer function, noise sources dividers, phase detectors, and fractional-N operation are all covered in this first study.

In the second work specifies low light and bad weather, radar systems according to the Frequency-Modulated Continuous-Wave (FMCW) transmissions can outrun optical and ultrasonic sensors. A quick settling frequency synthesizer is necessary for FMCW radar systems to decrease signal of chirp modulation and inactive times. Through the use of Ring-Based Pulse Injection Locking Oscillator (R-PILO) and Fast Settling Fractional-N DPLL (FS-FNDPLL), a new C-Band FMCW Transmitter is proposed. The suggested FS-FNDPLL implements an Automatic Controller-based TDC switching (AC-TDCSw) technique in the forward loop of FNDPLL to provide ultra-fast low-noise smooth narrowband chirp. A new Background Gain Calibrated Digital-to-Time Converter (BGC-DTC) is also used in the proposed FS-FNDPLL as a fractional divider in the feedback loop for the Quantization Noise Cancellation (QNC). After creating a narrowband chirp with FS-FNDPLL, recommended FMCW Transmitter provides an R-PILO to provide fast switching adjacent carriers. Ultra-fast chirps with lower spur levels and phase noise are made possible by the key characteristics of suggested FMCW to speed settling time with BGC-DTC, AC-TDCS, and combination of spur suppressing pulse generator in R-PILO. A 2-GHz chirp at the C-band is obtained by proposed emitter by up converting a 500-MHz narrowband chirp signal in four nearby carriers. According to simulation results, the suggested FMCW Transmitter uses 79 mW of power. Additionally, the suggested FS-FNDPLL's phase noise is decreased to 113 dBc/Hz at 1-MHz With the added AC-TDCSw system, the suggested, FS-FNDPLL decreases settling time to 1μs.

ACKNOWLEDGEMENT

The successful completion of any task would be incomplete without complementing those who made it possible, under whose guidance and encouragement, the efforts are made successful. First of all, I acknowledge without hesitation, the grace of god the Almighty, inthis arduous journey, it is he alone who deserves all the credit for this work. I owe my sincere gratitude to my project supervisor **Dr. Shanky Saxena**, Assistant Professor,Lovely Professional University, Punjab, India for his valuable guidance, direction, and persistent encouragement. He has always motivated me and supported me in the constructive and creative process of the entire research journey. Its really a matter of pride and joy for me to work under his guidance. I hope to seek his guidance for my future endeavors also. I owe my sincere gratitude to my project Co-supervisor **Dr. Govind Singh Patel**, Professor, SITCOE, Ichalkaranji, Maharashtra, India for his vital guidance, direction, and persistent encouragement. He has always motivated me and supported me in the constructive and creative process of the entire research journey. It is really a matter of pride and joy for me to work under his guidance. I hope to seek his guidance for my future endeavors also. I would also like to express my deeply felt gratitude to the Department of Research Program. I would also like to express my deeply felt gratitude to the Lovely Professional University, Punjab, India for providing me with an opportunity to work in the best academic environment.

I also would like to thank **Dr.Gaurav Sethi**, Professor & Dean, School of Electrical & Electronics Engineering, Lovely Professional University, Punjab for his kind support.

I also would like to thank **Dr. Sanjeet K. Sinha**, Associate Professor, HoD School of Electrical & Electronics Engineering, Lovely Professional University, Punjab, India for his kind support.

I would also like to express my deeply felt gratitude to **Capt.V.Lakshmikantha Rao Sir, Ex MP (Rajyasabha), Chairman** of Kakatiya Institute of Technology and Science, Warangal, for providing unconditional support during this journey .I also would like to thank **Prof. K. Ashoka Reddy Sir, Principal,** Kakatiya Institute of Technology and Science, Warangal, for his kind support**.** I also would like to thank **Prof. G. Raghotham**

Reddy Sir, for his kind support. I also would like to thank **Dr M.Raju Sir**, HoD ECE for his kind support. I also would like to thank all staff members of Kakatiya Institute of Technology and Science, Warangal, for their kind support. I am really thankful to **Dr. B. Arun Kumar** Assistant Professor, Lovely Professional University, Punjab, India for his kind support.

I am really happy to be blessed and encouraged by, My father **Md Abdul Aleem**, My Mother **Qursheeda Begum**. I also express sincere gratitude to all my family members. I really have no words to express my feelings for them. It is a great privilege to express my profound thankfulness, and fondness to my wife, and my dearest Sons, who stood like a rock in my difficult times. Their love, patience, persistent encouragement, and good virtuous understanding enabled me to complete the research work successfully. Finally, I express my sincere thanks to Almighty and his beautiful nature for allowing me an opportunity to complete this research work

.

Mohammad Abdul Muqueem

RegNo: 41800742

TABLE OF CONTENTS

List of Tables

List of Figures

ABBREVIATIONS

PLL	Phase-Lock Loop
VCO	Voltage Controlled Oscillator
LPF	Low-Pass Filter
CP	Charge Pump
PFD	Phase/Frequency Detector
FMCW	Frequency-Modulated Continuous-Wave
DPLL	Digital Phase Locked Loop
RF	Radio Frequency
FS	Frequency Synthesizer
PFD	Phase Frequency Detector
SoCs	System-On-Chips
SSC	Spread Spectrum Clocking
EMI	Electromagnetic Interference
DTC	Digital-To-Time Converter
TDC	Time-To-Digital Converter
DCO	Digitally Controlled Oscillator
QNC	Quantization Noise Cancellation
AFC	Automatic Frequency Control
ICs	Integrated Circuits
FMCW	Frequency-Modulated Continuous-Wave
BLE	Bluetooth Low Energy
FHSS	Frequency-Hopped Spread Spectrum
PI	Phase Interpolation
SSC	Spread Spectrum Clocking
DJ	Deterministic Jitter
ILCM	Injection Locked Clock Multiplier

TP-FPSC	Triple-Point Frequency/Phase/Slope Calibrator
SIL	Self-Injection Locking
ADDLL	All-Digital Delay-Locked-Loop
NCO	Numerically Controlled Oscillator
NOCs	Network On Chips
PCS	Personal Communication System
FPGA	Field Programmable Gate Array
GDI	Gate Diffusion Input
MOSFETs	Metal-Oxide Semiconductor Field-Effect Transistors
TA	Temporal Amplifier
DMRO	Dual-Mode Ring Oscillator
PVAPF	Photovoltaic-Active Power Filter
CDAC	Capacitor-Based Digital-To-Analog Converter
RSPD	Reference Sampling Phase Detector
MDLL	Multiplying Delay-Locked Loop
SPO	Static Phase Offsets
BBPD	Bang-Bang Phase Detector
DPO	Dynamic Phase Offsets
TPM	Two-Point Modulation
FFD	Fractional Frequency Dividing
DPI	Digital Phase Interpolator
LSB	Least Significant Bit
GEO-SA-BiSAR	Geosynchronous Spaceborne-Airborne Bistatic Synthetic Aperture Radar
SRR	Short-Range Radar
LRR	Long-Range Radar
EA	Error Amplifier
ADA	Azimuth Doppler Ambiguity
VSAR	Velocity SAR
RCMC	Range Cell Migration Correction

MIMO	Multiple Input Multiple Output
TBS	Time Domain Bandwidth Synthesis
MDLL	Multiplying Delay Locked Loop
SSPLL	Sub-Sampling-Based PLL
S-PLL	Sampling PLL
CP	Charge Pump's
NPS	Narrow Pulse Shielding
PG	Pulse Generator
SOGI	Second-Order Generalized Integrators
PID	Proportional Derivative Integral
FFT	Fast Fourier Transform
PMAF	Pre-Filtering Moving Average Filter

CHAPTER 1

INTRODUCTION

1.1 Overview

PLLs are necessary to synchronize and retime the input data on the receiver side. A Phase/Frequency Detector (PFD), Voltage-Controlled Oscillator (VCO), Charge Pump (CP), Low-Pass Filter (LPF), and frequency divider make up a typical single-loop PLL [1]. A fractional PLL is designed by choosing the PLL's constituent parts, such as the Phase Detector (PD), loop filter, fractional divider, and VCO, and then fine-tuning their parameters to attain the desired frequency constancy, phase noise, and stability achievement. Steps needed in creating a fractional PLL in general [2] identify the required input and output frequency. The output frequency is the preferred value of the output clock signal, and the input frequency is the reference frequency signal. To detect phase differences among reference and output signals. To produce an error of signal proportionate to that phase difference, choose the phase detector. There are various different types of phase detectors, each with advantages and limitations, including XOR, mixer-based, and D-type flip-flops. The most important part of PLL is the design of the loop filter, which stabilizes the PLL by removing noise from the error signal [3]. The fractional-N PLL synthesizers based on Delta-Sigma are commonly used as local oscillators for creating precisely specified frequencies in wireless communication applications. The approach-based FNPLL has many benefits that have led to its widespread application in electronic devices like mobile phones and wireless LANs, including high shift speediness, little phase noise (PN), and compact space between channels. Determine the outcome frequency of a $\Delta\sum$ f-N PLL and an integer-N PLL [4]. To integer multiples of reference frequency, loop some degree. Integer NPLL and FNPLL share many fundamental properties; however, different circuits are employed. Introduce the frequency accurately between a single or non-negative integer multiple. Fast-settling frequency synthesizers are becoming increasingly popular in Frequency-Modulated Continuous-Wave (FMCW) in the radar system because of their capacity to shorten the chirp signal's idle modulation and time period [5]–[7]. The quick response time of clock generators is crucial for supporting power management strategies like frequency scaling and dynamic voltage [8] as well as in digital SoCs. The Digital PPL (DPLL) is created as a switched scheme with a novel loop-order switching device included in its feed-forward channel in order to achieve a quick settling reaction [9]. The high-order integrator and differentiator are called upon by this adaptive mechanism to escalate error tracking responses

in the loop. A system that alternates among various loop orders and loop gains would be more likely to deviate from equilibrium or oscillate among various states. This chapter covered the history of phase-locked loops, fractional-n modulation techniques, fractional-n frequency synthesis, and applications of PLLs, as well as their benefits and drawbacks. This chapter also includes motivation, a problem description, research objectives, and a thesis organization.

1.2 Background information of Phase Locked Loop

The phase-locked loops (PLLs) were operated at high frequency and speed. Therefore, it is necessary to possess in-depth knowledge of the theory's foundational ideas on PLLs, dynamic behavioural traits, and transistor size scaling. Some performance measurement characteristics, such as speed, settling time, and hold time, and decreased jitter with minimal power consumption, are highlighted and elaborated for high-frequency operation based on the simulation findings attained. The fundamental need for charge pump phase-locked loops with very high clock frequencies in the range of GHz is growing quickly as high-data-rate transmission technologies. PLLs are usually used in radio frequency (RF) [10], digital, and analog communication systems. PLLs can produce low-jitter, high-frequency clocks with little temporal skew. To successfully recover the data broadcast from the transmitter, PLLs are also utilized in clock and data recovery [11] circuits. PLL refers to a system that locks to a specific phase or frequency dependent on input frequency. PLL cycle rate Synthesizers emphasize the need for a clear frequency signal when processing or synchronizing data. Software PLL, analog PLL, all-digital PLL, and digital PLL (DPLL) are some of the different types of PLL. These are categorized based on their analog and digital blocks.

These current system applications drive the designs of PLL, and as a result, the specifications required vary. A low power, completely integrated, low cost, and high performance Integer-N digital PLL frequency synthesizer is required by applications including frequency multipliers, radar, cell phones, data synchronization, and telecommunications. Research has confirmed the CP in the integer-N digital PLL [12]. In an indirect frequency synthesizer, the PLL is a crucial component. The frequency division and/or multiplication can be carried out by a PLL in conjunction with divider components. The majority of the frequency synthesizers sector is still held by a number of PLL design variants today. In addition to enhancing portability across coming CMOS technologies, a solid understanding of PLL frequency synthesizer (FS) design can save development costs and shorten time to market.

An essential component of an indirect frequency synthesizer is the PLL. A PLL in conjunction with divider elements can be used to multiply and/or divide frequencies. Today, a number of

PLL design variants continue to dominate the market for frequency synthesizers. In addition to enhancing portability across forthcoming CMOS technologies, a solid understanding of PLL frequency synthesizer (FS) design can save development costs and shorten time-to-market.

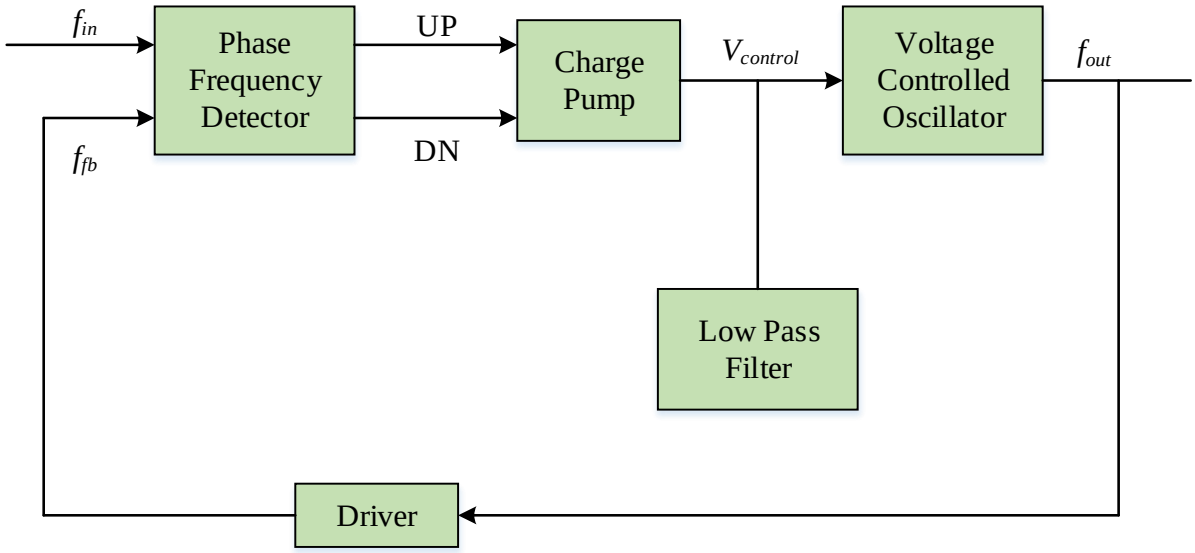

Figure 1.1: Block Diagram of Digital Phase Locked Loop [13]

The illustration of digital PLL is displayed in the Figure 1.1. The VCO, LPF, CP, and phase frequency detector (PFD) are the main components of these DPLLs [13]. PFD and divider in this case are digital in nature.

1.3 Fractional-N modulation methods

Modern system-on-chips (SoCs) are capable of performing a wide range of analog, mixed-signal, digital, and radio frequency tasks. A SoC often consists of a wide range of things, including wireless transceivers, modules, I/O interfaces, memory, and multicore processors [14]. These modules each operate in a separate clock domain tailored to their preferred outcome. In contrast, a CPU may need Spread Spectrum Clocking (SSC) to decrease Electro-Magnetic Interference (EMI) or quick frequency switching to provide power-saving strategies like Dynamic Frequency Scaling (DFS) [15]. For instance, I/O interfaces need low-jitter high-frequency clocks. Additionally, dynamically adjustable per-core clock generators are needed for today's multicore processors because they must offer quick frequency switching without frequency overrun and adhere to strict settling time, power, and area limits. SoC clock producers were commonly designed as Fractional-N Phase-Locked Loops (FNPLLs) to satisfy these various criteria. However, PLL bandwidth (BW) restricts the degree of EMI reduction and the shortest attainable settling time during frequency switching [16]. The BW restriction

can be bypassed using a two-point modulation approach and calibrated modulation routes [17]. However, its use in the dynamically variable SoC clock generators is constrained by the calibration's extremely sluggish settling time. Open-loop modulation of digital delay lines or multi-phase switching, on the other hand, can provide a great decrease in EMI and accurate depth of the modulation [18], but they have a significant deterministic jitter (DJ) issue. Multiple independent output clocks are produced between the frequencies of 20 to 1000 MHz using a digital PLL's low-jitter high-frequency clock.

The BW restriction of FNPLLs is overridden by the open loop architecture, which also achieves almost infinite modulation of the spread spectrum as well as instantaneous frequency switching without any frequency overshoot. A high-resolution Digital-to-Time Converter (DTC) is used to implement the suggested background calibrated quantization error cancellation approach, which results in outstanding jitter performance.

1.3.1 Fractional-N PLLs (Closed Loop)

The feedback divider is dithered using D modulator to operate in the fractional-N mode. Phase errors among reference and dithered feedback clocks are found using Time-to-Digital Converter (TDC) [19]. The diagram of typical Digital FNPLL is displayed Figure 1.2.

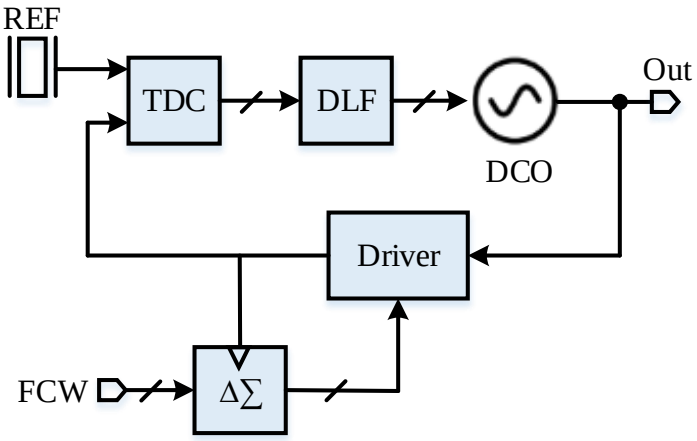

Figure 1.2: Block diagram of conventional fractional-N synthesizers using ΔΣ-digital FNPLL [16]

In order to adjust the frequency of the Digitally Controlled Oscillator (DCO), TDC output is filtered by a digital loop filter. The PLL-BW controls jitter performance and is difficult to optimize under opposing demands. Low-pass filtering of shaped quantization noise is aided by a narrow PLL-BW, but the modulation BW is constrained, and oscillator phase noise is

insufficiently filtered as an outcome [20]. In order to avoid this tradeoff and achieve excellent jitter performance, Quantization Noise Cancellation (QNC) methods [21] might be used. However, they are prone to mismatches between the two modulation pathways. Two-point processes and modulation approaches can expand modulation BW [22]. In order to accurate path mismatches across voltage and temperature differences, background gain calibration [23] can be used. However, because of the calibration's slow convergence, this method is not suitable for SoC clock generators where the modulation parameters and output frequency must be changed automatically.

1.3.2 Multi-Phase Switching (Open Loop)

The modulation BW constraint of FNPLLs was addressed by the proposal of open-loop frequency synthesis-based phase switching. Rotating M evenly spaced clock signals with similar phase and frequency gap between adjacent signals was used to accomplish fractional-N synthesis, as given in Figure 1.3.

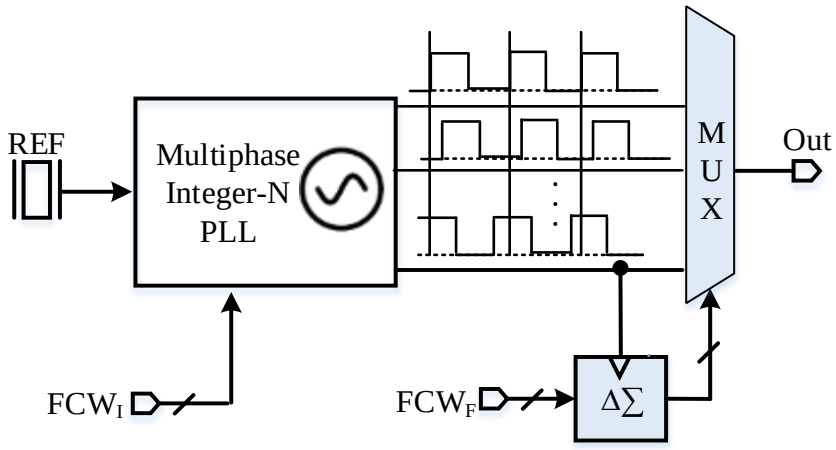

Figure 1.3: Block diagram of conventional fractional-N synthesizers using Δ∑-based phase switching [16]

Ring oscillators built into integer-N PLLs or conventional quadrature generating methods are frequently used to create these clock phases. A digital phase accumulator incorporates fractional frequency control words, or FCWF, and produces the phase multiplexor's control sequence. Phase interpolators are employed to increase resolution due to the output frequency resolution being determined by the very low phase separation [24]. By driving the phase accumulator with a digital modulator, it is possible to attain finer frequency resolution. In order to eliminate the shaped quantization error, a QNC technique is put forth that involves directly modifying the VCO of a multi-phase clock generator. This resulted in the simultaneous

achievement of low-phase noise and open-loop modulation performance. Perfect QNC is sensitive to PVT changes because it involves reasonably accurate knowledge of KVCO in VCO gain. Additionally, the multi-phase clock generator is not shared, so this solution is unable to produce several independent outputs. The performance of spurious and phase noise is diminished by digital-to-phase conversion's nonlinearity. To reduce performance degradation, routing pathways and VCO delay cells must be exactly matched [16]. The requirement for the determination of numerous high-frequency clocks dramatically raises the power consumption of strategy. An open loop FDIV method that can attain fine resolution and low jitter in light of the shortcomings of current open loop modulators.

1.4 Fractional-N Frequency Synthesis

In multi-standard transceiver systems, PLL-based frequency synthesizers are essential. When the frequency division ratio must be particularly high, the integer-N PLL struggles to meet design trade-offs. The block diagram for the device that produces 2 GHz output at a stable crystal frequency of 19.68 MHz is shown in Figure 1.4.

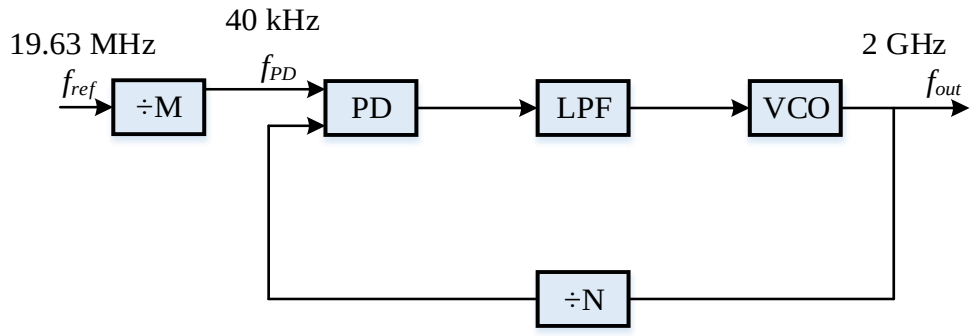

Figure 1.4: Frequency synthesis example with integer-N PLL [25]

In order to achieve the 200 kHz frequency resolution for channel rasters, such as WCDMA systems, the phase detector frequency must be set to 40 kHz and the frequency division ratio must be 50,000. In that situation, phase detectors and reference sources's in-band noise contributions are increased by 114 dB at VCO output. Additionally, PLL BW can only a few kHz for stability with a phase detector frequency of 40 kHz, causing VCO noise suppression and a protracted settling time. The fractional-N PLL provides the number of benefits over the integer-N PLL due to PD frequency being greater than resolution frequency. Unwanted spur production, which is brought on by the dual modulus divider's periodic operation, is the fractional-N PLL's special difficulty. If the fractional spurs are not suppressed, the fractional-

N frequency synthesis is useless for real-world applications. Therefore, more circuitry is required to reduce those fractional spurs.

1.4.1 Fractional-N PLL

The PD frequency cannot match the fine-resolution frequency of fractional-N PLL. The Digiphase methodology, which uses digital control of the phase to interpolate the frequency, is where the fractional-N method first emerged [26]. The illustration of conventional fractional-N PLL is provided in Figure 1.5.

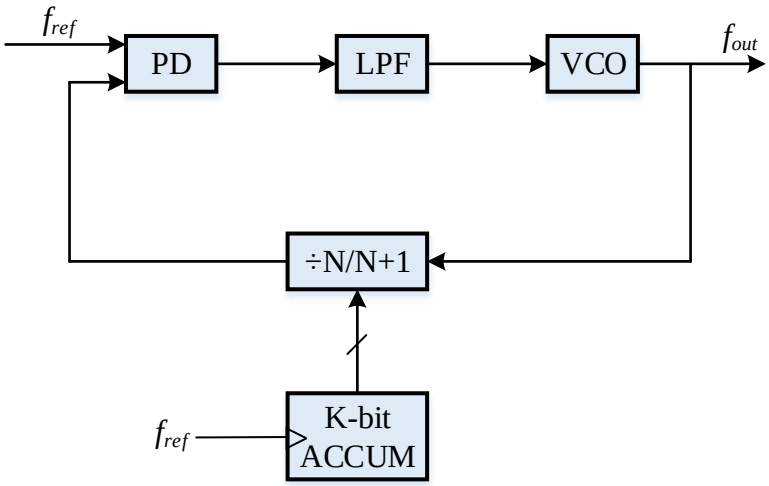

Figure 1.5: Block Diagram of Fractional-N PLL [26]

The dual modulus divider's control input is regularly modulated to produce a fractional division ratio. Such periodic modulation produces an undesirable spur.

1.4.1.1 DAC Cancellation Method

A common surge reduction technique is phase cancellation utilizing a Digital-to-Analog Converter (DAC). Figure 1.6 depicts the fundamental design and how it functions.

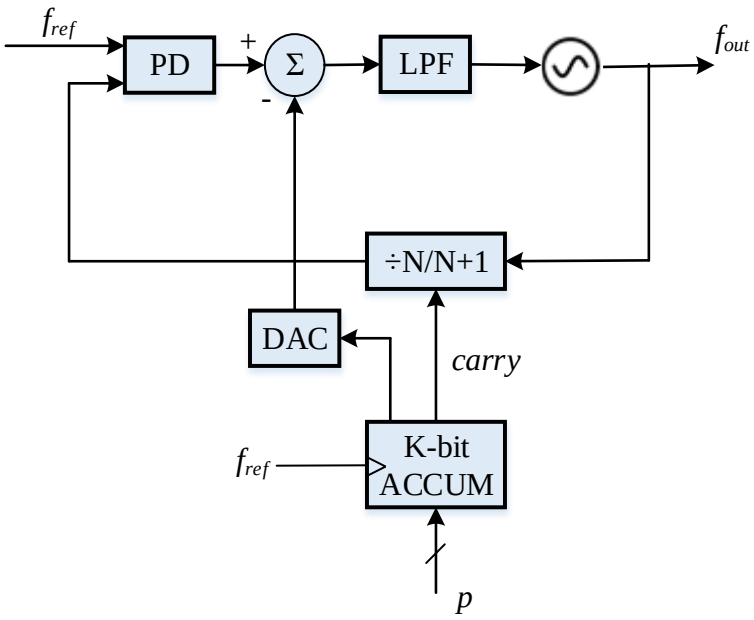

Figure 1.6: Fundamental Block Diagram of DAC Cancellation [27]

This method has analog flaws since phase error is corrected in the voltage field. The DAC resolution and accuracy limitations are the main causes of the discrepancy. The DAC only requires to match dc voltage for one reference clock period; this technique is highly efficient when an S/H phase detector rather than a phase/frequency detector (P/FD) is utilized.

1.4.1.2 Phase Interpolation Method

A fractional divider is implemented as shown in Figure 1.7 by taking use of the N distinct phases that N-stage ring oscillator creates.

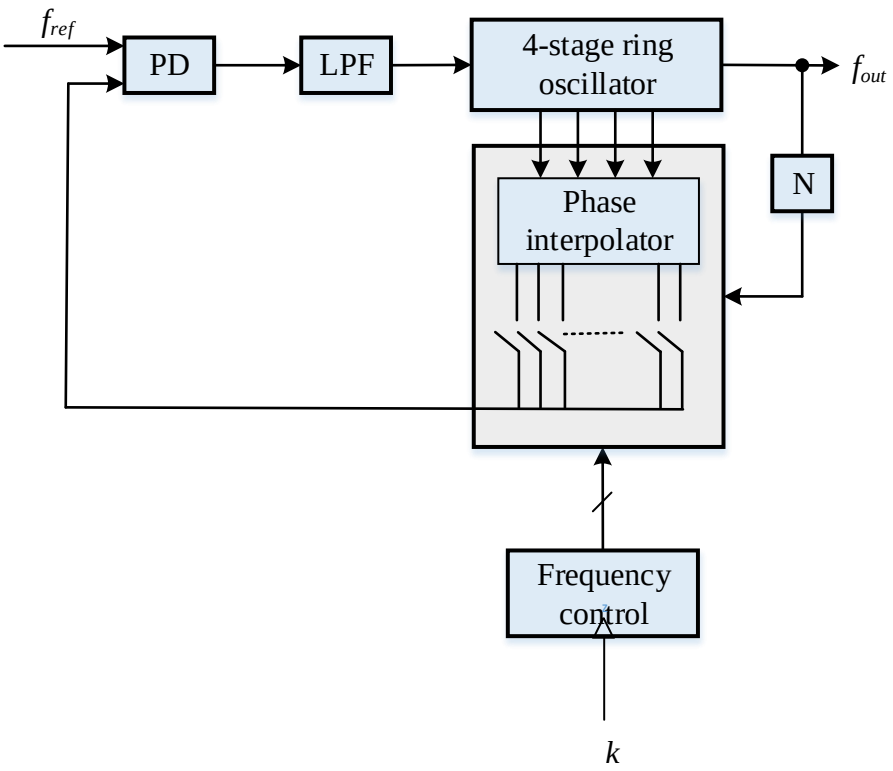

Figure 1.7: Block Diagram of Phase interpolation method [28]

The phase interpolator is provided to create finer phases using obtainable stages from multi-phase ring VCO because the ring oscillator's number of inverters is constrained. A fractional division is accomplished by picking the ideal interpolated phase from the available phases. Any mistake in interval of timing was inserted phase edges produce secure tones since phase edges provided for fractional division ratio are chosen frequently.

1.4.1.3 Random Jittering Method

The conventional fractional-N synthesizers perform poorly for fractional spurs when analog matching is not properly managed. In addition, the VCO output frequency affects design complexity. The section of the VCO time, which is as low as 10^{-3} rad, is the instantaneous phase error that must be negated at PD outcome. By digitally randomizing the sequence of dual-modulus divider control bits, a random jittering solution resolves the spur issue in the digital realm [28]. The illustration of a fractional-N divider with random jittering is shown in Figure 1.8.

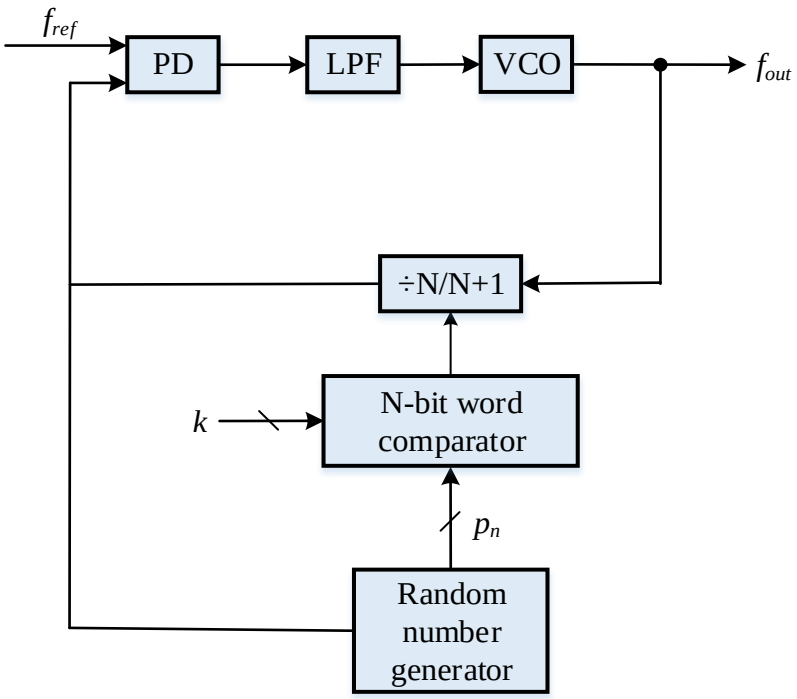

Figure 1.8: Block Diagram of Random jittering method [28]

The random number producer yields a new random word P_n at each outcome of the divider, which is associated with the frequency word K. The dual-modulus divider is controlled by the frequency word K so that the average value tracks the required fractional division ratio. The white noise injection in the frequency domain causes $1/f^2$ noise in the phase domain, which causes frequency jitter in this method.

1.4.2 Frequency synthesis with ΔΣ modulation

An essential component of contemporary transceiver systems, the ΔΣ fractional-N frequency synthesizer provides direct digital frequency modulation for low-budget transmitter construction. The fundamental method is to interpolate fractional frequency using a coarse integer divider and an oversampling ΔΣ modulator, as shown in Figure 1.9.

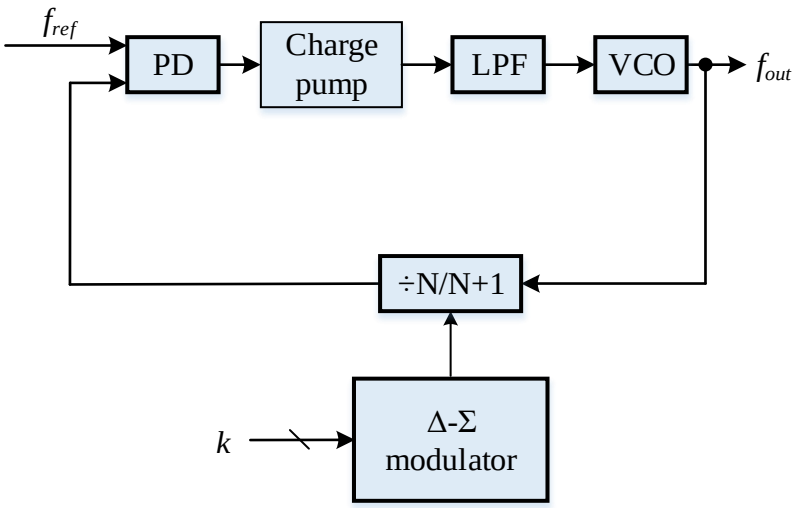

Figure 1.9: Block Diagram of ΔΣ fractional-N PLLs [29]

Higher VCO frequency causes greater spur reduction challenges for conventional finite-modulo ΔΣ fractional-N PLLs, although the resolution of these PLLs is independent of VCO frequency. One can easily achieve an extremely fine frequency resolution, such as 1 Hz, by simply increasing the modulation bit count. This technique is related to the random jittering technique; however, due to the shaping of the noise ability of the ΔΣ modulator, it does not produce a frequency jitter.

1.5 Applications of PLL

A PLL is flexible electronic circuit that finds applications in a different industries due to its capability to synchronize signals, regulate frequencies, and retrieve timing information. PLLs are used in the following typical applications:

- ***Clock Recovery***

  PLLs are frequently provided in communication schemes to recover the clock signal from a stream of incoming data for clock recovery. For accurate data demodulation, this is essential.

- ***Frequency Synthesis***

  PLLs are capable of producing precise and consistent output frequencies by securing with a source of reference frequency. This is necessary for many applications, such as RF transmission, the creation of local oscillators for transceivers, and the manufacture of clocks for microprocessors.

- ***Frequency Modulation and Demodulation***

PLLs can be used to demodulate a modulated signal (frequency demodulation) or to modulate a carrier signal with information (frequency modulation). This is used, for instance, in FM radio receivers.

- ***Phase noise reduction***

  PLLs are capable of helping oscillators in reducing phase noise, producing clearer and more stable signals. RF and microwave applications need to take this into consideration.

- ***Data Synchronization***

  In digital communication, PLLs are used to accurately recover data by synchronizing the receiver's clock with the incoming data stream.

- ***Frequency Tracking and Control***

  PLLs are capable of tracking and controlling a signal's frequency within a specific range. This is applied in radar systems and automatic frequency control (AFC) circuits.

- ***Signal locking and tracking***

  PLLs are employed in tracking systems to lock onto and follow a signal source's phase or frequency. This is typical in satellite communication, radar systems, and GPS receivers.

- ***Frequency Divider and Multiplier***

  PLLs have the ability to divide or multiple the frequency of an input signal, which is advantageous for both clock distribution and signal processing.

- ***Phase-Locked Loop Detectors***

  PLLs are used to monitor phase differences and retrieve signals buried in noise in a variety of detectors, including phase detectors and lock-in amplifiers.

- ***Spread Spectrum Communication***

  In spread spectrum systems, the dispreading spreading code is synchronized with the received signal using PLLs. Both GPS and wireless communication employ this technology.

- ***Motor Control***

  PLLs can be used in motor control systems to precisely manage the speed and position of motors in a variety of applications, such as industrial automation and robotics.

- ***Audio and Video Processing***

  PLLs are utilized in consumer electronics like DVD players and HDTVs for audio and video synchronization, jitter reduction, and clock generation.

- ***Frequency Hopping***

To increase communication security and dependability, frequency-hopping spread spectrum systems use PLLs to quickly switch between various carrier frequencies.

- ***Test and Measurement Equipment***

  To reliably create, modulate, and demodulate signals, PLLs are used in signal generators, spectrum analyzers, and other test and measurement instruments.

- ***Wireless Communication***

  PLLs are essential parts of wireless transceivers for the generation and synchronization of carrier frequencies as well as for the establishment of reliable communication links.

PLLs are essential in a variety of applications where accurate timing, synchronization, and frequency control are essential because to their flexibility and adaptability.

1.6 Advantages of PLL

PLLs are generally utilized in electronics and communications because of their many benefits, which include:

- ***Frequency Stability***

  PLLs can produce output frequencies that are extremely stable and accurate by locking onto a reference signal. Applications like frequency synthesis and clock generation depend on this stability.

- ***Frequency Control***

  PLLs are the best choice for applications that call for modulation or fine-tuning of the output frequency since they provide precise control over this parameter.

- ***Frequency Multiplication and Division***

  PLLs have the ability to be programmed to multiply or divide the input frequency, giving them flexibility in the creation and manipulation of signals.

- ***Clock Recovery***

  To ensure precise data reception and synchronization, PLLs are employed to recover clock signals from data streams.

- ***Noise reduction***

  PLLs can lower jitter and phase noise in signals, making communication clearer and more dependable.

- ***Synchronization***

  PLLs are used for synchronization to make sure that various signals or systems function in unison and at the same frequency.

- ***Signal Regeneration***

  PLLs may restore and correct weak or distorted signals, enhancing the quality of the signal in a variety of applications.

- ***Phase and Frequency Tracking***

  PLLs are capable of keeping track of changes in phase or frequency, which makes them helpful in systems like frequency hopping and radar.

- ***Data Demodulation***

  To enable data recovery, PLLs are used to demodulate analog and digital signals, including frequency and phase modulation.

- ***Phase Detection***

  Phase-locked loop detectors are useful in phase-sensitive applications such as phase-locked amplifiers and phase-locked detectors because they can precisely monitor phase differences.

- ***Wide Range of Applications***

  PLLs have a wide range of uses, including in telecommunications, wireless communication, audio and video processing, radar systems, GPS, motor control, and test and measurement equipment.

- ***Versatility***

  PLLs are flexible electronic system components that can be modified and designed to perform a variety of tasks.

- ***Real-Time Tracking***

  PLLs have the ability to modify their output in real-time to stay in sync with an altering input signal.

- ***Energy Efficiency***

  A significant number of contemporary PLL implementations are made with low power consumption in mind, which makes them appropriate for battery-operated gadgets and mobile applications.

- ***Reduced Component Count***

  A PLL can replace several discrete components in some applications, simplifying circuit design and cutting costs.

- ***Improved Signal Quality***

  PLLs improve the quality and dependability of signals in applications like communication and data transmission by minimizing phase noise and jitter.

- ***Ease of Integration***

Contemporary PLLs are frequently offered as integrated circuits (ICs), which make them simple to integrate into electrical systems.

- ***Security and encryption***

  PLLs synchronize spreading codes and improve security in spread spectrum communication systems, which contribute to secure communication.

- ***Efficient Signal Processing***

  PLLs can be employed in signal processing applications for effective frequency and phase alignment.

- ***Environmental Change Adaptation***

  Some PLLs can adjust to environmental changes, including temperature variations, to preserve frequency stability.

Due to these benefits, PLLs have become a crucial and adaptable part of contemporary electronics, enabling accurate frequency control, synchronization, and signal processing for a variety of applications.

1.7 Disadvantages of PLL

Although phase-locked loops (PLLs) have many benefits in a variety of electronic and communication applications, they also have several drawbacks and difficulties. PLL drawbacks include the following points:

- ***Phase Noise***

  Phase noise, or random and unwelcome fluctuations in the output signal's phase, can be introduced by PLLs. In RF communication and radar, for example, where low phase noise is essential, this may had effect on signal quality.

- ***Jitter***

  Jitter is the signal's departure from real periodicity, which is frequently brought on by phase noise. An excessive amount of jitter can cause data transmission mistakes in high-speed data transfer.

- ***Locking Time***

  PLLs may require some time to lock onto the reference frequency or input signal. In applications that need quick synchronization, this lock-in time can present a drawback.

- ***Spurious Signals***

When running close to the loop's bandwidth limit, PLLs are more likely to emit undesirable spurious signals or harmonics. Other nearby frequencies may be hampered by these erroneous transmissions.

- ***Design of the Loop Filter***

  To obtain the desired performance, a PLL's loop filter design, which might be intricate, needs to be carefully tuned. The performance or instability of a loop filter might be affected by improper loop filter design.

- ***Sensitivity to Reference Signal***

  PLLs are sensitive to the strength and consistency of the reference signal. The performance of the PLL might be impacted by any alterations or errors in the reference signal.

- ***Frequency Pulling***

  PLLs are susceptible to frequency tugging, in which the output frequency is affected by outside signals or noise. This may result in frequency variations from the desired value.

- ***Nonlinear Behavior***

  PLLs may display nonlinear behavior under specific operating situations, which can make their performance unpredictable and difficult to manage.

- ***Operating Frequency Range Limitations***

  The operating frequency range of PLLs may have several restrictions. Operating outside of this range could lead to performance degradation or lock loss.

- ***Power Consumption***

  PLLs have the potential to use an enormous amount of power, which could be problematic for battery-powered devices depending on implementation and operating conditions.

- ***Complexity***

  The design and implementation of PLLs, particularly in high-frequency and high-precision applications, can be challenging. They could need careful parameter adjustment and component selection.

- ***Cost***

  High-performance PLL components can be costly, which may be a factor in applications with tight budgets.

- ***Trade-offs***

Phase noise, lock time, power consumption, and frequency range are some of the trade-offs that are frequently made while designing a PLL. Finding the right balance can be difficult.

- ***Compatibility***

  Considering compatibility is important when integrating PLLs into existing systems since frequency output and phase of PLL must correspond to those of system.

- ***Vulnerability to External Interference***

  In sensitive applications like RF transmission, external electromagnetic interference (EMI) can impair PLL performance.

- ***Limited Bandwidth***

  Since a PLL has a limited bandwidth, it could not be appropriate for applications using wideband or rapidly changing signals.

PLLs continue to be a useful tool in many applications despite these drawbacks, and engineers frequently employ a variety of strategies to reduce these restrictions and enhance their performance for certain work.

1.8 Motivation

Periodic spurious tones at integer multiples of frequency orientation can be produced using $\Delta\sum$-fractional-N PLL with certain divider modulus. Although a small PLL bandwidth minimize the PLL's total performance is reduced, which can counteract the advantages of $\Delta\sum$-fractional-N approach. The delta-sigma modulator's high oversampling rate makes sure quantization noise produced by modulation is dispersed over a wide frequency range, with the majority of its power in a band that is above PLL's ideal BW. Because they are dispersed in large frequency range and it can be eliminated with a low-pass filter in PLL loop, spurious tones brought by the periodicity of divider modulus are no longer concern. Also, the current synthetic bandwidth-based FMCW SAR Transmitter is complicated due to the use of numerous PLLs, high-speed RF switches, as well as filter banks. Because of this, a fast-switching injection-locked oscillator (ILO) should be used to simplify the design of a FMCW SAR transmitter of synthetic bandwidth. The current SHILO, takes up more space, decreases power efficiency, and causes crosstalk. These arguments stimulate to produce a new FMCW SAR transmitter by refining the FNDPLL and ILO configurations to improve overall performance while lowering power and space requirements. The minimum settling time that may be achieved is constrained by PLL bandwidth of frequency switching. The FMCW chirp's bandwidth is also expanded

using a synthetic bandwidth technique. This method up converts narrowband chirp to other carrier frequencies. Additionally, it makes use of several PLLs, high-speed RF switches, as well as filter banks to facilitate rapid carrier frequency switching. Therefore, overall synthetic bandwidth structure becomes more complex. Therefore, the FMCW SAR Transmitter's architecture needs to be updated in order to decrease complexity and settling time.

1.9 Problem Statement

Modifying divider modulus resolves the issue of achieving non-integer multiples of reference frequency, cost is incurred as enlarged segment noise. The fractional-N-PLL technique is prepared to improve segment noise performance. Inaccuracies that are introduced into PLL and result in compounded section noise occur at some point during each reference period when actual divider modulus differs from common, or ideal divider modulus. The characteristics of the series of the divider are what determine how much the section noise is increased. There was the use of dual modulus and then the pulse swallowing technique, each of which had their own input limitations, so a new technique was introduced where the divider values will assume the fractional values also to reduce the addition of 20 dB noise in the procedure of frequency multiplication. Pre-scaler networks are used with integer N-PLLs to increase the upper frequency of the counter. Pre-scaler networks hinder the n value to the integers. The random noise group, along with periodic noise and phase noise, are the types of noise that have an effect on PLL performance. The PLL overcomes various challenges by reducing power, taking up less space, and increasing frequency. This comparison includes several PLL.

In order to achieve a quick PLL settling, previous techniques required a very wide PLL bandwidth, significantly raised spur levels and phase noise. Additionally, the phase detectors in the previous FNPLLs were either BBPD or PFD. The settling period of the FNPLL is lengthened by nonlinear Phase Error Detector unit like BBPD, despite its low power consumption. In contrast, PFD uses more power but has a longer settling period. Therefore, a different FMCW SAR transmitter with a quick settling time FNPLL is required. Additionally, for fractional division in low-noise Application, Existing FNDPLL Structures Frequently Rely On DTCs or TDCs. Due of its intricate structure, the DTC uses more energy and is constrained.

1.10 Research Objectives

The main research objectives is given below,

- To achieve improved noise reduction, quick simulation environment, and various methods to lower the phase noise in FNPLL, a FNPLL with a modulator is created in this study.
- To achieve power reduction, reduced area, and high frequency, this work describes the fundamental loop transfer function, noise sources dividers, phase detectors, and fractional-N operation.
- To implement an AC-TDCSw device in forward loop of the FNDPLL to produce an ultra-fast low-noise smooth saw-tooth wideband chirp.
- To design on-chip averaging strategy to lower measurement error and add a mutable TDC by a timing signal interpolation and counter.
- To increase settling time of FNDPLL excluding the need for reference clock, remove quantization noise, and create new DTC-based fractional divider with background gain calibration in feedback path.

1.11 Thesis Organization

The thesis is organized in following way, there are:

Chapter 1: Introduction

This chapter discussed about Background information of phase locked loop, fractional-n modulation methods, fractional-n frequency synthesis, applications of PLL, advantages of PLL and disadvantages of PLL. Additionally, motivation, problem statement, research objectives and thesis organization are provided in this chapter. And finally concluded with summary.

Chapter 2: Literature Review

This chapter discussed about the reviews of studies related to PLL based method. Additionally, the comparison of advantages and disadvantages of reviews are provided in tabular representation.

Chapter 3: Preliminaries of PLL and DDS

This chapter discussed about Preliminaries of PLL and DDS. This chapter includes different existing PPL algorithms, DDS various approaches, comparison analysis among PLL and DDS. Finally the chapter concluded with summary.

Chapter 4: Fractional PLL Performance Improvement through an Optimized Algorithm

This chapter discussed based on the optimized algorithm to achieve improved performance of fractional PLL. This chapter includes about proposed method and result analysis. Finally this chapter concluded with summary.

Chapter 5: Fast-Settling FNDPLL Synthesizer

This chapter discussed about proposed Fast Settling Fractional-N DPLL synthesizer. This chapter includes about proposed scheme and result analysis. Finally this chapter concluded with summary.

Chapter 6: FMCW Transmitter with the utilization of R-PILO to produce fast switching adjacent carriers

This chapter discussed about ultra-low-power C-Band FMCW Transmitter utilizing a Fast Settling Fractional-N DPLL as well as ring-based pulse injection locking oscillator approach. This chapter includes about proposed scheme and result analysis. Finally this chapter concluded with summary.

Chapter 7: Conclusion and Future scope

This chapter discussed about the conclusion of the entire research and the direction for future enhancement in the area of PLL based technology.

1.12 Summary

A PLL is control system-equipped device that produces an outcome signal which phase is correlated with phase of input signal. A variable frequency oscillator and PD with a feedback loop make up the fundamental electric circuit. It is a closed loop control system structural circuit design whose primary goal is to make it easier for the fed input signal to be phase and frequency synchronized. Nowadays, radar/ranging applications require a transceiver engine with an ultra-low power limitation. Different radars, FMCW radar, pulse, and a including UWB, are used for the range applications. FMCW is a pulsed waveform that has become widely employed in SAR recently to increase transmit power and sensor range. Modern CMOS technological advancements have made it possible to manufacture FMCW radar sensors on a single chip. This chapter covered the background information of phase locked loops, fractional-n modulation techniques, fractional-n frequency synthesis, applications of PLLs, as well as its benefits and drawbacks. This chapter also includes motivation, a problem description, research objectives, and a thesis organization.

CHAPTER 2

LITERATURE REVIEW

2.1 Overview

The development of low-power, low-jitter frequency synthesizers for transceivers that adhere to the IEEE802.15.4 & Bluetooth low-energy (BLE) specifications has been the subject of numerous studies [29]. Nonetheless, fractional-N PLLs with a quick settling reaction are necessary for certain applications. For instance, the channel-switching period was a crucial part of frequency-hopped spectrum dispersion (FHSS) devices and needed for vital security applications as well as commercial standards like wireless USB with ultra-wideband (UWB). Quick settling frequency synthesizers were being used more often in frequency-modulated continuous-wave (FMCW) sensors because they could lessen the idle time and modulation length of the chirp signal. [30].

Wide chirp bandwidth busing narrowband chirp capability of an FMCW transmitter based on synthetic bandwidth approach had the potential to decouple the aforementioned PLL tradeoff [31]. Only discrete solutions using DDFS, which consumes a lot of power, were exhibited. The SoC project was defined using such a technique. The problem of substituting DDFS with PLL is addressed in this letter, along with suggestions for enhanced efficiency [32]. Ultimately, this leads to the suggested fractional-N PLL including randomised interpolation of phase and a wide loop filter bandwidth (BW).

A wide variety of digital, analog, mixed-signal, and radio frequency jobs can be performed by modern system-on-chips (SoCs) [33]. A SoC frequently comprises of a variety of modules, including memory, I/O interfaces, wireless transceivers, multicore CPUs, and memory. Each of these components runs in a unique clock domain which was developed to satisfy its unique performance needs. For instance, I/O interfaces need low-jitter, high-frequency clocks, whereas a CPU would need EMI (electromagnetic interference) to allow power-saving strategies like dynamic frequency scaling or spread spectrum clocking (SSC) to decrease frequent frequency switching. The amount of EMI decrease and the quickest attainable time to settle during frequencies switching are, nevertheless, constrained by PLL bandwidth (BW). BW restriction can be bypassed using a two-point modulation approach and calibrated modulation routes. However, because to the calibration's incredibly slow settling period, its application in the dynamic adjustable SoC clock generator was limited. [34].

While looping modulation using multi-phase switches and digital delay lines can provide great EMI suppression and precise modulating depth, they have a significant deterministic jitter (DJ) problem.

2.2 Related Works

The PLL model is a phenomena, a process, or a logical description of a mathematical or physical system. The model operates on a block's inputs and outputs without regard to its internal parts. The model is actually implemented using a simulation. A simulation illustrates how a certain entity within the block behaves. A lot of labor, money, time, and effort go into simulation. Therefore, in the real world, a notion is represented in a model before it can be put in action. They belong to the category shown in Figure 2.1 based on the way they modelled.

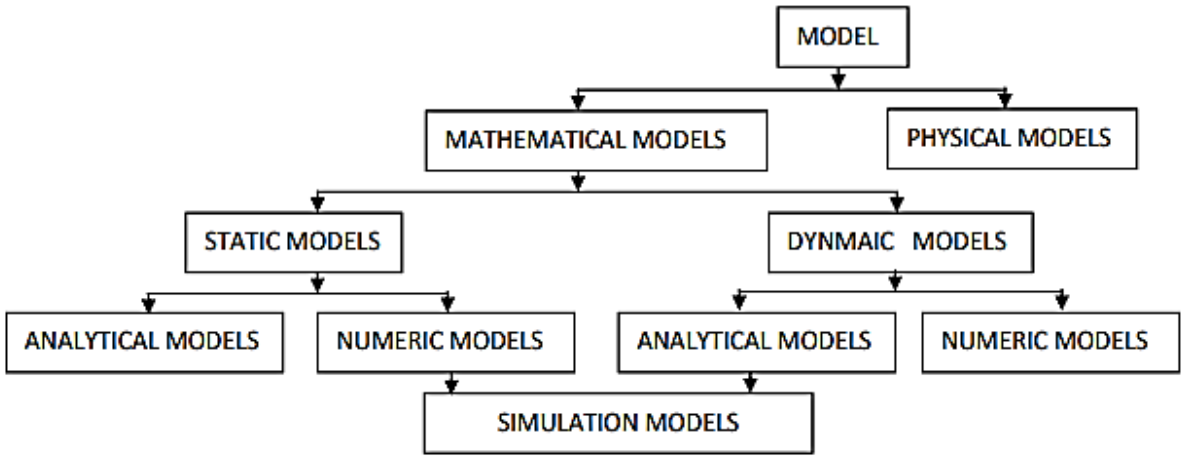

Figure 2.1: Classification of PLL model

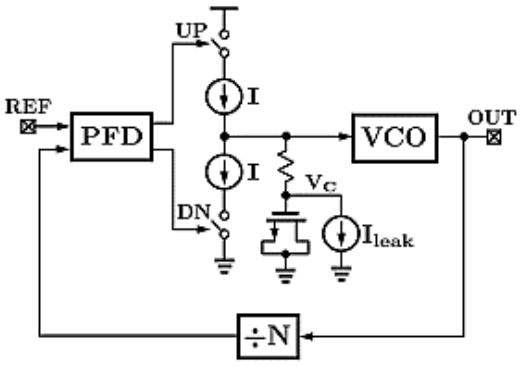

2.1(a) Analog PLL (APLL) [116]

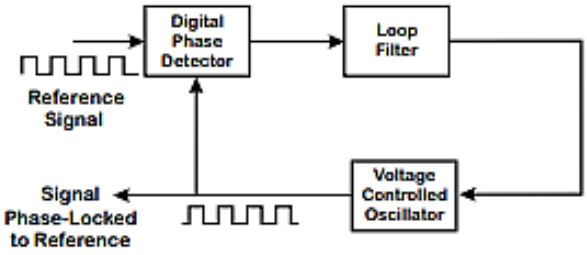

2.1(b) Digital PLL (DPLL) [117]

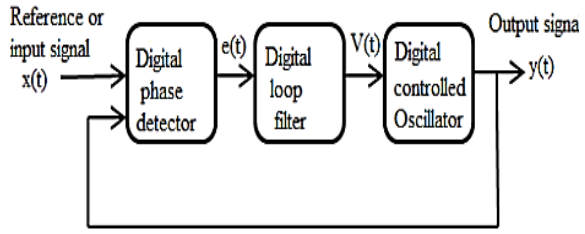

2.1(c) All Digital PLL (ADPLL) [118]

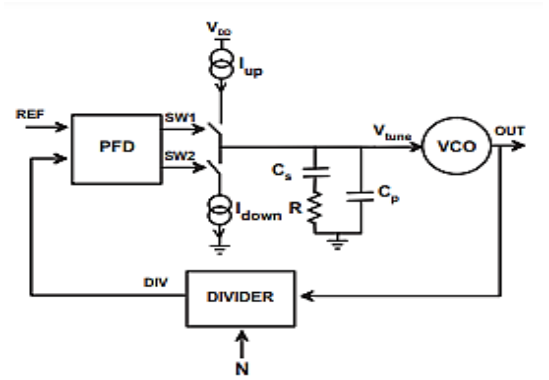

2.1(d) Charge-pump PLL (CP-PLL) [119]

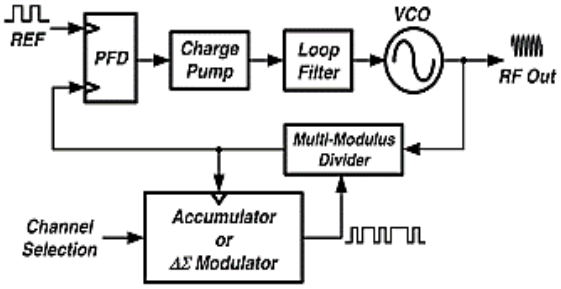

2.1(e) Fractional- PLL (FPLL) [120]

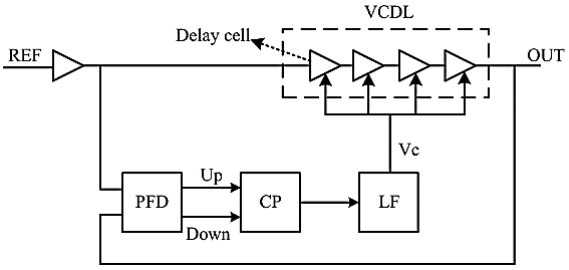

2.1(f) Delay Locked Loop (DLL) [121]

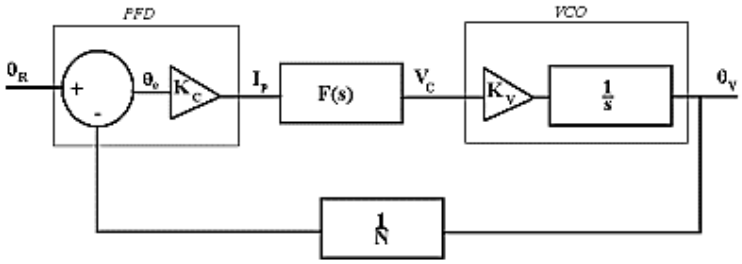

2.1(g) Linear PLL [122]

Figure 2.2: Different types of PLLs

Rakesh Varma Rena et al. [35] this proposed design makes use of the 3rd harmonic of the occurrence of quarter-rate subsampling. , f_s , to simultaneously achieve Impedance matching and quadrature direct down-conversion. Utilizing the 8-path active mixer transparency characteristic, impedance matching is accomplished. The frequency synthesizer's power requirements, distribution circuits, & no overlapping timer generation were decreased by this architecture's usage of samples that were three times lower than those of RF sampling receivers. A 65 nm, 1.2 V CMos test chip was developed to validate the intended architecture. Novel technique for RF port matching in impedance and indirect down-conversion RF the front- end design was presented. To verify the theories, a proof-of-concept test device for CMOS technology at 65 nm and 1.2 V was created. The measurement outcomes show that the

recommended sub-sampling down-conversion approach was a wise decision for configurable RF front-end designs that prioritized mixers and were low power.

Ali M. Kalkhoran and Seyed H. Sedighy [36] had explained the creation of a 64-element transportable digital satellite broadcasting receiver through simulation, cost-effective implementation, and design. Additionally, the electronic beam formation's speed and range were established. The methodology and architecture that were proposed were notable for their cost-effectiveness, utilization of readily available commercial elements, and avoiding of high-frequency designs by employing Delay-line-PLL for phase changing instead of costly RF phase shifters with intricate control buses. The design allowed for the construction of an antenna out of easily accessible parts and household receivers. Phase shifters with a 6-bit resolution and a 16-degree 2D half-power electronic beam scanning range were produced by the design. The array's prototype had been successfully created and put to the test for feasible in practical applications. The sampling of the array output power and obtaining the phase shifters' resolution were also described. For the purposes of performing the platform movement-related tracking task, grating lobes reduction, and SNR maximization, a straightforward and efficient technique is proposed. Moreover, the PLL lock time was the sole aspect of this method's design that slows down beam forming, but adopting very quick locking PLLs could alleviate this issue.

P. Meenakshi Vidya and S. Sudha [37] had explained the design process, simulation, and cost-effective implementation. This intrinsic EMI interferes with the hearing aid SoC's fundamental operating concept. Thus, an all-digital clock generator driven by looping fractional dividers was included in the suggested SoC for hearing aids. A high quality digital-to-time converters with calibrated duty cycle and background bandwidth helps reduce jitter. In addition, a dynamic element matching technique based on switching blocks is included in the suggested hearing aid SoC to reduce the analogue front-end circuit's nonlinearity. Additionally, a multiband complicated spectrum subtraction technique using a pitch-based speech action detector is proposed to enhance the functionality of the deployed hearing aid SoC. The open loop clock generating circuit had a DTC gain & duty cycle adjustment mechanism added to its front to enhance the suggested architecture's jitter/phase noise performance. The open loop FDIV implementations have resulted in distinct clocking needs for the AFE circuit & DSP platform within the hearing aid SoC. That AFE circuit's not linearity’s have been decreased by the addition of the SBDEM calibration method. The DSP platform's performance had also increased as a result of the adoption of new NR, WDRC, and FC methods.

Seyeon Yoo et al. [38] had produced an injection lock clock multiplication with little jitter and a reference spur based on a ring voltage-controlled oscillation (ring VCO). The in-band phase noise of the output signal was also significantly decreased by the TP-FPSC's calibration loop for frequency drift. The TP-FPSC's characteristics, along with the injection-locking mechanism's inherent broad bandwidth, enable the ILCM to produce exceptionally low RMS jitter. Utilizing 65-nm CMOS technology, ILCM was developed. Because of its wide bandwidth, the calibration loops for frequency drift can help further reduce the flicker sound of the ring VCO. The mean spur & RMS jitter fluctuations for the 2.4 GHz signal output for five different processors were found to be 72 dBc & 136 fs, respectively, thanks to strict TP-FPSC control.

Alessio Santiccioli et al. [39] designed a fractional-N frequency synthesizer (FNFS) that can get around the drawbacks of traditional phase-locked loops using bang-bang technology. Fast lock became possible with the introduction of an electronic frequency error recovery technique that required little power or circuit overhead. A suggested architecture for a low-jitter and spur digital-to-time converting with decreased static and dynamic nonlinearity was made. The PLL, It had a 0.17 mm2 core area and was produced using a conventional 28-nm CMOS technology. It takes 18.55 seconds to accomplish a 1-GHz hop to inside 70 ppm of the value of steady-state frequency. After being integrated over 1 kHz to 100 MHz, the prototype's rms-jitter for the fractional-N & integer-N mode was 66.20 & 58.96 fs, respectively. At 61 dBc, a worst-case within a band partial spur is conceivable. Approximately jitter-power figure-of-merit for all fractional-N channels became 250.6 dB as a result of the 19.8 mW overall power usage. Described a 19.8 mW power, fractional-N digital PLL operating at 12.8–15.2 GHz with 66 fs-rms jitter. The system comprised an enhanced DTC design for low-jitter & low-spur fractional-N operation. For speedy lock, it additionally employed a low-power supplementary BBPD and the DFER technique. It is implemented using CMOS technology using a 28-nm process.

Davide De Caro et al. [40] had been demonstrated that SSCG, a spread-spectrum signal generator, could generate either spread- and un-spread-spectrum clocks. The spread clock's carefully crafted modulation profile allows for a major decrease in EMI as well as a smooth, synchronization-free interface across the spread & un-spread clock domains. The study discusses the construction specifics of an all-digital SSCG which can generate the desired modulation waveform, together with the innovative extremely discontinuity modulation profile that enables EMI reduction of up to 15.8 dB. A unique dual-output digitally controllable delay line was used to produce a test chips in UMC 65nm CMOS technology. Route can either create

just a spread clock (single output mode) or a spread clock coupled with an un-spread clock (double output mode). This study demonstrated that, under certain synchronization conditions, both modulation and unmodulated clocks might be generated. SoC applications that require both modulated and unmodulated clocks can incorporate this SSCG. A novel, extremely continuous modulation profile was designed to boost modulation gain because the temporal restriction limits EMI mitigation. By employing a digital frequency generator using phase offset to prevent phase drift caused by error accumulation, the clock synchronization was preserved. The experimental findings showed that synchronized clocks plus a reasonable EMI decrease could be achieved. Spread & un-spread clocks were created in this SSCG using two different synthesizers. The power dissipation, at 48.5 mW in double output mode & 34 mW within single output mode, was similar to various other all-digital SSCGs proposed in the literature, though. Area occupation is associated with SSCGs based on single-output PLLs.

Kang-Chun Peng et al. [41] had created (SIL) self-injection locking loop that was a FNFS. The SIL loop had the potential to significantly enhance the FNFS's phase-noise performance, as it can mitigate noise from the injection-locked oscillatory (ILO), delta-sigma modulator, and reference signal. Experimental outcomes show that a 17-ns SIL loop can reduce 2.4 GHz fractional-N frequencies synthesis phase fluctuations by up to 36.5 dB.

Gujjula Ramana Reddy et al. [42] had developed a hybrid M-GDI numerically controlled oscillator was designed and its memory was optimized. The NCO was a type of electronic design that takes shifting time bases' range of frequencies into account. The NCO was ideally adapted to integrate the vast variety of precise recurrence proportions, unlike a simple recurrent synthesis using stage bolted circles. Additionally, NCOs-often abbreviated as DDS, were a comprehensive technique employed in the era of radio recurrence signals for a variety of purposes, including radio collectors, sign manufacturers, and surely more. According to the findings, hybrid GDI NCO memory optimization offers superior performance in terms of latency, MOSFETs and Nodes with relation to hybrid GDI NCO and NCO-based 8-bit Microchip.

Yu-Lung Lo et al. [43] Clock generators that were entirely digital, low-power, fast-lock, delay-locked-loop (ADDLL) oriented, and that generate fractional numerous of the reference frequency have already been developed. For a hybrid M-GDI dynamically controlled oscillator, its design and memory optimization. The suggested clock generator consists of a fractional frequency multiplication and a dual-loop-designed ADDLL. The suggested ADDLL may

decrease the amount of static phase error and achieve a low locking time because of its coarse & fine tune loops. That 28-phase output clocks of the ADDLL may also be synthesized by the proposed frequency multiplier to produce high multiples. The ADDLL uses the SAR and RSAR to dynamically track phase variations and reduce locking time. The fraction many of the standard frequency can also be obtained using the proposed flexible multiplier.

Ramana Reddy Gujjula et al. [44] had (NCO) One of the various digital oscillation signal generators is the numerically controlled oscillator. It could generate waveforms that were discrete, asynchronous, timed, and generally sinusoidal. Direct digital synthesizers (DDS) were typically made using NCOs in DAC (digital to analog converter) output combinations. Network on chips (NOCs) have been employed in a variety of applications, including the generation of random waves, precise control for ultrasound systems and phased array radar, technological down/up converters, all digital PLLs to stay cellular and personal network communications bases stations, and motorists over acoustic or optical transmissions. Less hardware will be used to enhance and improve the NCO's fundamental design, enabling complete system level support for a numerous modulation types with a lowest use of FPGA resources. In this suggested study, a FPGA is used to optimize the memory of a hybrid gate diffused input (GDI) statistically driven oscillator. The memory optimization performed on the hybrid GDI dynamic controlled oscillator using an FPGA yields favorable outcomes in terms of MOSFETs, nodes, and latency when compared to an 8-bit NCO-based microchip.

Yushan Liu; Runchuan Ye et al. [45] had shown a DDS-based integrative MW source, whose performance is experimentally shown on one NV center in diamond. The quantum electric resonance systems used it for quick frequency sweeping operations. This MW source is much more compact and precisely integrated on just a single PCB board than normal commercial equipment, and it had a lot of possible applications in the engineering industry for emerging quantum technologies and gadgets. While the corrected output frequency range of this MW source is currently 1.4 to 3 GHz, it is theoretically possible to increase this range to 7.4 GHz by modifying the LO frequency & replacing the required parts. Think about switching to on-board chips in place of the current external peripherals to further enhance integration. The MW source could be used in a variety of electrically detecting magnetic-resonance and ODMR systems with the right modifications.

Enrique Alvarez-Fontecilla et al. [46] had proposed all-digital upgrades based on FDC for digital fractional-N PLLs. Among the improvements were a method for assessing digital

background gain and an enhanced DMRO-based FDC design. By reducing the range of the PFD output pulse-width, the former significantly eases the timing limitations placed on the digital component and dividing of the FDC and allows for simpler divider implementations and higher-frequency reference signals. The latter makes it easier to use simple DMRO topologies by correcting for inadequate DMRO frequency in the digital domain with fixed f_{high} and f_{low} values and improving how high-bandwidth PLLs present phase noise. However, it required a very wide PLL loop bandwidth.

Min-Seong Choo et al [47] had stated that although an ILO may generally produce excellent jitter performance if injection time is appropriately regulated, the significant phase fluctuation an ILO encounters at a given injection rate generally reduces spur performance. This work gives a quantitative description of the dynamics of a digital ILCM and investigates a behavioral framework of the ILO that deals with the digital control for a BBPD in a discrete-time domain. To improve spur performance, the frequency mismatch across the injection input with free-running oscillator must be adjusted. However, it was difficult to properly adjust for the time offset brought on by the device mismatches. However, uses more power and causes spurs and increased phase noise.

Marsida Ibro et al. [48] had illustrated the VHDL language's use in the Direct Digital Synthesis (DDS) circuit synthesis. These days, the DDS was widely employed in telecommunications-related sectors, including signal generating circuits. Using digital circuits, the DDS circuits were utilized to produce analog signals. The purpose of this study was to demonstrate how DDS may be implemented using the VHDL language, which was compatible with FPGA hardware. In order to enhance the output of the automatically generated code and the functionality of the DDS circuit, the VHDL code is updated. This optimization of the VHDL code results in a 15% improvement in power consumption and a decrease in resource usage.

Junting Jin et al. [49] had proposed a proposal for an analog integer-N PLL as well as open-loop fractional divider-oriented multi-output clock generator. A high-frequency intermediate clock (600 MHz–900 MHz) is produced from the lower frequency reference using the three-stage VCO-based PLL. This allows for the generation of a broad frequency spectrum between 500 kHz and 150 MHz using the open loop fractional divider. The clock generator's open-loop control feature makes instantaneous frequency changeover possible. The addition of phase-adjusting circuitry to the divider greatly reduced the jitter of the output clock. Its RMS jitter is currently 5.2 ps. A multi-output clock producer is suggested to meet different clock necessities

in SoCs. The DSM-induced quantization error was successfully minimized by charging the capacitor from a variety of current sources. Instantaneous frequency switching and outstanding jitter performance were achieved by this novel open-loop divider architecture.

Eslam Helal et al. [50] had demonstrated a wide-range input-range phased-N digital PLL based delay chain temporal amplifier (TA) operating at 6.5 GHz. While the TA employed an updated dual-mode ring oscillatory FDC, the PLL was constructed utilizing a delay-averaging linearity amplification technique. At higher bandwidth settings, the PLL's phase noise would otherwise worsen, but the TA reduces both the delta-sigma FDC and the DMRO flicker noisy quantization error. These two factors have an impact on the PLL's in-band phase noise. First experimental trial of recently created delta-sigma FDC digital gain calibration method is provided in this paper, together with a delay-free asynchronous DMRO phase sampling methodology.

Darryn Anton Jordan et al. [51] Fractional-N PLLs provide an affordable way for FMCW sonar to meet its precise frequency ramp requirements. Regrettably, the synthetic output of these PLLs is known to generate unwanted spur. Recent research had demonstrated that some of these spur appear as frequency chirps, also recognized as spur chirps, inside a deramped beats signal. Conventional Fourier processing converts these so-called spur chirps into Fresnel waves in the range domain. Spur chirps were especially dangerous for heterodyne receiver systems due to the Diffraction ripples can occur at noise-floor or even higher levels. Authors of that article provide advice for avoiding spur chirps as well as a list of approaches for reducing interference that can be used to address this problem. A list of transferable suppression approaches was also given, along with guidelines for eliminating these spur chirps. A novel suppression technique was also demonstrated. Simulation results demonstrated that in RMSE, SSIM, and PSLR, RDSM performed noticeably better than time-domain zeroing. But it was shown that the efficiency of RDSM was influenced by its frequency resolution. When RDSM was fitted on the measured data, the spur chirps in the ensuing SAR imagery were meaningless. An important step toward expanding the usage of fractional-N PLLs and heterodyne FMCW radars was taken by this study. Subsequent studies could employ the sparse representation methods under investigation to do a complete computing complexity comparison.

Zhijun Li et al. [52] had suggested a method of adjustable size of steps adaptive harmonic detection that was more efficient. In order to perform the step size modification, the method uses a sliding integrator to discover feedback which may accurately represent the tracking state.

The amount of steps per iteration based around the L2 norm was then calculated using this feedback instead. The updated approach was used on the photovoltaic-active power filtering (PVAPF) system, and simulated verification was done using MATLAB, to further bolster its superiority and viability. The simulation outcomes demonstrate that, with the same modeling parameters, the new algorithm had a lower steady-state error and a half-cycle faster rate of convergence than the traditional methods. In PV-APF system application, grid-connected solar systems and harmonic compensation were both accomplished under standard illumination conditions. This work provided a better variable size for the adaptive harmonics detection technique to overwhelmed the inherent shortcomings of the traditional adaptive detection algorithm. Using a sliding integrator, this method determines the error factor that accurately captures the tracking error. The step size is then dynamically adjusted and the calculation is made simpler by inserting the error variable into the newly constructed variable step dimension iteration function, which is depend on the L2 norm. Comparing the updated algorithm to the conventional detection method, the simulation results demonstrate that it achieves both a small steady-state misalignment and a fast dynamic response time. The PV-APF system can now quickly and correctly detect harmonics and adapt itself in response to variations in load and light intensity thanks to the improved algorithm.

Dongyi Liao et al. [53] There was an introduction of a fractional-N RSPLL. To reduce the divider error in quantization in fractional mode, a capacitor-oriented digital-to-analog conversion was set up at the baseline sampling phase detector (RSPD) output. By keeping the sample capacitors discharge current constant, the RSPD was linearized. However, compared to a sampling PD, the current flowing through the source could produce some noise. But once locked, the noise of the loop can be successfully muffled by using the high-gain setting of the RSPD. Without deteriorating the PLL n-band phase noise, the linear spectrum of RSPD can be changed to compensate for quantization error in a frac-N mode. The CDAC was created using a high order cancelling technique that uses many reference voltages but just a single capacitor array to reduce the nonlinearity of RSPD. The prototype was made using 45-nm pitch partly depletion silicon-on-insulator (PDSOI) CMOS technology. Since it doesn't require phase interpolation at the VCO output or loud, power-hungry DTCs on the reference channel, the suggested PLL also offers low noise for fractional synthesis. The reference sampler's amplitude can be adaptively adjusted to attain a broad detection range with acquisition as well as increased strength for decreased phase noise after lock. The recommended RSPLL had a simpler and more stable loop structure than the SSPLL since it does not need a second frequencies locking

loop Even though the sampler's current amplifiers adds more background noise than a pure SSPD, overall noise was still less than that of a typical PFD/CP-oriented PLL since it had fewer sources of noise & a quicker remaining turn on time. Furthermore, by altering the sampled edge's slope and putting the RSPD in high gain mode, noise created by the CDAC canceller may be reduced even lower below the PLL input threshold. The sampler's linearity constraint is loosened by the proposed high order quantization error canceller. Using several reference voltages on the CDAC helps further reduce higher order quantization error.

Bangan Liu et al. [54] Even although the sampler's present amplifier adds additional noise than a pure SSPD, overall noise remained lower than that of a standard PFD/CP-oriented PLL despite a smaller amount of noise and a faster residual turn on time. Furthermore, by altering the sampled edge's slope and putting the RSPD in high gain mode, the noise generated by the CDAC canceller may be reduced even lower under the PLL noise threshold. The sampler's linearity constraint is loosened by the proposed high order quantization error canceller. Using several reference voltages on the CDAC helps further reduce higher order quantization error. This work introduced a fractional-N MDLL that is fully synthesizable and calibrated. A low-power, high-performance programmable DTC was suggested and developed, along with a suggested digital nonlinearity calibrated that was customized for the synthesizable design, oriented on noise as well as linearity tests of many DTC architectures. Additionally, the initial spur was reduced by calibrating a SPO and the DPO. The DPO was calibrated by a recommended complimentary switching MUX and BBPD, whilst the SPO was measured using a two-step hybridization with arbitrarily fine resolution.

Jeffrey Prinzie et al. [55] had shown off an all-digital fractional-N synthesis with aggressive type-I with type-II loop settling, fast frequency hopping, and linear frequency tuning word estimation. With a linearized DCO that enabled wide-band as well as closed-loop operation, it used digital zero phase reset to lessen phase fluctuations during switchover that were caused by type-I settling. For closed-loop activities in the 5.8–7.2 GHz band, a hybrid binary–thermometric segmentation is utilized with routing inductances that equalize the DCO gain, resulting in increased DNL efficiency.

A Shansho et al. [56] had outlined the operation of a phase-locked loop-stabilized reverse wave oscillator. An automatic phase-locked loop was utilized to secure the backward waves oscillator using the frequency range of the direct-drive digital synthesizer. The approach for optimizing the frequency synthesizer parameters is given. This makes it possible to make small

adjustments (less than 1 Hz) to get the best reaction time, the quietest phase noise, and the least amount of spurious. It was demonstrated that phase noise, spurious level, and response time were all simultaneously impacted by the kind and arrangement of the looping filters of the frequency synthesizer. The study's findings demonstrate that open resonators can be utilized to test a small sample's properties using a frequency synthesizer.

Zhengkun Shen et al. [57] The study yields fast, high-linear FMCW signals using a revolutionary ADPLL. Two-point modulating (TPM) technology allows for fast chirp slopes, while a broad loop bandwidth reduces ramp linearity distortion caused by a DCO. To minimize quantization noise and overcome loop bandwidth constraints, a digital phase interpolator (DPI) based calibration-free retiming fractional division of frequency (FFD) method was presented. High-linear phase interpolation was produced using the retiming FFD approach using the parasitic insensitive DPI. To further decrease the quantization noise, a vernier temporal-to-digital convertor (TDC) having 2.3 ps time resolution and a high frequency determination DCO and 9.8 kHz/bit corresponding to the LSB were used. That order to produce FMCW signals, this paper introduced a quick and highly linear 12-GHz ADPLL. Examined the necessary loop bandwidth for producing linear and fast chirps. To reduce quantization noise and improve loop bandwidth, a calibration-free retiming the FFD method oriented on DPI is recommended. A high-linear phases interpol for FFD was presented, utilizing a 9-bit parasitic unresponsive DPI. Good PN efficiency for the ADPLL was achieved by further optimizing the quantization noise using a high resolution frequency DCO and a high time accuracy TDC. The 40-nm CMOS technology was used to develop the ADPLL prototype. But that wasn't a very effective system.

Hongyang An et al. [58] Because it can produce excellent quality photographs of the ground target via frequent coverage and a wealth of scattering information, which comprises of a GEO transmitter and an airborne receiver, was indicated to have a wide range of potential applications in both the armed forces and civilian sectors. Sub-Nyquist sampling results from the Doppler width in this setup being larger compared to the PRF of the broadcast pulses. The receiver had been enhanced with a Mult receiving technique to enhance the similar sampling rate and rebuild a comprehensible image. In order to restore the clear image using GEO-SA-BiSAR with less receiving channels, this study employed a unique technique. Initially, a precise echo concept predicated on the "non-stop-and-go" latencies in dispersion model set the groundwork for accurate imaging. As such, the GEO-SA-BiSAR image problem was treated as a combined recovery problem involving sparse and low-rank matrices. The computationally costly observation matrix is neither computed or stored using the modified alternative direction

method of multiplication (M-ADMM), which was developed to shorten the computation time of the conventional recovery methodology. To mitigate the severe sub-Nyquist sample echo of GEO-SA-BiSAR, an M-ADMM approach with multiple reception channels was also implemented. This technique combines the multiple reception of information theory with recovery theory. Simulation findings show that the suggested approach had a good computing efficiency for recovering the original image scene. Compared to the Multi receiving approach, fewer receiving channels were needed.

Zhe Chen et al. [59] had for a radar system operating at 76–81 GHz, It is recommended to generate chirps using an integrated circuit block in conjunction with a fractional-N PLL. The linearity, stage noise, chirp BW, and buzz rate of the FMCW synthesizer were capable of being designed for immediately apparent radar and distant radar applications, via switch at ON/OFF states that respectively, depending on different specifications and concerns, as a result to the moved inductor voltage-controlled the oscillator changes (VCO) topology. Comparing the suggested FMCW synthesizer to traditional single-varactor VCOs and cap-bank VCOs, it shows superior phase noise for switching OFF-state, making it appropriate for LRR applications. With the Q-boosting method, the switch loss in the ON-state is even decreased, enabling the FMCW synthesis to provide good phase noise, steep modulating rates, and an extended chirp spectrum all at once for SRR application. Inbuilt waveform generator also makes it possible to create multi-slope chirp generators and provides extensive chirp rate, duration, and bandwidth programmability.

Jun-Hee Lee et al. [60] A high-precision FMCW radio is described using a direct input FVF LDO. For minimizing the impact of electrical ripple upon the magnification of the FMCW radio sensor and boost open-loop gain, a folded cascode errors amplifier (EA) was connected to the outer looping of the FVF. Power supply ripple path is decreased and PSRR is improved while maintaining a transient response with the direct feedback system. A fast feedback loop was created by the super source follower and inverted voltage follower. The state matrix breakdown technique was used to examine the multi-loop FVF LDO's dependability and susceptibility to parameter changes. Using a 1.2 V source of energy, the constructed FVF LDO generated a maximum current at load of 20 mA. It was suggested to use a FVF LDO with direct feedback. The outcomes of the circuit modeling, the traditional ac analysis, with the state-space framework of the LDO were compared. The state matrix approach was used to examine how sensitive the LDO was to changes in parameters. The outside loop's folded cascode EA improved the low-frequency closed-loop gain, while the local FVF loop produced a high unity-

gain frequency and rapid response. A less complicated design and a power supply ripple path were features of the proposed direct feedback topology. Theoretical predictions were validated by experimental results.

Jianxi Wu et al. [61] had demonstrated a mixed-mode FMCW generator with TDC counter support working at 77 GHz. An innovative solution to the delay mismatch issue was the introduction of a dual rising-edge fraction phase's detector. A Vernier TDC utilizing an automated calibration, a 2.3-ns detection range, and a 10-ps resolution identified two successive climbing edges of the extremely fast clock in the detector. To save space and electricity, the generator used a divider-less frequency mistake estimator and a coarse-fine segmentation DAC. By using sample edge selection, the issue with digital phase identification was also resolved. A split varactor LC VCO with a wide tuning range was suggested to achieve the requisite wide FMCW modulation bandwidth. The offered FMCW generator was produced using CMOS 65 nm technology. The Vernier TDC employs a self-calibrated delayed chain to account for changes in manage, voltage, and temperature (PVT). In order to avoid phase detection errors, the sampling-edge selection technique was adopted. A frequency mistake estimator without dividers was described in order to save space and energy. The generator creates FMCW chirps with customizable period and bandwidth that mimic triangles and sawtooth patterns using a coarse small segmentation digital-to-analog converter (DAC).

Ying Zhang et al. [62] possesses a type of bistatic SAR called GEO-SABM SAR, which combines an airborne multichannel receiver with a GEO transmitter. One major advantage of SAR-GMTI is the regular covering of earth views via GEO-SABM SAR. Azimuth spectrum aliases (ASA) was caused by the azimuth spectrum folding into many sub segments since the azimuth spectra's bandwidth in this configuration was bigger than the pulse repeating frequencies (PRF). The azimuth Doppler ambiguous (ADA) can additionally occur concurrently with the moving object due to its increased radial velocity. Following an analysis of the effects of ASA and ADA on the signal of movement targets, a signal architecture was inferred using coarse images and static target attributes. To recover every single Doppler frequency found in every signal sub segment, an improved VSAR can be applied. The slope of the sub segment range migration after a range movement of cells correction (RCMC) depending around the static target parameter values can be used to estimate the Doppler ambiguous integer. Additionally, dependent on determined spectrum and projected Doppler shifts spectrum sub segments.

Fang Zhou et al. [63] The benefits of small satellite artificial aperture radar (SAR), such as its low cost, rapid development, and customizable deployment, have made it a viable alternative for space-borne SAR. On dispersed small satellite multiple input multi output (MIMO) SAR, however, little study had been done. A distributed tiny satellite highlight MIMO-SAR ultra-high resolution imaging approach is presented in this paper. It makes use of the sub-aperture image coherence fusion algorithm and the sub-aperture division methodology. The sub-aperture signal being deblurred, an improved time domain BW synthesizing (TBS) method was used to generate the large bandwidth signal, a sub-aperture imaging coherent fusion method was utilized to construct the ultra-high resolution image, and so on. The suggested strategy's practicality and effectiveness were supported by simulation findings. In this study, a distributed tiny satellite spotlight MIMO-SAR imaging technique with ultra-high resolution was suggested. The amount of echo data and the possibility of range ambiguity were significantly decreased when PRF is able to recover the sub-aperture unambiguous signal. Furthermore, a more efficient TBS technique for bandwidth synthesis was introduced, which improves frequency band synthesis effectiveness while streamlining the typical TBS operating procedure. The outcome of the simulation indicates that this tactic is workable and efficient.

Darshana Saravanan et al. [64] had provided SARI, a straightforward NPLL framework that carries out classifier training and pseudo-labeling iteratively. Weighted KNN is used for pseudo-labeling, while label smoothing and other common regularization techniques were used to train a classifier on the labeled data. Through a wide range of tests with different partial rates and noise rates, SARI produces SOTA results. As noise and the number of classes rise, the benefits become more noticeable. SARI is very good at fine-grained classification problems. SARI maintains its performance as the dataset's ambiguity rises, in contrast to many other approaches. On datasets collected by the public in real life, SARI also generalizes well. Give comprehensive ablation studies that clarify how the SARI framework operates. The findings highlight the steady contributions of Mix-up and Consistency Regularization to gains in overall performance. It also emphasize the significant advantages of label smoothing, especially in high-noise environments.

Nikolay V. Kuznetsov et al. [65], a 2nd-order type 2 PLL with a sinusoidal PD characteristic is analyzed in this paper. By using phase plane analysis, an asymptotic lock-in range formula that improves on the current formula is found. The lock-in range estimations from engineering and computer simulation were compared with the analytical formulas. The comparison demonstrates that while the lower estimation given in this research promises frequency

reacquisition without cycle slipping for all parameters, it is unable to offer a dependable solution for the Gardner problem. In contrast, engineering estimates have the potential to cause cycle slipping in the matching PLL model.

Kalpana Kasilingam et al. [66] had new design had been finished and incorporates a feed-forward ring oscillator, dynamic PFD, and a sophisticated, low-power PLL. The dynamic PFDs (proposal) were designed to give PLLs superior jitter management while assisting them in finding their lock fast. Utilizing them results in applications that were less complex and use less energy than static logic designs. The high-end PLL's CP had an upgraded loop filter that operates flawlessly on an ultra-low voltage supply without any current mismatches. It had been possible to reduce oscillator frequency fluctuation caused by power supply noise by developing a low-voltage FRVCO. By adjusting the driving intensity ratio between the direct and feed-forward paths, compensation is achieved.

Jiaxing Lei et al. [67], dependent on the precise system model of the progressive PLLs, the suggested method reversely calculates the PLL controller and parameters from the preferred closed-loop transfer function. The sophisticated PLLs that have been designed have the potential to attain any desired dynamic performance. Specifically, the overshoot is eliminated from over 40% and the settling time is lowered from above 40 ms to lower 30 ms. In the meantime, there is no impact on the removal of unbalanced components and the filtering capability is further enhanced. Reshaping a grid-connected converter's frequency response to improve the stability performance of the PLL is a potentially useful application of the suggested technology.

Ziqian Zhang and Robert Schuerhuber [68], Large-signal models were used to simulate a grid-side converter that was linked to a power system via two transmission lines. This study looked at the fault dynamics of the converter-grid system and came up with a stability criterion depend on the mathematical explanation of this model. It was determined and confirmed that injecting reactive current into the grid during a severe grid fault increased the phase-locked loop circuit of the converter's stability, which in turn improved the converter system's overall stable performance during the fault. The study also looked into a reactive current's escape strategy following fault clearance. Phase deviations from a PLL may result in reactive current, which could trigger the converter to backfill grid power to the DC link. This would throw off the DC's power balance and perhaps trip the converter owing to DC link voltage constraints. Many exit solutions for reactive current were put forth in an effort to overcome this problem. After fault

clearing, the study's methods involved raising the active current reference while swiftly lowering the reactive current reference value. Moreover, the PLL's control time constant was rapidly raised following the fault to enhance the DOA and hasten the PLL's convergence.

Tong Zhou and Gaetan Kerschen [69] had suggested approach uses adaptive filters in conjunction with phase-locked loop control to provide online Fourier decomposition. In order to do this, the objective stage lag to be adhered to during the experimental maintenance process is defined by utilizing the idea of a resonant phase lag. Two systems with cubic nonlinearities: a numerical Duffing oscillator and a practical experiment with a clamped-clamped narrow beam were used to illustrate the methodology. The obtained findings demonstrate that the control method is capable of tracking the backbone curves of secondary resonances and precisely characterizing them. One noteworthy aspect of the created method is its ability to automatically and smoothly move the dynamic state toward a single point on a subharmonic isolated branch, hence causing branch switching, all from the rest position.

Rachana Arya et al. [70], Using CMOS technology for approximation in digital PLLs offers a convincing route to more scalable and effective integrated circuits. Through comprehension of the associated trade-offs and use of the most recent developments, designers were able to produce high-performance PLLs that satisfy the requirements of contemporary electronic systems. DPLLs were highly amenable to future CMOS scaling methodologies. It performs exceptionally well over a broad frequency range. This research conducts a relative examination of DPLL building blocks. The DPLLs have improved mid-frequency tuning range, little power consumption, and good phase noise. Locking time is primarily determined by the PFD, VCO, and loop filter parameters. Therefore, an increased lock range can be obtained by adjusting the parameters. The improved center frequency would be attained by scaling the transistors. The circuit bandwidth will be regulated by the filter's order. The relationship among the locking time and circuit bandwidth is inverse. BW and noise jitter will also decrease as soon as the PLL reaches the locking range.

Shahriar Khan Hemel et al. [71] had centered on accurately optimizing a PFD circuit using sophisticated methods that combine 90 nm CMOS technology and the cadence virtuoso spectral parametric analysis. This study's methodical parametric analysis optimized the PFD. Upon simulating the optimized symmetrical PFD under diverse conditions, it was discovered that the optimized circuit shown a remarkable enhancement, attaining an operational frequency of 0.9 GHz higher at a power consumption of 61 µW lower than the other designs. Additionally,

the optimized PFD produced a dead zone that was just 25 ps smaller. These outcomes support This method's efficacy in optimizing operational efficiency and reducing power consumption in PFD circuits. The circuit exhibited a dead zone of 25 ps even though the suggested design obtained a higher frequency and consumption of low power. This can be further decreased in the future to significantly increase the PFD's performance.

Hongyu Lu et al. [72] had presents a conversion matrix approach for digital phase-locked loop (DPLL) phase noise modeling that is linearly periodically time-variant (LPTV). This method allows for quick design iteration and optimization by providing accurate and computationally economical results. The suggested conversion matrix technique allows the designer to signify the LPTV systems with excellent accuracy utilizing intuitive LTI-like transfer functions, in contrast to many previous studies that either solve LPTV systems with noise folding as well as multiple sampling rate conversions, which heightens modeling as well as complexity in computation, or assume linear time-invariance (LTI) and thus overlook phase noise aliasing effects. Furthermore, the uncorrelated upsampling method improves computing efficiency by removing the requirement to take into account the beat frequency of noise sources with varying sampling rates. Simulink transient simulations were used to verify the modeling correctness of a DPLL with time-varying proportional loop gain, which is modeled using the suggested algorithm.

Yuqing Mao et al. [73], Using 28nm FDSOI technology, a ILCDR is demonstrated. By using UTBB-FDSOI transistors with back-gate auto-biasing decrease the size and power consumption of the QRO. This circuit can be used to create a low-jitter ILO by injecting a digital signal. It suggest a low power ILCDR with rapid locking time as well as low jitter for burst-mode applications because of this oscillator's good performance. The primary innovation is the use of FDSOI technology to create a complementary QRO oriented on back-gate control, resulting in the realization of an easy-to-use and effective ILCDR circuit.

Table 2.1 Comparison of different existing works

Authors	**Technology**	**Objective**	**Advantages**	**Disadvantages**
Rakesh Varma Rena et al. [35]	mixer-first straight	The suggested design uses the	• It does away with the	• Uses more power

	down conversion with quarter-rate sub sampling RF	3rd harmonic of the quarter-rate subsampling frequency to accomplish simultaneous direct down-conversion and match the impedance concurrently.	requirement for a separate matched network for sub samples RF front-ends • Uses minimal power	
Ali M. Kalkhoran and Seyed H. Sedighy [36]	PLL	Explains how to create a handheld digital satellite receiver using simulation, cost-effective implementation, and design principles.	• Implementing array radars becomes easier.	• PLL lock time is the sole aspect of this method's design that slows down beam forming
P. Meenakshi Vidya and S. Sudha [37]	delta–sigma modulator (DSM)	The suggested hearing aid SoC had an open circuit fractional divider driven all-digital clock generating functionality.	• Power consumption was significantly lower than on any other DSP platforms.	• The DTC gain modifications were not found and fixed by the current structures.
Seyeon Yoo et al. [38]	PLL	Demonstrates a reduced jitter	• to attain and preserve	• uses more power and

		and reference spur injection locked clock multiplication (ILCM) based on a ring voltage-controlled oscillation (ring VCO).	minimal reference spur and RMS jitter	causes spurs and increased phase noise
Alessio Santiccioli et al. [39]	PLL	Suggested a fractional-N frequency generator concept that can get beyond the drawbacks of traditional bang-bang phase-locked loops.	• Offer fractional-N operation while minimizing jitter and spur operation	• Need more complex tuning loops
Davide De Caro et al. [40]	PLL	Spread-spectrum clocking generator (SSCG) which can produce both un- and spread-spectrum clocks was demonstrated.	• To improve modulation gain	• required a very wide PLL loop bandwidth

Kang-Chun Peng et al. [41]	loop for self-injection locking (SIL)	Created a FNFS with SIL loops that is low-noise.	• The synthesizer was built and shown to have exceptional phase-noise performanc e as a outcome of this remarkable phase-noise reduction.	• Time consuming
Gujjula Ramana Reddy et al. [42]	DAC	A hybrid M-GDI numerically controlled oscillator was designed and its memory was optimized.	• Gives more effective outcomes	• used more power and had limitations
Yu-Lung Lo et al. [43]	SAR and RSAR	It is recommended to use a fast-lock, low-power ADDLL clock synthesizer to generate fractional several of a	• The planned design was appropriate for system on chip, mobile communicat ion, and microchip applications .	• More complex system

		reference clock.		
Ramana Reddy Gujjula et al. [44]	digital to analog converter (DAC)	Memory optimization and hybrid GDI numerically driven oscillator design were accomplished using field programmable gate arrays (FPGAs).	• In regard to delay, metal-oxide semiconductors field-effect transistors (MOSFETs), and nodes, PGA provides effective results.	• Difficult for implementation
Yushan Liu; Runchuan Ye et al. [45]	DDS	A fast frequency-sweeping integrated MW source based on DDS for quantum magnetic resonance systems	• Efficient model • Cost effective	• Does not electrically detected magnetic-resonance systems.
Enrique Alvarez-Fontecilla et. al. [46]	PLL	Proposed enhancements to digital fractional-N PLLs based on FDC.	• Enhances PLLs with large loop bandwidths' phase noise efficiency.	• required a very wide PLL loop bandwidth
Min-Seong Choo et. al [47]	injection-locked	A TDDC technique is	• To achieve a stable	• uses more power and

	oscillator (ILO)	recommended to produce stable jitter performances on RMS combined jitter and referencing spur metrics.	jitter performance on the reference spur and RMS integrated jitter metrics.	causes spurs and increased phase noise
Marsida Ibro et al. [48]	DDS	Utilizing the VHDL language, describe the synthesis of the Direct Digital Synthesis (DDS) circuit.	• It is possible to reduce resource use and improve power usage.	• Does not electrically detected magnetic-resonance systems.
Junting Jin et al. [49]	PLL	To satisfy various clock requirements in SoCs, a multi-output clock generator is suggested.	• Provided rapid frequency switching and great jitter performance.	• Does not added spread spectrum clock (SSC)
Eslam Helal et al. [50]	DMRO	Offered a temporal amplifier (TA) with a broad input range based on a delay chain.	• Consumes only low power	• It is not an efficient system

Darryn Anton Jordan et al. [51]	FMCW radar	give suggestions for avoiding spur chirps and list current interference suppression methods	• SAR images can be made free of the effects of spur chirps by masking just 0.15 percent of the available Doppler bins.	• High Computational complexity
Zhijun Li et al. [52]	photovoltaic-active power filter (PVAPF)	Presented an enhanced method for adaptive harmonic detection with variable step size. The software finds input that accurately describes the tracking condition using the swiveling integrator and adds it into the procedure of value iteration calculation.	• to get over the limitations of conventional adaptive detection technique • A sliding integrator locates the error variable that accurately depicts the tracking error. • Achieves, in comparison to the conventiona	• Uses large amount of time • High cost system

			l detection method, both a quick dynamic reaction speed and a minimal steady-state misalignment. • The equipment can quickly and accurately recognize harmonics and make modifications when the load or light intensity changes. As a result, this improved strategy is applicable and helpful.	
Dongyi Liao et al. [53]	PLL	Introduce a fractional-N reference sampling PLL (RSPLL).	• Because it doesn't use noisy components, fractional	• No reduction in higher order quantization

			synthesis produces low noise. • A high gain for reduced phase noise after lock is attained along with a large detection range for acquisition.	error is possible.
Bangan Liu et al. [54]	MDLL and DTC	Described based on digital-to-time (DTC). The suggested synthesizable DTC with two stages	• Uses low-power, • high-performanc e system	• uses more power and causes spurs and increased phase noise
Jeffrey Prinzie et al. [55]	PLL	Demonstrated a fast frequency hopping fractional-N synthesizer that is fully digital and had linear frequency tuning word estimate.	• Minimize phase transients between gear-shifting	• Used more power and had more limitations.
A Shansho et al. [56]	DDS/PLL/ BWO	The frequency synthesizer	• good performanc	• Complex System

	frequency synthesizer	parameters optimization method is described.	e in phase locked BWO	
Zhengkun Shen et al. [57]	two-point modulation (TPM) method and digitally-controlled oscillator (DCO)	This work presents the all-digital phase-locked looping (ADPLL), a new rapid and high-linear FMCW noise generator.	• Cost effective	• Not an efficient system
Hongyang An et al. [58]	Technique for obtaining a clean picture for GEO-SA-BiSAR with fewer receiving channels.	The proposed method had a much lower computing complexity than the most current imaging method that relies on joint patchy and low-rank matrices' recovery.	• Uses a low-power, • high-performanc e system	• High cost system
Zhe Chen et al. [59]	FMCW frequency synthesizer in the K-band	Give a description of the design of a multi-chip frequencies synthesis that	• Results in low phase noise, a wide chirp BW, steep modulation	• Used more power and had more limitations.

		combines an FMCW frequency synthesizer operating in the K-band.	rates, and acceptable chirp linearity.	
Jun-Hee Lee et al. [60]	radar with frequency modulation continuous wave (FMCW)	Radar's direct feedback Flipped Voltage Follower (FVF) LDO is explained.	• minimal ripple in the power supply without a complicated design	• High cost system
Jianxi Wu et al. [61]	digital-to-time converter	This paper presents a demonstration of a mixed-mode FMCW converter running at 77 GHz.	• Reduce area and power consumption.	• Used more power and had more limitations.
Ying Zhang et al. [62]	GEO-SABM SAR	For moving objects, a more effective azimuth wave reconstruction technique based on VSAR is advised.	• Most effective system • improved VSAR processing	• Time consuming system
Fang Zhou et al. [63]	MIMO-SAR	This research presents a high-resolution	• increases effectiveness of	• More complex for developing

		imaging approach for networked micro satellite spotlight MIMO-SAR based on a coherent fusion algorithm and sub-aperture photography coherent fusion strategy.	frequency band synthesis while streamlining the operation of conventional TBS.	
Darshana Saravanan et al. [64]	KNN	Provide SARI, a straightforward NPLL framework that carries out classifier training and pseudo-labeling iteratively.	• More robust	• Time consuming
Nikolay V. Kuznetsov et al. [65],	PLL	A 2nd-order type 2 PLL with a sinusoidal PD characteristic is analyzed	• Provide Reliable method	• High complex
Kalpana Kasilingam et al. [66]	FRVCO	To lower oscillator frequency	• High Energy-efficient	• Limited bandwidth

		fluctuation due to power supply noise, a low-voltage feed-forward ring	• low complexity	
Jiaxing Lei et al. [67],	PI-based DSOGI-PLL	to improve the dynamic performance of the frequency-adaptive advanced PLL without affecting the removal of unbalanced component	• Optimal performance • Improved stability	• Complex controller
Ziqian Zhang and Robert Schuerhuber [68],	converter-grid system	Large-signal models were used to simulate a grid-side converter that was linked to a power system via two transmission lines.	• Stability enhancement • Improved performance	• Voltage limitations
Tong Zhou and Gaetan Kerschen [69]	PLLT	The suggested approach uses adaptive filters in conjunction with phase-locked loop	• Accurate • Efficient	• Complex model

		control to provide online Fourier decomposition.		
Rachana Arya et al. [70],	CMOS technology	focusing on quantifying their impact on key performance metrics such as lock time, jitter, and settling time	• High Efficiency • High Scalability	• High Complexity
Shahriar Khan Hemel et al. [71]	PFD	Concentrated on accurately optimizing the PFD with sophisticated methodologies in order to optimize a PFD circuit.	• Uses Higher Frequency • Lower Power consuming	• Less efficient
Hongyu Lu et al. [72]	DPLL	presents a conversion matrix approach for digital phase-locked loops that were periodically time-variant (LPTV) (DPLL)	• High Efficiency	• Limited Scope

Yuqing Mao et al. [73]	UTBB-FDSOI	Using 28nm FDSOI technology, a low-power Injection-Locked Clock and Data Recovery (ILCDR) is demonstrated.	• Low power • Fast locking • Low jitter	• More complex

2.3 Research Gap

- The complexity of the existing synthetic bandwidth-based FMCW SAR Transmitter is very high due to multiple PLLs, high-speed RF switches, and filter banks.
- Hence, a synthetic bandwidth-based FMCW SAR Transmitter architecture should be simplified by employing a fast-switching injection-locked oscillator (ILO).
- However, the existing SHILO consume more area, reduces power efficiency and introduces crosstalk.
- These points motivate to develop a new FMCW SAR Transmitter by optimizing the structures of FNDPLL and ILO to reduce the overall performance of the transmitter, power consumption and area requirement.

2.4 Summary

This investigation demonstrates that mixed-mode PLL, DDFS, or FNPLL were used in the design of the existing FMCW synthesizers. However, DDFS uses more power and causes spurs and increased phase noise. An analog FNPLL synthesizer is created as an alternative that uses less power and produces FMCW signals with narrower chirp bandwidths. As a result, when the radar was employed for the actual detection range of the application, its range resolution was decreased and a high-gain antenna became required. Analog and digital PLLs were discovered to work well together in this mixed-signal mode architecture. In order to give a larger chirp bandwidth, the mixed-mode based architecture needed a high VCO gain, which reduced the

phase noise performance. An option is the programmable loop architecture of the FNDPLL, which can generate chirps at different chirp speeds.

When trying to achieve a quick PLL settling using earlier approaches, a very wide PLL loop bandwidth was required, which significantly raised the phase bruit and spur levels. Furthermore, the previous FNPLLs employed PFD or BBPD phase's detectors. Its linear Period Error Detection unit, like the BBPD, increases the time it takes to settle of the FNPLL despite its low power consumption. On the other hand, PFD takes more time to settle. It follows that an additional FMCW SAR transmitter with a quick FNPLL time of settle is needed. Moreover, the current FNDPLL structures often use Digital-To-Time Converters (DTCs) or Time-To-Digital Converters (TDCs) for fractional dividing in the low-noise application. Due to its complexity, the DTC which was initially provided needed more support and had limitations. A bias pin was also required for the current mirror. Additionally, the DTC gain changes were not found and fixed by the current structures. To automatically adjust the DTC strength in the background, a way should be looked at. So design efficient systems.

CHAPTER 3

PRELIMINARIES OF PLL AND DSS

3.1 Overview

In many systems with high performance, including wireless communications [74], data converters, and clock generators, a PLL (phase locked loop) with minimal jitter and noise in phase is frequently utilized. Key performance indicators for the traditional PLL are integrated jitter, reference spur, power consumption, phase noise, and power supply.

Typically, the PLL has strict trade-offs between these aforementioned characteristics in order to promise the steadiness of a system. The bandwidth (BW) loop of a traditional PLL is only permitted to be most at one-tenth of reference frequency due to the stability constraint. The in-band phase noise (PN) caused by charge-pump (CP) and the out-of-band PN caused by voltage-controlled oscillators (VCO) cannot be efficiently inhibited due to the restricted BW. To decrease the noise in phase of PLLs, numerous research strategies have recently been presented, including the use of a sub-sampling-depend PLL (SSPLL), multiplying delay locked loop (MDLL), a leakage-free digitally calibrated PLL , a sampling PLL (S-PLL) [75]-[80], and sub-harmonically injection locked PLLs [81]-[85].The traditional MDLL architecture, shown in Figure 3.1, has the benefit of removing the accumulated jitter from the blaring edges of the VCO. To switch among the noisy edges and the reference clock of the VCO clock, a multiplexer is essential for this purpose. The division is responsible for totaling the clock pulses that are used to create the 'SEL' signal via the block of logic selector in Figure 3.1 and observe the multiplexer's time of switching to and fro. This choose logic circuitry enables the input reference clock edge to be directed into the delay cells. In the meanwhile, any misalignment at this point for the duration of the replacement of noisy edges in VCO results in extremely high reference spur and deterministic jitter. This is this architecture's primary flaw.

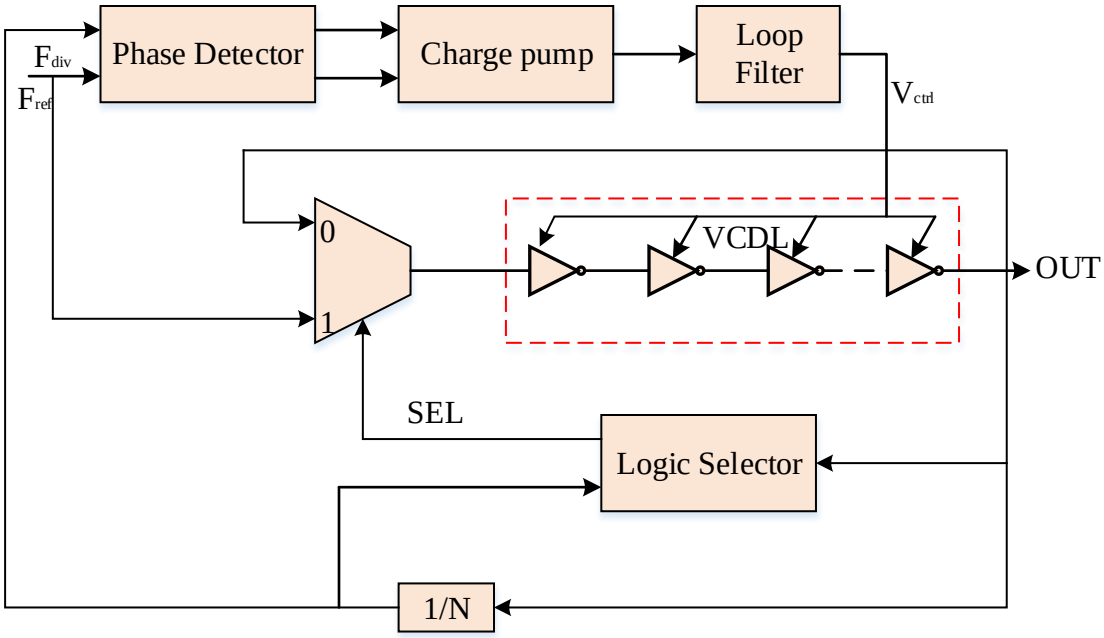

Figure 3.1: Conventional MDLL

Similar to the divider-less PLL, the sub-sampling-dependent PLL is well-known. This reduces the CP's noise by N2, where N is the divider's size. The system's total phase noise performance is directly impacted by the consequence of CP noise reduction. To prevent false locking caused by the lack of a divider block, this design always needs an extra frequency tracking loop. As a result, this architecture required switching circuits, PLL, and FLL.

Controlling the changeover between dividerless PLL and frequency locked loop (FLL) requires proper synchronization. Any misalignment results in a significant reference spur. A single-path sampling PD (S-PD) is frequently developed utilizing a narrow pulse shielding (NPS) method in order to advance the reference surge and RMS jitter that are assimilated in a type-I PLL sampling PLL (S-PLL) [79]. The S-PD actually entails of two sampling stages: a master sampling stage as well as a slave sampling stage for, respectively, identifying the error in phase via the controlled switch, displaying the sampled DC voltage, and dealing with the consequence of reference-feedthrough via the controlled-T shaped switch. In order to reduce the sampling operation's non-idealities, particularly injection of charge and leakage of varactor gate, a high-frequency narrow-pulse shielding method cascading a switch and a 1^{st} orderlow-pass filter (LPF) has been used with help of the T-shaped switch to prevent the spur on control line Vc.

The injection time of the pulse that injected can be calibrated automatically or manually in an injection-locked PLL (ILPLL). The fundamental diagram of ILPLL is presented in Figure 3.2. Additionally, Figure 3.2 depicts the suppression of noise in phase as an outcome of the

employed approach. By pumping a clean pulse (PUL_{INJ}) from the outcome of pulse generator (PG) to input of VCO, the out-of-band PN is immediately suppressed.

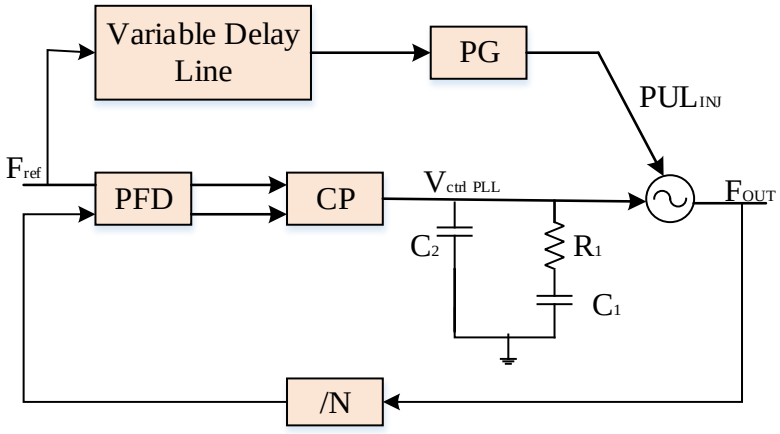

Figure 3.2: Block diagram of the fundamental ILPLL

By using this method, N2 is able to reduce phase noise. N is the divider's size. The latency of the line is manually adjusted in this fundamental ILPLL. ILPLL performance is subject to voltage, process, and temperature (PVT) change since the delay-line lacks self-calibration control. Additionally, if the frequency changes, the variable delay line required to be manually changed several times. The injection signal is inserted into VCO with help of the pulse generator's delay (PG_{delay}) when the ILPLL is locked, aligning F_{OUT} with the reference input F_{ref}. Due to the manual timing control, if this injection is not handled appropriately, it results in a significant reference spur.

3.2 Different existing PPL algorithms

In this section discussed about various existing PLL in the researches like APLL, DPLL, ADPLL, SRFPLL, DDSRFPLL, FLPLL, and goes on. Some of these are described in further detail in the subsections that follow:

3.2.1 Analog PLL

It is possible to generate a linear model for studying the dynamic behavior of the APLL by taking into account that the PLL is already locked with the input signal [86]. Despite the possibility of some components having nonlinear gain characteristics, a linear characteristic is assumed in this context.

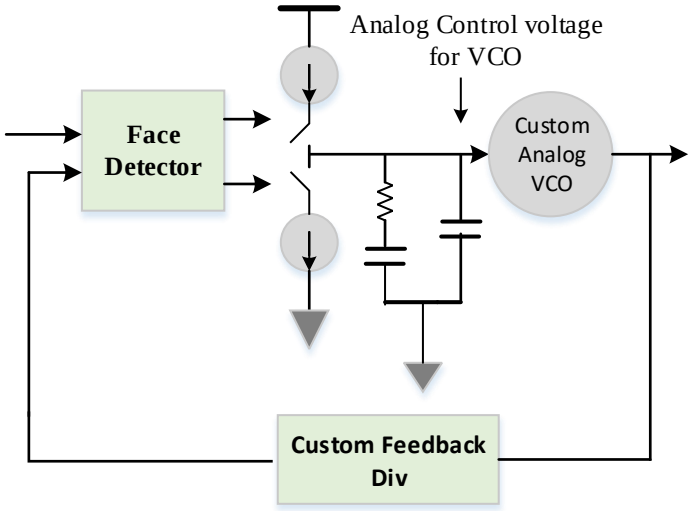

Figure 3.3: Structure of APLL

The outcome of the PD (eq. 3.1) is proportionate to the difference in phase among its inputs. With a gain factor of k_w, (eq. 3.2) the VCO regulates the instantaneous frequency ($w_0 = d\phi_0 / dt$) at its output.

$$\phi_d(s) = k_d[\phi_j(s) - \phi_n(s)] \tag{3.1}$$

$$O(s) = k_w / s, w_0 = \Omega_0 + k_w v_F \tag{3.2}$$

The traditional first- or second-order pole/zero pairings are not the only ones that the loop filter can handle [1, 21]. Instead, a general filter structure (eq. 3.3) is taken into consideration, which supports any order.

$$F(s) = F_0 \frac{\sum_{k=0}^{M-1} a_k s^k}{\sum_{k=0}^{M-1} b_k s^k};\ a_0 = b_0 \tag{3.3}$$

By defining a loop gain factor $[1,2], \lambda = k_d F_0 k_w / N$, the APLL transfer function, $\phi_0(s)/\phi_j(s)$, may be established as follows:

$$T(s) = \frac{N\lambda \sum_{k=0}^{M-1} a_k s^k}{\sum_{k=0}^{M-1} (\lambda a_k + b_{k-1}) s^k}, \begin{cases} a_M = 0 \\ b_{-1} = 0 \end{cases} \tag{3.4}$$

The APLL components parameters may be directly related to the transfer functio1n coefficients (eqs. 3.5 and 3.6), as the loop transfer function is predetermined (eq. 3.5), allowing any APLL design to be solely dependent on its specification.

$$T(s) = \frac{\sum_{k=0}^{M-1} a_k s^k}{\sum_{k=0}^{M-1} \beta_k s^k}, \lambda = \frac{1}{\frac{\beta_1}{\beta_0} - \frac{\alpha_1}{\alpha_0}}, N = \frac{\alpha_0}{\beta_0} \tag{3.5}$$

$$a_k = \frac{\alpha_k}{N\lambda}, b_k = \beta_{k+1} - \frac{\alpha_{k+1}}{N} \tag{3.6}$$

3.2.2 Digital Phase-locked loop (DPLL)

When precise frequency synchronization is necessary, control application systems frequently use digital phase-locked loops (DPLL) [87]. Phase frequency detectors (PFDs), loop filters, and DCOs (digital-controlled oscillators) are the three essential components of a DPLL, or "all digital PLL," as depicted in Figure 3.4. The PFD creates an error signal to represent the difference in phase values after comparing the DCO's final signal with the reference signal.

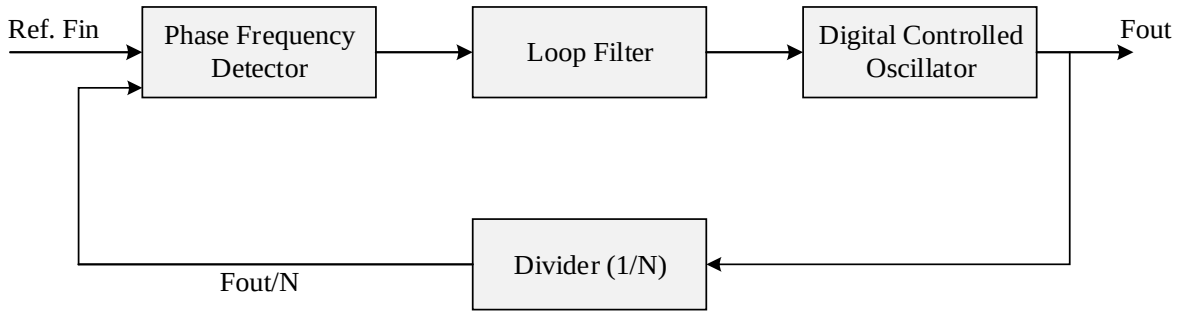

Figure 3.4: Structure of DPLL

The loop filter filters the phase error signal to provide a value for the control signal that is proportionate to the difference in phase among the two signals. The DCO frequency is changed using this control signal value to decrease the phase discrepancy. When the DCO frequency matches the reference-input signal frequency exactly, an equilibrium condition is reached.

The DCO frequency can be synced to a multiple of reference frequency by including a frequency divider (often a digital programmable counter) in the feedback line, as shown in Figure 3.4. A frequency synthesizer is a setup like this that's typically used in communication systems to generate exact frequencies. The lock range of the DPLL is the range of frequencies between the minimum and maximum value from its reference where the DPLL will remain in

the locked condition. When the PLL is initially locked and input signal frequency falls below f_{min} or rises above f_{max}, the PLL is unable to maintain its rated speed at the reference input signal frequency and unlocks. The stated digital PLL method can be useful for controlling dc motor speed since it offers a reliable way to synchronize motor speed with a precise clock signal. In order to replace the DCO, the basic frequency synthesizer configuration or the PLL configuration can be utilized. In these configurations, a dc motor (with a motor driver) and speed encoder are combined to generate a pulse train with a frequency inversely proportional to motor speed.

3.2.3 ADPLL Architecture

ADPLL is a negative feedback control system that includes an oscillator that is digitally controlled, a PD, and a loop filter. All of the digital blocks are present. The feedback loop additionally includes a divide-by-N clock that provides a frequency synthesis function. The signal could be a single parallel digital transmission or a mix of them. ADPLL's basic structure is depicted in Figure 3.5 [88].

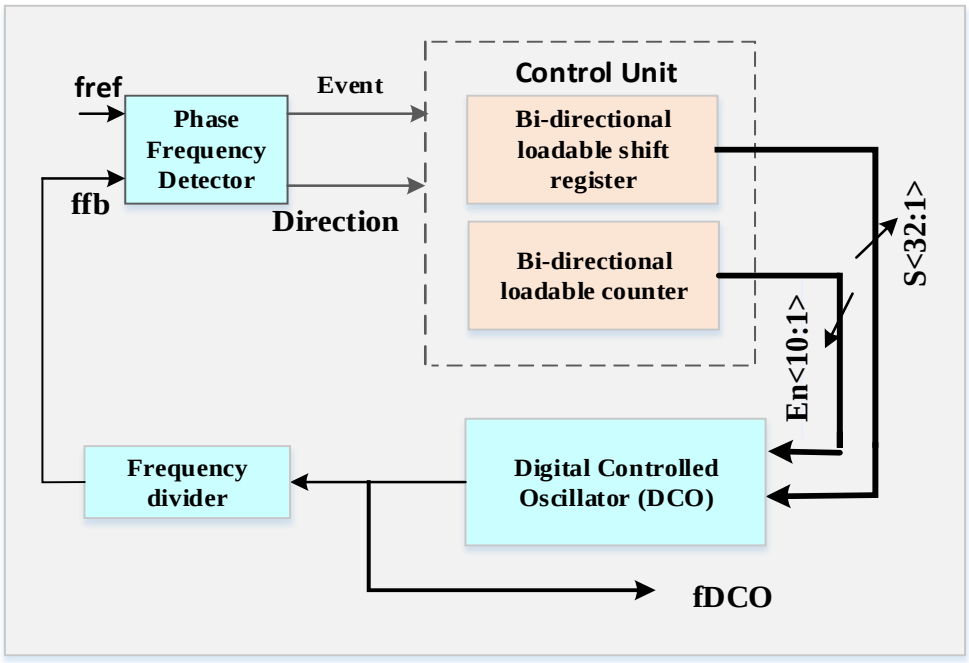

Figure 3.5: ADPLL structure

The ADPLL's goal is to interlace the frequency as well as the phase input v1 and output v2'. The usage of a phase detector helps to minimize the difference between two signals. Loop filtering is used to remove noise. Finally, the signals from LF are obtained by the digitally controlled oscillator (DCO), which then moves closer to the input signal. Existing elements

must be digital circuits in order to realize an ADPLL. There are a few benefits: Insensitive to technology and no off-chip components.

3.2.4 CP-PLL

The CP-PLL can be used to resolve the phase locking issue [89]. Many current fast-speed and low-spur devices employ this strategy. The CP-PLL architecture entails of a regulated oscillator, a loop filter, a CP, and a PFD. A charge pump PLL's schematic layout is shown in Figure 3.6. In this typical CPPLL, a first order passive filter is utilized in series with the charge-pump. The PFD differs from previous methods in that it tracks frequency while detecting phase. Traditional PFDs have two output signals (UP and DOWN), and because the fourth state (UP=DOWN=high) is not enabled, they operate as tristable devices.

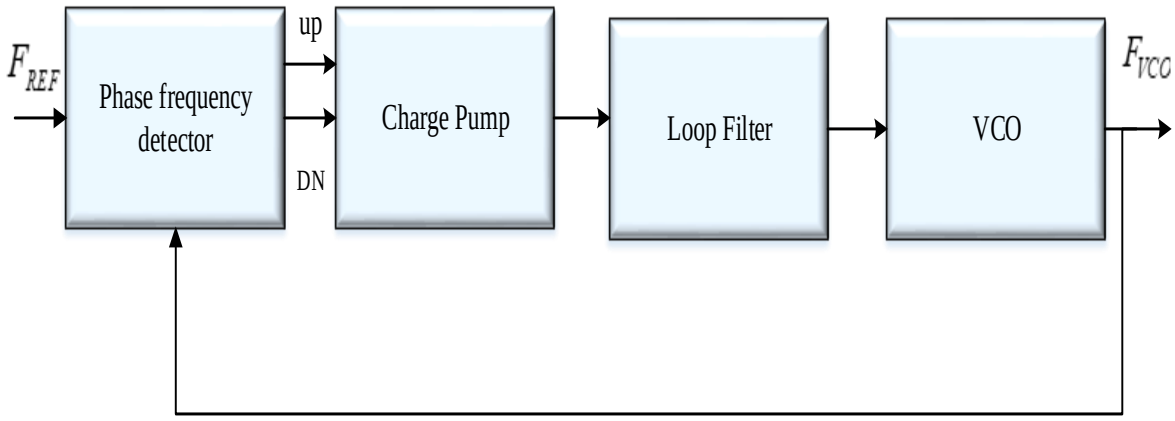

Figure 3.6: Structure CP-PLL

A PFD is a digital phase-detector that can be in one of three states, depending on how the input signal's phase differs from each other: up, down, or high impedance. Two current sources with switches are used to create a charge pump that can drive a filter with plenty of resistors and capacitors and a pole at the origin. The switches on the charge-pump are controlled by the PFD's two outputs, UP and DOWN. Because the width of the pulse on the UP or DOWN signal defines the degree of inaccuracy happening in phase of the PFD input, the charge pump will charge (discharge) capacitor Cz properly when switch S1 (S2) is on.

3.2.5 Fast lock DPLL

One benefit of the digital PLL is the ability to quickly alter loop parameters and behaviors to create some advanced locking characteristics. A fast phase lock DPLL is described in [90] and

Figure 3.7 depicts its block diagram. The frequency comparator and phase detector are both used in this DPLL.

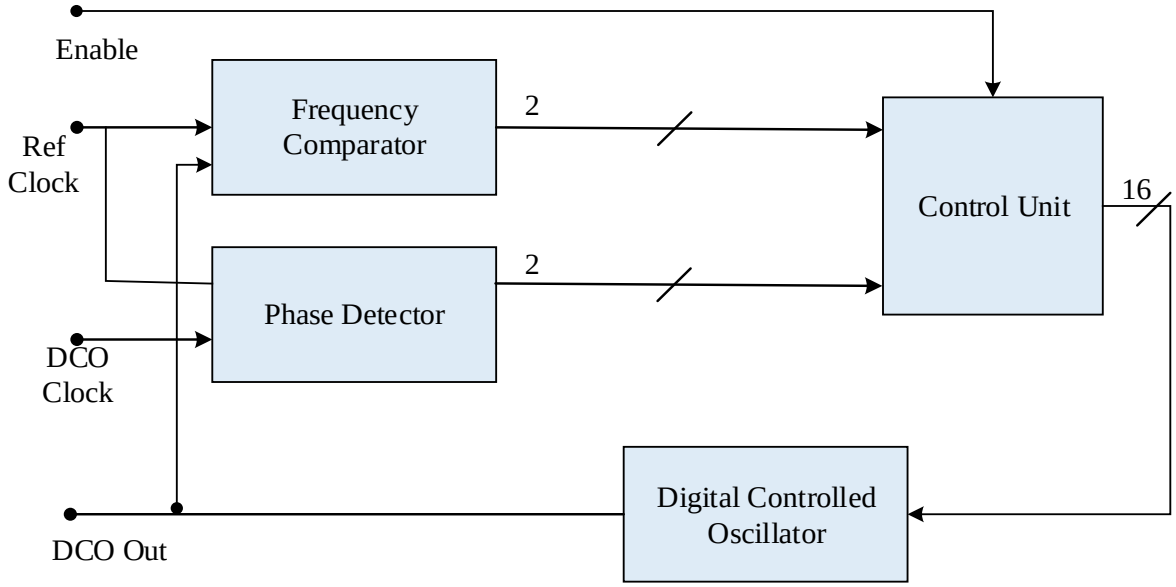

Figure 3.7: FL-DPLL Structure

The DCO output is first aligned to the reference edge, and then the Nth DCO transition edge is related to the next reference edge. The comparator then generates "slow" or "fast" signals to indicate if the DCO frequency is lesser or greater than intended frequency. The DCO in this ADPLL is depend on a ring oscillator, like many other DCOs, and the tuning is accomplished by adjusting both the delay in propagation of one signal stage and the overall number of inverters. Four modes (frequency bands) can be obtained by varying the number of inverters. The inverters' current can be adjusted to adjust the propagation delay. 14 bit control MOS devices are cascaded in front of each inverter. The control device size ratios are two times larger. The largest control devices correlate to bit 13, the most important control bit. When the most significant control bit (bit13) is asserted, the simulation indicates that the least significant bit resolution is 177ps. The upshot is that each of the DCO's four frequency bands has 214 different frequency levels. This ADPLL uses a fast frequency/phase acquisition approach and can complete both frequency/phase acquisitions in 47 reference cycles. Only 8 reference cycles are required to find the correct mode/band, 28 reference cycles are required to acquire the frequency using a binary search method, and 11 reference cycles are required to acquire the phase.

3.3.6 SRF-PLL Algorithm

Many complex PLLs are based on the Clarke and Park transformations, which change the normal abc reference frame to a synchronous reference frame (SRF) [91]. The SRF-PLL is regarded as a basic PLL. Additionally, the grid frequency is output by the proportional integrator controller (PI controller), which is in turn used to regulate the q variables. Additionally, the grid frequency is integrated to provide the utility phase angle, which is given back into the PD (-dq transformation). The SRF-PLL technique, which is employed in three-phase grid-connected power converters, has been extensively studied due to its straightforward implementation and quick and precise calculation of the phase/frequency under normal grid circumstances. The configuration of the SRF-PLL is exposed in Figure 3.8.

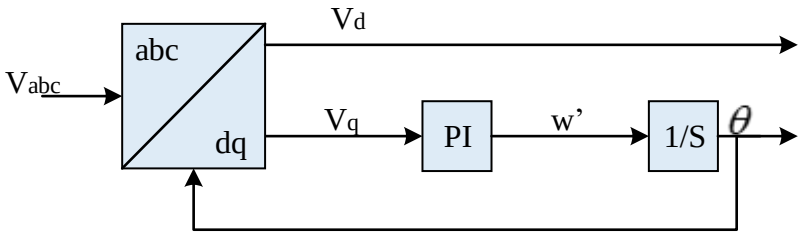

Figure 3.8: SRF-PLL Structure [92]

As previously indicated, the traditional SRF-PLL enables for quick and exact approximation of the grid voltage frequency as well as phase angle under ideal circumstances and functions as intended in the presence of balanced grid faults subsequently the SRF rotates with a positive angular speed. On the other hand, when an imbalanced fault occurs, it will be unsuccessful to track the angle of phase. This is a result of the twice-grid frequency fluctuations that are brought about by the negative sequence constituents that upset the dq-constituents that occur in the disparity of Vd from the positive sequence magnitude. In addition, harmonically distorted voltages prevent the SRF-PLL from functioning correctly.

3.3.7 DDSRF-PLL Algorithm

The SRF-PLL's performance is imprecise on an unbalanced grid, which prevents the loop filter from being able to completely exclude the occurrence of harmonic components. Since the algorithm known as DDSRF-PLL, which decouples the coupling among the negative and positive voltage sequences, expresses the vector of grid voltage through its inverse and direct sequence constituents utilizing a double synchronous reference frame, utilizing two various reference systems is crucial [92]. As seen in Figure 3.9, the DDSRFPLL is accomplished by splitting the grid voltage into positive as well as negative SRFs. While the estimating procedure

is highly difficult and delicate to the phase-angle jump of grid voltage, this approach may totally eliminate the estimation mistakes in traditional SRF-PLL. The next section explains the theoretical underpinnings of the DDSRF-PLL and its decoupling network structure (Figure 3.9).

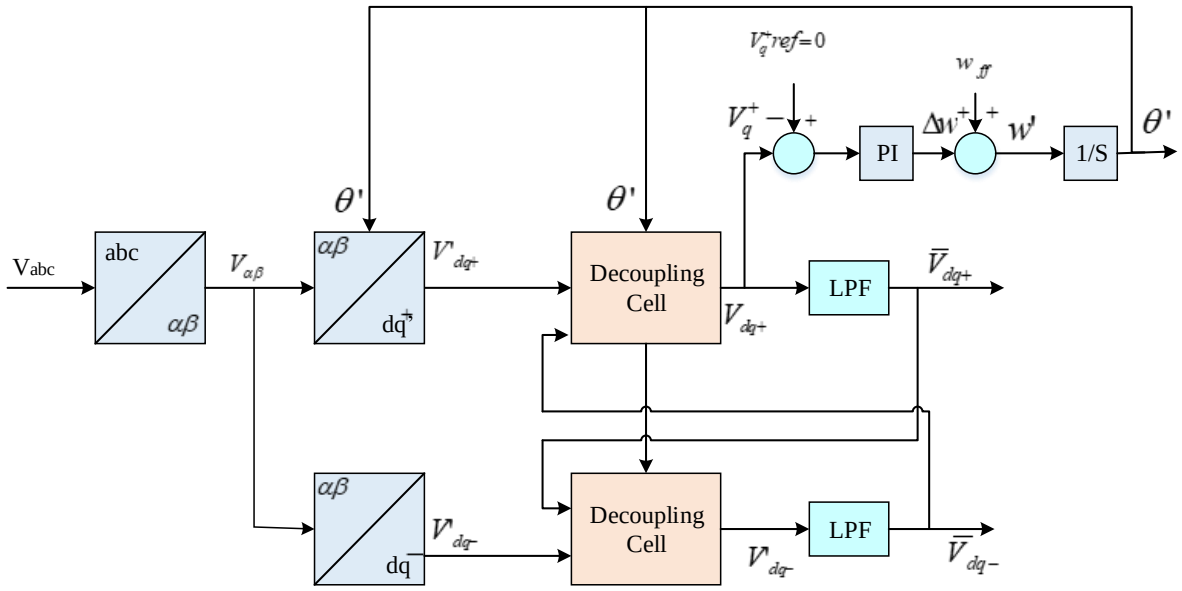

Figure 3.9: Structure of SRF-PLL [92]

The DDSRF-PLL ensures a successful functioning during imbalanced grid failures as a result of the decoupling procedure. But in addition to the low pass filter (LPF), a cross-feedback decoupling network is required for obtaining the direct sequence grid voltage vector.

3.3.8 Second-Order Generalized Integrators PLL (SOGI PLL)

In PLL structures seen in grid-tie power inverters, second-order generalized integrators (SOGI) have recently been suggested for use as phase detectors.

In essence, SOGI structures are band-pass notch filters that are easy to tune to the grid frequency. Additionally, they have the appealing benefit of giving users access to both the filtered output and a quadrature-shifted version of the same output at the same time. By employing the Park transform as the phase detector, they provide a simple application that can match that of conventional SRF-type PLLs. The following is the SOGI-based PLL's general operating principle:

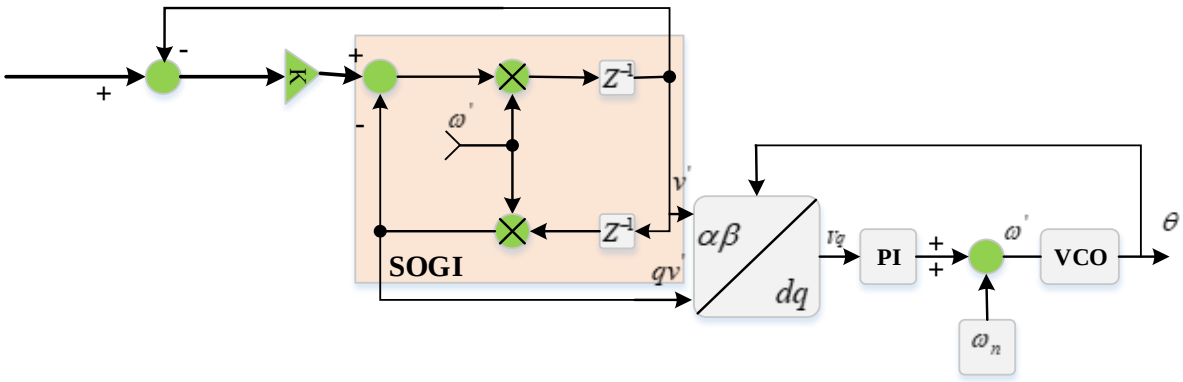

Figure 3.10: Structure of SOGI-PLL [92]

3.3.9 Proportional Integral Derivative (PID)-based PLL

The huge overshoots of frequency in the DDSRFPLL can be avoided by using a PID controller in the loop filtering stage instead of the traditional PI [93]. The additional derivative parameter effectively lowers the anticipated frequency's overshoot. However, the additional zeros in the transfer function have an impact on the PLL's low pass filtering properties. As a result, the PLL will be less sensitive to errors brought on by higher order harmonics due to the usage of PID controller. As a result, when it comes to situations where it is essential to reimburse for the undesirable effects of high-frequency grid voltage harmonics, the PID controller is typically avoided.

3.3.10 Adaptive or Notch Filtering Techniques

Notch or adaptive filters used in PLL procedure can be employed to reduce the undesirable oscillations brought on by atypical and defective grid circumstances. Infinite impulse responses of adaptive notch filters are built depend on the Schur lattice structure in [94] to augment the performance of standard SRFPLL under unbalanced grid voltage and changing frequency situations. Under unbalanced and harmonically biased voltages in grid, the approach may successfully synchronize despite any sudden changes in the grid frequency. According to a similar technique described in researches, the standard SRF dqPLL is altered utilizing a low-pass notch filter (LPN), as seen in Figure 3.11.

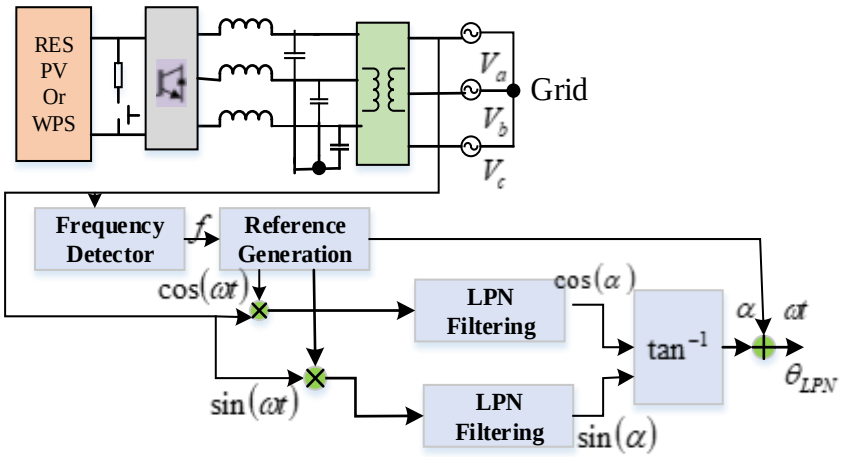

Figure 3.11: Adaptive or Notch Filtering based PLL [94]

The Fast Fourier Transform (FFT) depending PLL is an alternative, and the LPN-PLL has increased performance and allows for correct response below harmonics and grid voltage imbalance. The LPN-PLL and FFT-PLL are applied without PI controllers, in contrast to the SRFPLL. As a result, the tuning of the PI controller has no effect on the dynamic response, and they are simpler and less complex. However, the application of adaptive filtering in the PLL's estimate process results in unwanted sluggish dynamics, which has an impact on the effectiveness of grid-connected RES systems as a whole.

3.3.11 Pre-filtering Moving Average Filter (PMAFPLL)

By adding a pre-filtering stage, the PMAFPLL [94] solves the problem of sluggish dynamics and enables simple adjustment. The pre-filtering stage involves moving the MAF, while the phase detector portion merely has the SRFPLL. The PLL's dynamic responsiveness is sped up by this shifting. The second-order equation describing the PMAFPLL transfer function may be simply modified using well-known inputs like the settling time and damping ratio. Figure 3.12 depicts the PMAFPLL's structural layout. When the grid voltage passes through the MAF, certain harmonics that were present along with the fundamental component and harmonics are eliminated. The phase angle is then retrieved using a typical SRFPLL after the filtered signals v are transmitted there. Under a non-nominal grid frequency, the calculated phase's offset inaccuracy is not taken into account.

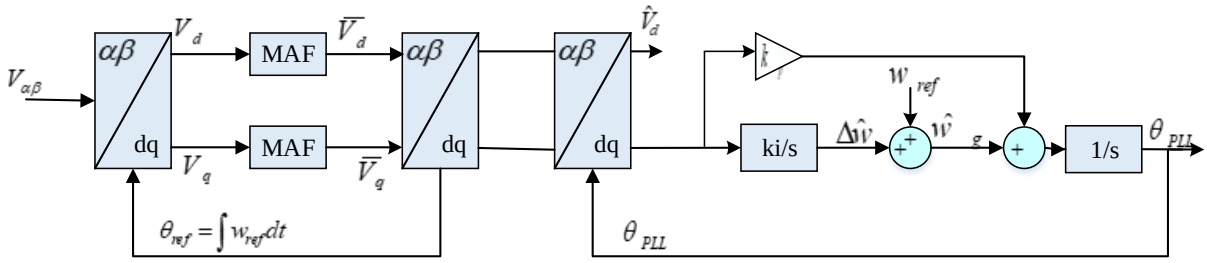

Figure 3.12: PMAFPLL Structure [94]

3.3 DDS: Concept and various types

Direct digital synthesizers (DDS) are essential components of current radio electronic equipment. Frequency reordering, high resolution, and a large synthetic band of frequencies are only a few of the numerous major advantages offered by them. Due to its capability, dependability, potential for minimization, and special technical characteristics (continuity of phase in the duration of frequency switching, the ability to form complex signals, and digital control of amplitude, frequency, as well as phase of output oscillation), multi-level DDS is now used in communication systems. Particularly interesting is the application of DDS in radio engineering information transmission systems with improved stability and security. One of the restraining constraints for such synthesizers' maximal speed and qualitative spectral composition is the speed of individual arithmetic operations in the cores.

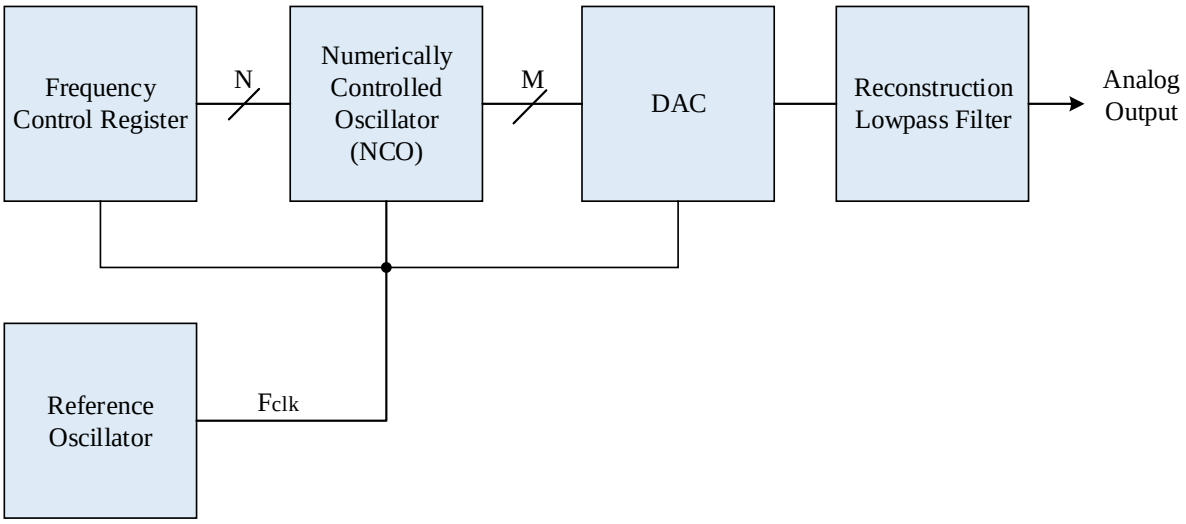

Figure 3.13: DDS Structure

(https://en.wikipedia.org/wiki/Direct_digital_synthesis)

As seen in Figure 3.13, the fundamental components of a DDS are a numerically controlled oscillator (NCO), a frequency reference (often a SAW oscillator or crystal), and a DAC.

The reference oscillator establishes the frequency accuracy of the DDS and gives the system a steady time base. It supplies the clock to the NCO, which produces a discrete-time, quantized form of the anticipated output waveform (typically a sinusoid) at its output. The period of this waveform is determined by the digital word found in the Frequency Control Register. The digital waveform that was sampled is transformed into an analog waveform via the DAC. The output reconstruction filter discards spectrum replicas as a result of the zero-order hold present throughout the analog conversion process.

There has been study on several different DDS architectures [95, 96]. The spectral purity of each architecture's performance varies. Lack of spectral purity would result in in-band spurious content production and a whole power degradation of the target signal. For low power and timing applications like the global positioning system (GNSS), this is a challenge. The receiver would experience acquisition issues if the total strength of an already weak signal was reduced further. Because the spurs would be inside the signal's bandwidth, the development of in-band spurious content would pose issues with the receiver's ability to correlate signals. There are six main categories of DDS architectures: Wheatley Random Jittering Injection, Triangle Output, Sine Output, Triangle Output, and Pulse Output. The spectral purity of the signal will be impacted by the performance of each architecture. Analog and digital components must be used in conjunction in every architecture. The architecture's potential to be software-defined is increased by diminishing the amount of analog components. Pulse and fractional divider DDS are described below:

3.3.1 Pulse Output DDS

The Pulse Output design, as seen in Figure 3.14, is the most straightforward of the different DDS designs and is capable of producing a wide range of waves at a provided carrier frequency (fc).

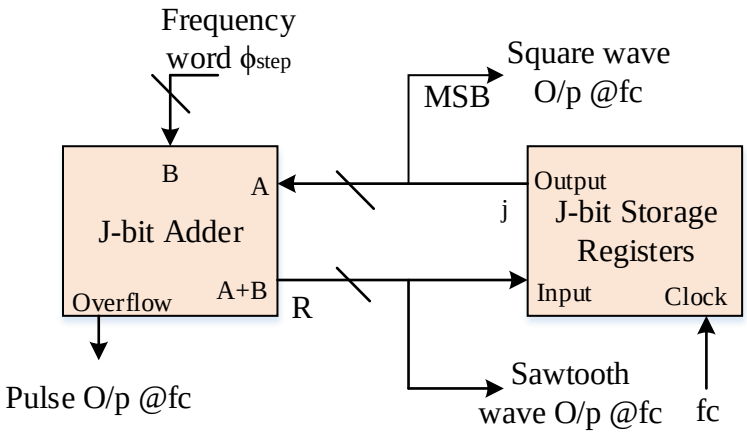

Figure 3.14: Pulse Output DDS

It comprises of a j-bit resolution accumulator. The previous value is increased by step for each iteration of the sampling clock frequency (fs). The description of the Pulse Output architecture, which generates pulses, square waves, and sawtooth waves at fc, is

$$f_c = \frac{\phi_{step}}{2^j} . f_s \tag{3.7}$$

The MSB of the storage register's output creates a square wave. The accumulator's final result value is what creates the sawtooth wave. The output of the accumulator is represented by

$$R(n) = \mathrm{mod}(\phi_{step} .n, 2^j) \tag{3.8}$$

The accumulator's overflow flag from adder produces the pulses. When the accumulator value exceeds j-bits, the overflow flag is set. Due to the sudden shift in energy, high frequency content is produced, which results in significant in-band spurious emissions. The Pulse Output design has the highest phase jitter and in-band spurious content of the six architectures.

3.3.2 Fractional Divider DDS

The Pulse Output design has been updated to become the Fractional Divider architecture, as seen in Figure 3.15.

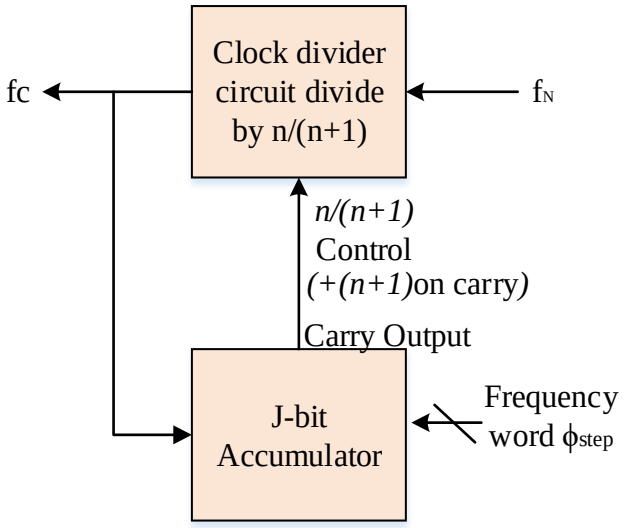

Figure 3.15: Fractional Divider DDS

A clock divider circuit controls the accumulator's clock. When the accumulator performs its addition operation, the clock divider circuit controls the clock. Pulses are generated using the Fractional Divider architecture, which is defined as

$$f_c = \frac{f_s}{n + \frac{\phi_{step}}{2^j}} \tag{3.9}$$

As a result of this design, pulses are produced. Because of the ability to have partial control over the accumulator, the quantity of in-band spurious content is comparable to the Pulse Output design, but the phase jitter is lower.

3.4 Comparison Analysis

The table 3.1 provides a comparison of some of the PLL architectures based on their key parameters, including architecture type, reference frequency, VCO type, output frequency, divider ratio, RMS jitter, reference spur, power consumption, and chip area which seen in existing researches.

Table 3.1: Summary and Comparison

Ref	Architecture	Technology	VCO Type	Output frequency (GHz)	Reference frequency (MHz)	Divider ratio	RMS Jitter (ps)	Reference spur (dBc)	Power (mW)	Area (mm^2)
[97]	Analog ILPLL	32nm	Ring	4G	125M	32	0.71	-61.6	11.4m	0.09
[79]	Type -1 -SPLL	28nm	LC	3.36	105	32	0.124	-78.6	3.37	0.22
[81]	SIL PLL	65nm	Ring	1.7	566	3	0.197	-47	11.77	0.017
[82]	SS-SIPLL	90nm	LC	2.4	40	60	0.37	-44	0.5	0.26
[83]	SIL-TPLL	45nm	Ring	2.4	150	16	0.91	-44.4	5.6	0.013
[77]	SILPLL	65nm	LC	8-12	2000-3000	4	0.1-0.11	-47.6	8.3-8.6	0.6
[78]	ILPLL+PNF	65nm	Ring	1.2	50	24	1.48	-57	19.8	0.6
[90]	fast-lock PLL	40nm	LC	25	390	N/A	N/A	N/A	64	0.1
[98]	fractional-N PLL	28nm	LC	22.25	104.5	N/A	N/A	-68	31	0.24

The table showcases a diverse range of PLL architectures with varying characteristics. The Analog ILPLL [97] employs a ring oscillator and offers a high output frequency of 4 GHz but consumes 11.4 mW of power. It excels in low RMS jitter at 0.71 ps but has a relatively lower reference spur of -61.6 dBc. In contrast, the Type-1 SPLL [79] utilizes an LC oscillator, achieving a lower output frequency of 3.36 GHz but consumes less power at 3.37 mW. It boasts impressively low RMS jitter of 0.124 ps and a reference spur of -78.6 dBc, making it suitable for applications demanding high precision. The SIL PLL [81] employs a ring oscillator, offering a modest output frequency of 1.7 GHz but with minimal power consumption at 11.77 mW and a relatively higher RMS jitter of 0.197 ps. The SS-SIPLL [82] employs an LC oscillator, achieving 2.4 GHz output, and 0.5 mW power but has a higher RMS jitter of 0.37 ps. The SIL-TPLL [83] offers a 2.4 GHz output with moderate power consumption (5.6 mW) and RMS jitter of 0.91 ps. In contrast, the SILPLL [77] provides a wide output range (8-12 GHz) with varying power (8.3-8.6 mW) and jitter (0.1-0.11 ps). The ILPLL+PNF [78] exhibits a lower output frequency (1.2 GHz) with a high RMS jitter of 1.48 ps but with relatively lower power consumption at 19.8 mW. The fast-lock PLL [90] stands out with a high output frequency of 25 GHz and low power (64 mW), but specific jitter and spur values are not

available. Lastly, the fractional-N PLL [98] operates at 22.25 GHz, offering moderate power consumption (31 mW) and a reference spur of -68 dBc. Comparison for existing DDS are shown in Table 3.2.

Table 3.2: Summary and Comparison of various DDS researches

Technology ft/fmax (GHz)	**InP 300/300 [99]**	**InP 300/300 [99]**	**InP 137/267 [100]**	**InP 406/423 [101]**	**InP 250/280 [102]**
Accumulator size (bit)	8	8	8	9	8
Average SFDR within Nyquist frequency(dBc)	- 21.56	- 26.67	- 30	- 30	-18.1
DAC resolution (bit)	5	7	7	—	4
Die size (mm^2)	2.7 x 1.45	2.7 x 1.45	8x5	—	2.2 x1.6
Emitter area of minimal dimension transistor(mm^2)	0.4 x 2	0.4 x 2	1.5 x 4	0.25 x 1	0.7 x5
FOM (GHz/W)	3.386	2.4	0.5	1.5	2.3
Max clock frequency (GHz)	32	13	9.2	12	17
Power consumption (W)	9.45	5.42	15	8	7.4
Transistors number	1891	1646	3000	8800	1700

3.4.1 Comparison of PLL and DDS

PLLs are widely utilized for frequency synthesis and clock generation in integrated circuits. Among the PLLs discussed, the Multiplying Delay-Locked Loop (MDLL) offers precise frequency multiplication and synchronization capabilities. It excels in applications where low jitter and fast locking times are crucial. However, it may be complex to design and calibrate. The Sub-Sampling-Based PLL (SSPLL) is suitable for applications with power constraints. It operates at a fraction of the input frequency, conserving power. Nevertheless, it may suffer from higher jitter and limited output frequency range [103]. The Sampling PLL (S-PLL) is known for its simplicity and little power consumption but may not provide the highest performance in terms of jitter and frequency range. The Leakage-Free Digitally Calibrated PLL as well as Sub-Harmonically Injection Locked PLLs offer specific advantages in terms of power efficiency and noise reduction, respectively.

On the other hand, DDS technology provides an alternative approach for frequency synthesis. Wheatley Random Jittering Injection DDS offers randomness in frequency generation, which can be advantageous in certain communication applications. Triangle Output DDS is excellent for applications requiring linear frequency sweeps, and Sine Output DDS is ideal for generating clean sinusoidal signals. Pulse Output DDS is useful in pulse modulation applications.

To provide a comparative analysis, we can summarize the advantages and disadvantages of PLLs and DDS in a table 3.3:

Technology	**Advantages**	**Disadvantages**
PLLs	1. Precise frequency multiplication and synchronization	1. Complex design and calibration
	2. Low jitter and fast locking times	2. Power consumption may vary
	3. Can operate over a wide frequency range	3. Limited output frequency range (SSPLL)
	4. Various specialized PLLs for specific applications	4. Higher jitter (SSPLL)
	5. Noise reduction (Sub-Harmonically Injection Locked)	
DDS	1. Versatile waveform generation (sine, triangle, etc.)	1. Limited to discrete frequencies
	2. Precise frequency control	2. May have spurious components (non-ideal DDS)
	3. Low power consumption	*3. x.* May require more complex circuitry
	4. Excellent for pulse modulation (Pulse Output DDS)	

	5. Linear frequency sweeps (Triangle Output DDS)	

Table 3.3: Advantages and Disadvantages of PLL and DDS

PLLs excel in precise frequency synchronization and offer a wide frequency range but may be more complex and consume variable power. DDS technology is versatile and power-efficient, providing various waveform options, but it may have limitations in discrete frequency generation.

3.5 Summary

In this chapter, an extensive exploration of Phase-Locked Loops (PLLs) within the context of CMOS technology is provided, covering a wide array of PLL variants and their architectures. Among the PLLs discussed are the MDLL, Sampling PLL (S-PLL), Sub-Sampling-Based PLL (SSPLL), Leakage-Free Digitally Calibrated PLL, and Sub-Harmonically Injection Locked PLLs. Furthermore, this chapter delves into the comprehensive details and architectures of various PLL categories, including All-Digital PLLs (ADPLL), Analog PLLs (APLL), Digital PLLs (DPLL), Fast Lock Digital Phase-Locked Loops, Charge Pump-Based PLLs, Synchronous Reference Frame PLLs (SRF PLL), Decoupled Double Synchronous Reference Frame PLLs, Second-Order Generalized Integrator (SOGI) PLLs, Proportional Integral Derivative (PID)-Based PLLs, and Pre-Filtering Moving Average Filter PLLs (PMAFPLL). In addition to PLLs, the chapter provides a comprehensive overview of Direct Digital Synthesizers (DDS) and their various types, such as Wheatley Random Jittering Injection, Triangle Output, Sine Output, Triangle Output, and Pulse Output DDSs.

CHAPTER 4

FRACTIONAL PLL PERFORMANCE IMPROVEMENT THROUGH AN OPTIMIZED ALGORITHM

4.1 Overview

The PLL serves as the brain of wireless communication circuits and systems, using a local oscillator to generate precisely defined frequencies. In the third order $\Delta-\sum$ modulator, which is made easier to use for changing the feedback division modulus instantly. Because numerous samples have to be implemented to plot the frequency response spectrum of the adjusted PLL because of a fractional N's outcomes, the PLL along with Delta Airlines Sigma value being greatly reliant on the data provided reference frequency, we chose Simulink to perform the mathematical experiments while continuing to transmit the parameters to what was intended modules through Matlab. The 3rd order delta sigma modulator through a dual modulus pre-scaler has been successfully simulated and proven in the discussion that follows. We have also plotted the frequency spectrum and retrieved the phase noise values. Background data and the rationale for the study please accept the PLL, one of the most often used frequency synthesizer designs, is constantly improved to reduce noise and increase efficiency. A divider circuit of division value N has been added to the feedback path of the initial integer N PLL that was developed after the discovery of and years of research. This circuit made it easier to divide the output frequency of VCO, which could then be fed into a phase frequency divider to generate several frequencies. [104].

A phase-lock looping (PLL) is a piece of machinery with a system of controls that produces an output signal that is phase-correlated with an input signal. A frequency-varying oscillator featuring a feedback structure loop and a phase-shifting monitor make up the basic electrical circuit. [105]. The fraction number of the dividing ratio must be generated, and additional electrical circuits must be linked to the feedback loop, in order to preserve a positive bandwidth as well as reduce noise. This is the only distinction among the integer-N PLL and the fractional-N PLL. The fundamental idea behind fractional-N PLL is to obtain the correct fractional value by switching between two different divider ratios. The pulse swallowing method, which moves the outcome to the next adjacent integer on the second half of the time period and replaces the divide numbers for the first, can be used to do this. Quantization noise, which manifests itself in FNPLL, can be reduced using an accurate multielement divide (fractional). Using FNPLL,

frequencies can be grouped according to a percentage of the reference. It can be utilized by analog and digital PLLs [106]. The higher frequency and wider band width it offers hasten the settling process. Quantization error noise is an extra source of noise that is introduced by the modulator that creates a division ratios in the FNPLL.

4.2 Proposed Methodology

The first way being considered in the suggested methodology is the design of fractional NPLL for low phase Noise. The PLL, a structural design feature for a system that controls closed loops, is primarily used to make phase and frequency synchronization of the input signal more straightforward. Frequency synthesizer, which takes the form of PLL, is one of the most crucial components of integrated transceivers. The explanation that follows provides an example of the $\Delta\sum$ 3rd order - modulator design model. Changing your approach can help with this. Creating a new PLL architecture that is suitable for wireless applications and has low noise. The PLL overcomes several obstacles by reducing power, taking up less space, and increasing frequency. This comparison includes a diagram that illustrates various PLL. The design of fractional NPLL for low phase Noise is the first method that is taken into account in the suggested methodology. The PLL, a structural design element for a system that regulates closed loops, is primarily utilized to facilitate the phase and frequency synchronization of the input signal.

Since no RF transmitting equipment might take up these low frequencies, the spurs' frequency range can be ignored while charting phase fluctuations at various offset numbers, the spurs' frequency range, and undesirable spurs generated at the references. Second is the enhanced Fractional-NPLL for lower phase noise. A 3rd order delta Sigma modulation has been developed, with a starting frequency of 26 megahertz and an established frequency of 3.5 GHz. It is designed for usage in communication transceivers that and makes use of system on chips. It may additionally be utilized in technologies for embedded systems. The clock must be produced and synchronized through additional timer occurrences in the circuit using a local oscillator. The frequency of the spur can be ignored when showing phase variability at different offset numerals, the range of spectrum, and undesired spurs formed at the references because there are no RF transmitting devices that might pick up this low frequencies. A piece of equipment with a control system known as PLL generates a signal for output whose phase is associated with its input signal. A stage detector and an adjustable frequency oscillator with a feedback process loop make up the basic electrical circuit. In order to maintain the optimistic

frequency and further minimize noise, the fraction value of the division ratio must be created, and extra circuits for electricity have to be included to the feed loop. This is the sole difference among the integer-N PLL and the fractional-N PLL. The fundamental idea behind fractional-N PLL is to obtain the correct fractional value by switching between two different divider ratios.

4.2.1 Design of Fractional-NPLL for Low Phase Noise

There are many methods for modeling simulations; to summarize the features of different approaches, the following table is provided. Fake tones at multiples of an integer of 40 kHz were used to construct it. Majority of the erroneous tones happen at low frequencies. Fractional N of 3rd Ordered Delta Sigma Ordering Design The architecture of the FNPLL is virtually identical compared to that of the number N PLL; the only variations are the generation of a fractional value to represent the divider ratio, the use of additional circuitry to maintain the ideal bandwidth of the feedback path, and the practical reduction of noise levels. Granular N PLL relies on cycling between two distinct divider ratios to determine the right fractional value. It is accomplished via the pulse swallowing approach, which swaps the divider's value for half of the time before shifting it to the next nearest integer for the other half. The following equations can be used to determine how the control circuitry functions:

$$Mfrac = M\frac{Q}{2^{Q}} = M + m \tag{4.1}$$

$$f_{out} = f\_ref * (M + m) \tag{4.2}$$

$$Q = m * 2^{q} \tag{4.3}$$

Where M the ratio of integer division, m is the ratio of fractional division, Q is value equal to the control circuitry, q is the number of bits in the Q.

The aforementioned equations illustrate the manner in which the signal being input, output signal, and control system are interconnected, requiring only adjustments to the control system's characteristics to obtain an alternate tuning frequency. Even this pulse swallowing method has a flaw. When the VCO is observed, this pulse swallowing method produces a signal that is not an exact multiple of the reference signal, but instead spends half of his time above the necessary level and the other half at a low level. This non-exact multiple to the reference

introduces noise spurs for every half time cycle; this noise spur is known as a fractional spur and is controlled by the fractional coefficient.

$$spur = -20 * \log\log \tag{4.4}$$

fm is the frequency of the spur located, and Δf is obtained from the vco sensitivity. To get over all the restrictions, the feedback path adjusts the division ratio using a novel technique called the Delta-Sigma Modulator.

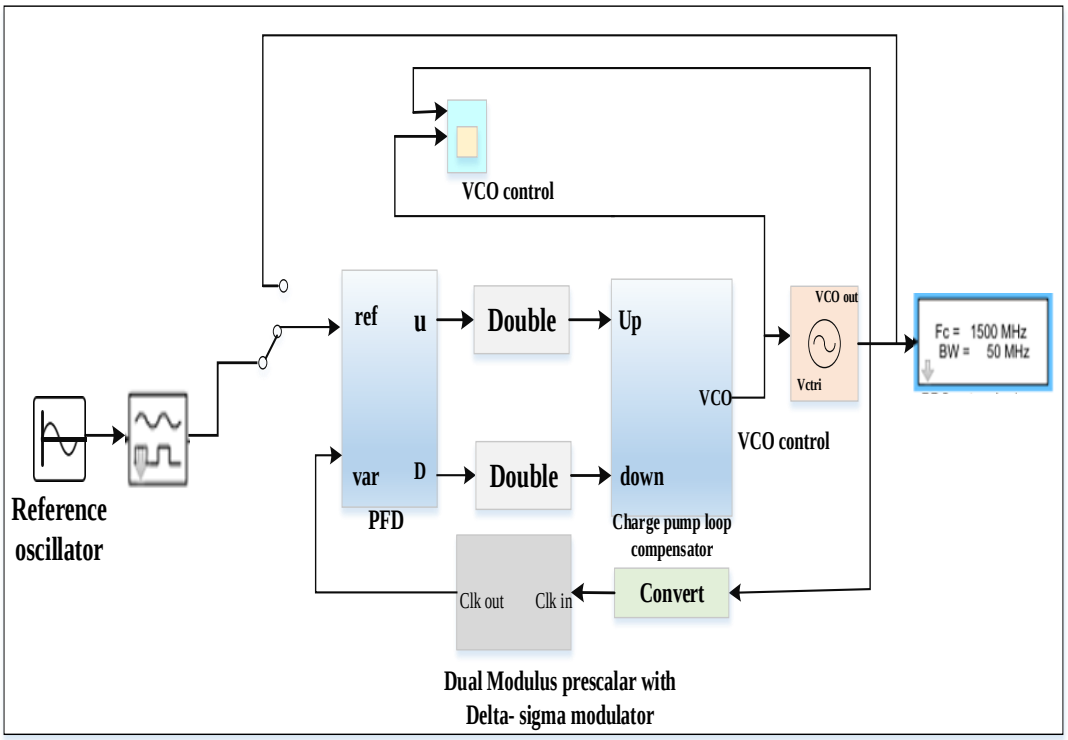

Figure 4.1 Block Diagram

The phase frequencies detector receives input from both the feedback signals and the source of the reference signals. The frequency and phase detector then produces two signals, UP and DOWN, through contrasting the input signals and acting as an error amplification circuit. These signals are then converted by respective information converters and cause the associated switches to become active.

The pulse Swallower circuit's accumulator overflow is something that is controlled by the $\Delta - \sum$ modulator, which also controls the control word, which is 2^q, where q the number of accumulator bits utilized in is. This indirectly influences the division ratio.

4.2.2 An Intensified Fractional-NPLL for Deepened low Phase Noise

The PLL is used in the suggested method, which causes multiple section noise. According to the definition below, the characteristics of the sequence of divider moduli determine how much the section noise is increased. A specific solution addressed in the literature you provided. In this implementation, the division ratio, or divider modulus, is set to either 123 or 122 different for each instance period. For an ensemble of 492 consecutive reference durations, the average modulus is calculated as 122 + 51/492, with 122 being the division factor for 441 units as 123 for 51 times.

The series of modulus has a length of 492, is periodic, and oscillates at an oscillation frequency of forty kilohertz. This periodicity leads to a periodic collection between the initial value division moduli and the average of them with an annual frequency that's 40 kHz. This periodicity results in erroneous sounds at integer times of 40 kHz in the PLL output, which can cause phase noise and distortion. Unfortunately, the N-fraction technique's advantages are defeated because suppressing these unwanted tones calls for an extremely narrow PLL bandwidth. The trade-off between consistency and noise performance is impacted by wider bandwidths, which allow faster settlement times but generate more noise in a PLL. The comparatively small bandwidth needed to suppress the unwanted tones generated through the N-fractional divider limits the PLL's ability to perform.

Finally, periodic spurious tones can be observed at an integer multiple of the reference rate utilizing a fractional-N PLL having a specific division modulus. The PLL's efficiency as a whole is decreased, which can work against the benefits of the fractional-N strategy even though a short PLL bandwidth helps to limit this. The delta-sigma fractional-N PLL is an alternative way to design a fractional-N PLL that overcomes the misleading tones caused by the periodic of the divider modulus. A delta-sigma modulation is used to create the pattern of fractional divisional ratios in a fractional-N PLL rather than directly setting the modulus of it for each reference period. A superior resolution digital signal produced by a delta-sigma modulator, which is oversampled very quickly in comparison to the reference frequency, controls the fractional division ratio. The quantization noise generated by the modulation is spread out over an extensive frequency range thanks to the high oversampling rate of the delta-sigma modulator, with almost all of its power concentrated in a band that is well over the PLL's optimum bandwidth. Because the spurious tones caused by the frequency of the divider factor are distributed over a wide frequency range, they may be eliminated with a low-pass filter that is included in the PLL loop. As a result, they are no longer a problem.

Using a $\Delta\sum$ modulator to operate in fractional-N PLL gives an array of advantages over traditional fractional-N PLLs. It first provides high-resolution frequency adjustment without the recurrent spurious tones of the divider modulus. Second, a wider PLL width can be employed without hampering stability or increasing the noise floor because the quantization bruit is spread out over a wide frequency range. There is more flexibility in choosing fractional division ratios thanks to the modulator's ability to generate any desired arrangement of fractional ratios.

In conclusion, by using a delta-sigma modulation to generate a sequence of fractional divide ratios and quantization noise scattered over a wide frequency range, a fractional-N PLL removes periodic spurious tones caused by the divider modulus. Versatility, PLL bandwidth, and accuracy of frequency resolution are all advantages of this. Input port type: The output signal in a system having a trigger is delayed by the signal it produces, which establishes the rate at which the system operates for the input in the previous step. Turning on this feedback signals used by the calling method's output when calling a function in a subsystem stops input from coming in once the function is running.

The output port's model the initial result will still be applicable to the active subsystem even if the output is unavailable. The output can be dependent on any type of value or be assigned to the first result if it cannot be accessed when the operation is being executed. In the above charge pump circuit compensator, as 1 rises and 2 falls, the input transforms from a Simulink is source to a Physical Signal. A convergent thinker can also provide them ports that appear to be done if they require input in the form of derivatives. One derivative is provided by the first-order filter, while the first and second derivatives are provided by the second-order filter. Constant voltage between its output terminals enables uninterrupted current flow from the source [107]. With the help of a voltage sensor block, you can see the voltage differences that are restricted between circuits that are linked to tangible signals based on voltage. A switch is a device that is controlled by an external physical signal. If the outside physical signal [PS] above a threshold value, the switch is locked; otherwise, the switch is open, then solver settings are applied to the simulation, which This third-order delta sigma modulator divides by variable with two input operations, a constant value for the fraction, and a different port as a trigger to apply the relational operator to the proportional component before checking the static bound. The third order differential sigma modulator further accepts a fraction as input and outputs min out as well as deltas. Based on whether its input information has increased or lowered since the last sample, a 1-bit quantize produces a digital output that has the third order of either 0 or 1.

Despite being straightforward and low-complexity, this quantizer performs poorly in terms of resolution and noise. A 2-bit quantize may produce the output numbers 00, 01, 10, or 11 depending on the quantity and orientation of the input signal. This can reduce the noise and distortion of the DSM and provides more precision than a 1-bit quantize. A 3-bit quantize produces 8 possible value streams (000, 001, 010, 011, 100, 101, 110, or 111) and offers even more detail than a 2-bit quantize. It may be possible to significantly improve the DSM's deformation and noise performance, but doing so would need more complexity.

Overall, which quantizes should be utilized with the DSM depend on the trade-offs between solution, noisy performance, and complexity needed for the specific application. The Delta Sigma Modulator takes inputs from the delta and sigma and averages all of the components using a 1-bit, 2-bit, & 3-bit quantize. FPLL uses a fractional division ratio to produce accurate frequency resolution. The reliability and noise efficiency of the FPLL can be enhanced by adding a 3-bit, 1-bit, 2-bit, and 3-bit quantizer 3rd degree Delta Sigma the modulator (DSM) into the feedback loop. Utilizing the delta and sigma components of the input signal, the DSM in the FPLL generates a high-resolution output that is the fractional division proportional. The delta component typically represents the difference among the reference rate & the PLL's output frequency, whereas the sigma portion is a filtered & decimated version of the phase error signal.

The DSM quantizes the delta & sigma components using a 1-bit, 2-bit, a 3-bit quantizer, depending on the FPLL's required resolution. The quantized outputs are then filtered by the DSM's delta and and sigma components to produce a high-quality digital output needed to control the PLL's fractional partition ratio.

A third order DSM used in the FPLL has a number of advantages. First, it gives the FPLL access to high-precision frequency control, enabling precise frequency resolution. Second, it improves the noise performance of the PLL by altering the quantization noise & dispersing it over a broader frequency range. Thirdly, it improves the stability of the PLL by minimizing the impacts of phase disturbances and jitter. Delta part of component compared the reference frequencies to the PLL output frequency, whereas the sigma component represents the phase error signal in its filtered and decimated form. Combining these components in the DSM yields a digital representation for the phase difference across the reference frequency & PLL output frequency. In general, the combination of an FPLL together with a 3rd order DSM and a 1-bit, 2-bit, or 3-bit quantized provides great resolution, low noise, and improved stability for frequency synthesis applications.

And while sigma includes the Fourier transformation and channel-specific filtering. The quantized delta & sigma components undergo processing through the delta & sigma elements of the DSM to provide an excellent quality digital output that is used to modify the fractional division ratio of the PLL. Using an additional order Delta-Sigma oscillator helps reduce quantization noise by improving the noise shaping effect. The performance of the PLL is improved by the higher order modulators, which reduce quantization noise over a wider frequency range. Multi-bit quantization: Multi-bit quantization reduces noise by increasing the number of bits in the quantized. By increasing resolution and reducing quantization noise, multi-bit quantizes like two-bit of three-bit quantizes can achieve this. For fractional-N PLL, a mix of software and hardware techniques is required. These methods allow for the creation of high-performance PLLs with little quantization noise. Figure 4.2 shows the Pulse Swallowing technique.

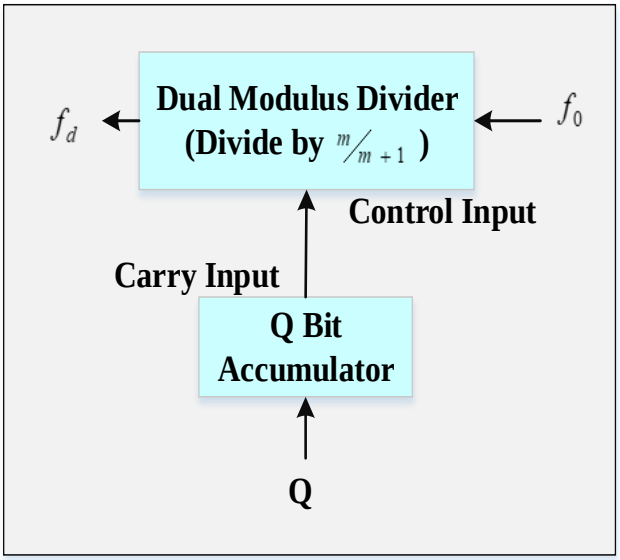

Figure 4.2 Pulse swallowing technique

The Pulse Swallowing Technique (PST) is a method used in Phase-Locked Loop (PLL) design to lessen the impact of high-frequency reference noises on the phase detector. The PST's repeated "swallowing" of a small portion of the baseline signal effectively filters out high-frequency noise and improves the phase detector's instantaneous response. For the implementation of the PST in a PLL, a pulse generator is connected to the reference input. The pulse generator produces brief, fixed-frequency pulses that are added to the reference signal. To generate an oscillation period that is a multiple times the reference frequency, the PD

analyzes its input signal to oscillator output. The frequency of the VCO is then changed using the filtered signal that results from the PD.

When a pulse generator is constantly running during the PST, a little portion of the signal used as a reference is "swallowed" or removed from its connection to the phase detector.

4.3 Result and discussion

4.3.1 Results of Fractional-NPLL

Figure 4.3 Wave form of VCO

We can see the erroneous signals that regularly emerge and lower the system's efficacy in Figure 4.3, which depicts the frequency spectra of the VCO output. . Contrary to what the term "reference spurs" suggests, these erroneous signals are not caused by the reference frequency utilized but rather by non-linearities that appear at various phases of PLL construction. The reference spurious that generates will be at multiples of the fed reference signals due to the multiplication. The offset settings are adjusted, the appropriate parameters are calculated, and the noise phase plot and spectrum of frequencies are plotted on a PLL test bench in Simulink. There are several advantages to using a 3rd degree Delta Sigma Modulators in fractional PLL. The FPLL then has the capability of high-precision frequency control, enabling accurate frequency determination. By reducing quantization noise and distributing it over a broad frequency range, it also enhances the PLL's noise performance. Third, it improves the stability

of the PLL by minimizing the impacts of phase disturbances and jitter. While the sigma element provides the phase mistake signal in its filtering & decimated form, the delta element component matches the reference frequencies to the PLL output. A computerized representation of the phase's error in the middle reference frequencies and PLL outputs frequency is produced by combining these elements in the DSM. In general, for frequency synthesis applications, an FPLL and a 3rd order DSM coupled to a 1-bit, 2-bit, or 3-bit quantized offer greater resolution, enhanced stability, and less noise. Sigma changes the PLL division ratio while providing good resolution through the application of channel-specific filtering & the Fourier transformation.

4.3.2 Results of Intensified Fractional-NPLL

The result of a DSM is a high-quality digital word with a size of 24 to 32 bits that corresponds to the PLL's fraction division ratio. With the use of this digital word, the PLL's output frequency may be precisely and consistently tuned to coincide with the selected reference frequency. By utilizing a high-resolution digital signal output derived from the DSM, which provides fine frequency resolution, the FPLL may achieve precise frequency control in frequency synthesis applications. Better noise or stability performance are also provided by the DSM and FPLL combination, which makes it a desirable choice for many applications.

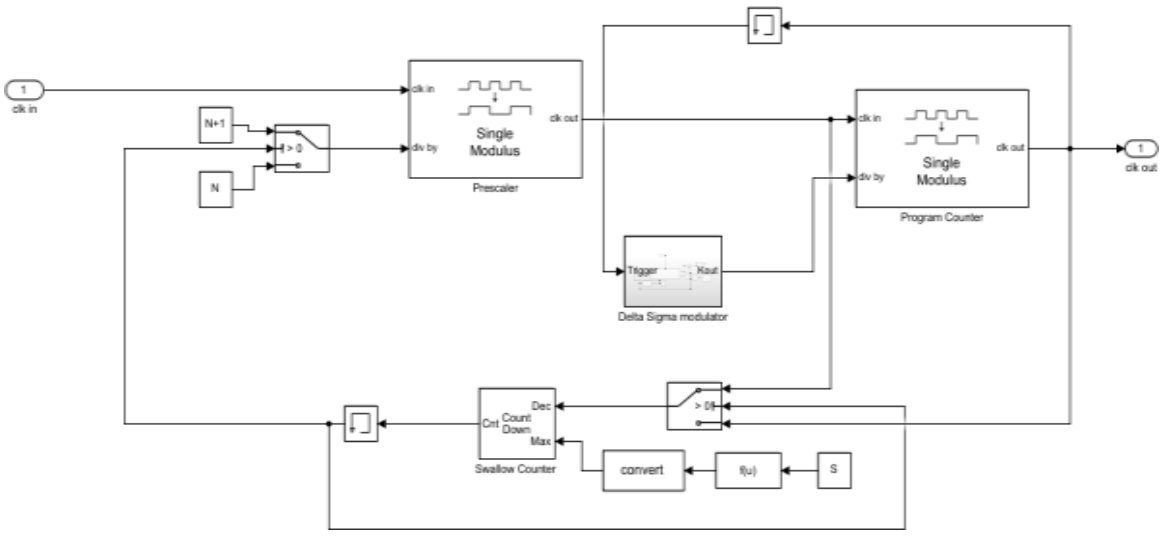

Figure 4.4 Feedback network through pulse swalloer circuit

The feedback system with a pulse swalloer circuit is depicted in Figure 4.4. The phase detector's response period is accelerated as a result, and high-frequency noise is successfully filtered out. The PST can be modified to adjust its performance for a particular PLL design by changing the pulse frequency and breadth. PLLs can operate better in noisy situations overall because to the PST approach, which is frequently employed in a variety of applications, such as communications, instrumentation, and control systems. Figure 4.5 depicts the first passage filter layout and the charging pump. Furthermore, the operation of the charge pump at different frequencies is displayed in table 4.1.

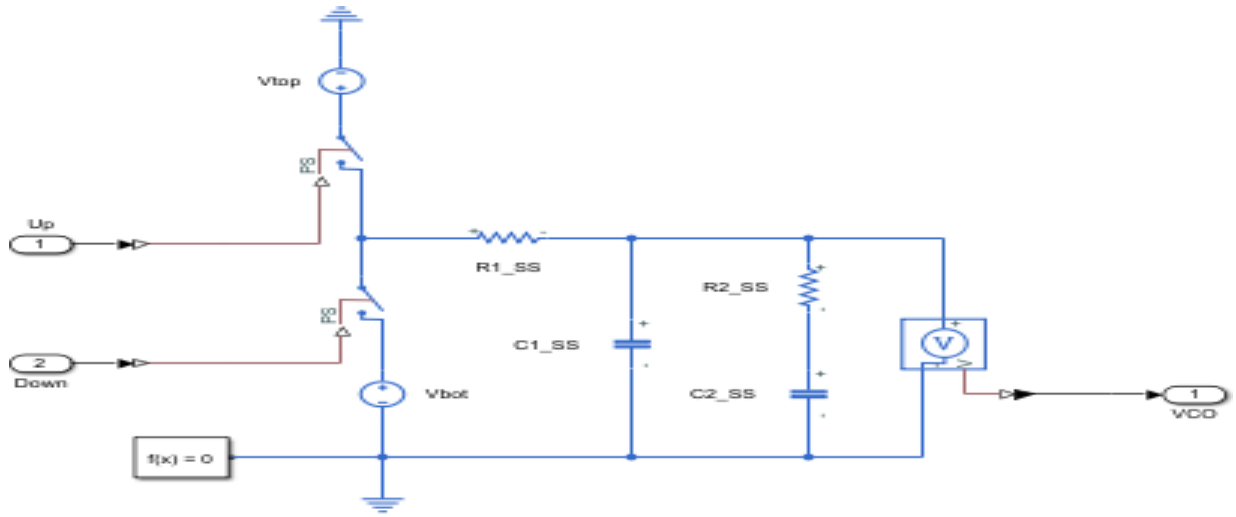

Figure 4.5 Charge Pump & low pass filter design

A charge pump is a circuit that has the ability to produce voltages that are greater or less than the input voltage. A signal can be cleaned of high frequency noise using a low pass filter circuit. The diagram represents a simple two-switch charge pump. The two switches that operate S1 and S2, are managed by the clock signal. When both S1 and S2 are open, voltage source V1 charges capacitor C1. When switching S1 and S2 are open, a charge from the capacitor C1 gets drained into the capacitor C2. In the diagram, the low passes filter is a straightforward RC filter. The charge pump's input is filtered by a low-pass rate filter consisting of the resistors R, a capacitor C2, & the capacitor C2. With the help of the charge pumps and the low passes filtering shown in the diagram, a steady voltage that may be greater or lower than the input voltage can be produced. The output voltage of the charge pump is determined by the duty cycle of the clock-generated signal & the values of the capacitors C 1 and C 2. These kinds of low pass filters and charge pumps are commonly used in phase-locked loops (PLLs). Numerous

electrical applications, including telecommunications, computing, and consumer electronics, require PLLs.

The diagram's extra details are as follows:

- The charge pump's input voltage comes from voltage source V1.
- The capacitors that are utilized to store the charge are C1 and C2.
- In order to build the low pass filter, a resistor called R is utilized.
- The switches S1 and S2 are managed by the clock signal.
- The low pass filter's output voltage serves as the charge pump's output voltage.

Table 4.1 Represent charge pump operation by different frequencies

Offs set frequencies	**Gained results of phase noise**
@20 KHz	-79.40 dB
@50 KHz	-80.00 dB
@10 KHz	-79.23 dB
@200 KHz	-75.00 dB

The phase noise across different carrier offset frequencies is shown in the table. The phase disturbances are expressed in dBc, or decibels compared to the carrier. The table demonstrates that the phase noise grows as the offset frequency drops, peaking at the lowest offset frequency of 20 kHz. Higher offset frequencies, such as 50 kHz and 200 kHz, have less phase noise as well. Understanding the phase noise performance of a specific oscillator or other signal source is made easier with the help of this table. The performance of communication systems and other applications might be impacted by phase noise, so it's critical to select a signal source with a low phase noise level. Here are some more specifics regarding the table:

- The offset the frequency is the difference between the noise frequency as well as the carrier frequency in frequency.
- Stage noise is characterized as phase noise on a single side of the carrier's frequency, or single-sideband phase noise.
- The unit of measurement for relative phase noise in relation to carrier power is dBc.

The table demonstrates that the signal source's phase noise is rather low, with values at offset frequencies of 200 kHz and higher falling below -75 dBc. For many applications, this level of phase noise is suitable.

Figure 4.6 Wave form of VCO

A VCO is a type of electronic circuit that produces periodic waves whose frequency can be adjusted by applying an external voltage. The image's waveform is a square wave. A signal known as a square wave has two separate voltage levels and alternates between them on a regular basis. The square wave in the image has a frequency of roughly 10 kHz.

VCOs are employed in numerous electronic applications, such as:

- Synthesizers: The carrier frequencies for synthesizers, which are instruments that can produce any desired frequency, are produced by VCOs.
- Phase-locked loops (PLLs): PLLs use VCOs to generate an oscillation that is synchronized with another frequency. A number of sectors, such as telecommunications, computers, and consumer electronics, use PLLs.
- Phase modulation (PM) and frequency modulation (FM) transmitters: The modulated signal is produced by VCOs in FM and PM transmitters.

The implementation of VCOs can be done using a wide range of circuit designs. The astable multivibrator is the most typical type of VCO. A circuit that oscillates in the absence of any external input is known as an astable multivibrator.

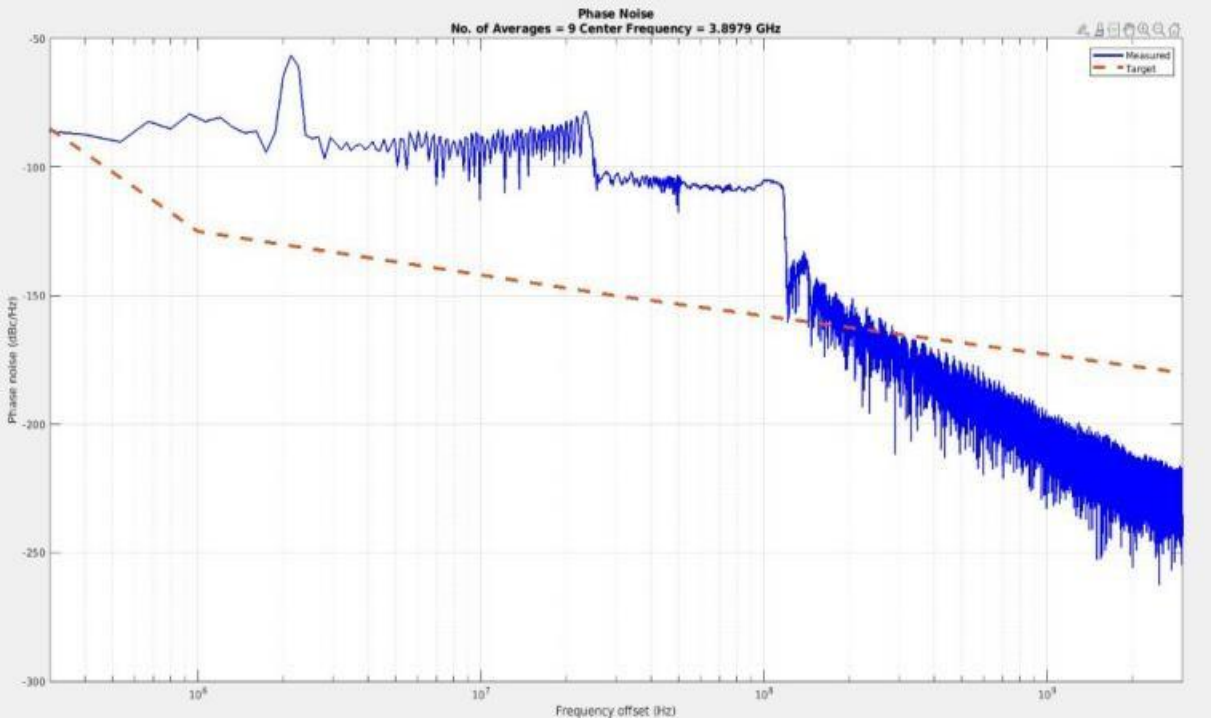

Figure 4.7 Phase Noise Plot

A signal's phase's short-term instability is measured by phase noise. It results from irrational changes in the frequency of the signal. Phase noise can be a serious issue in communication systems since it can reduce the system's performance. The PN of a signal source is shown on the graph at different offset frequency from the signal's carrier frequency. The difference among the frequency used by the carrier and the frequency of the noise is known as the offset frequency. Degrees compared to the carrier, or dBc, are used to measure phase noise. According to the graph, the phase noise increases as an offset frequency decreases and reaches its maximum at the lowest deviation frequency. This is due to the fact that random changes in the frequency of the signal, which are what generate phase noise, are more likely to occur at lower frequencies.

The graph also shows that the phase noise increases with increasing carrier frequencies. This is true because the transfer power—which is bigger for higher transfer frequencies—is used to compare the phase noise to that of the carrier power. A signal source's specific phase disturbance performance will depend on how it is designed and implemented. However, the

graph in the image is a typical illustration of a signal's source. Here have been some other facts about the graph:

- The phase noise is shown on the graph's y-axis, while the offset frequency is shown on its x-axis.
- The noise phase is stated in proportion to the transmission power and is measured in dBc.
- The graph displays a signal source's phase noise at various offset frequencies from its carrier occurrence.
- The speed of the signal being conveyed is known as the carrier frequency. The offset frequency is the frequency at which the carrier frequency and the noise frequency are separated.

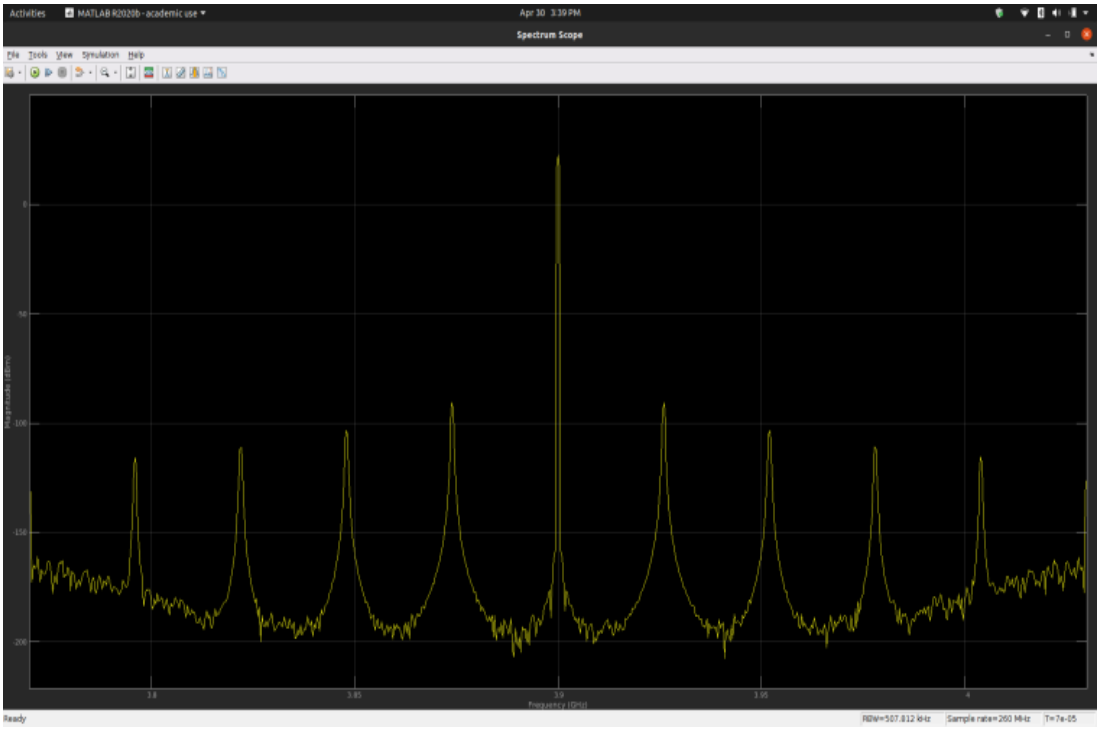

Figure 4.8 Frequency Spectrum plot of the Design

A frequency range graphic shows the magnitude of a signal at different frequencies. Plotting shows the amplitude along the y- and x-axes, respectively, as well as the frequency. The plot shows that there is a noticeable peak in the noise signal at roughly 10 kHz. Smaller peaks can be seen in the signal at various frequencies like 5 kHz and 15 kHz. The various frequencies that make up a signal can be located using the frequency spectrum depiction of the signal. Additionally, it can be used to gauge the strength of the signal at various frequencies. According to this particular frequency spectrum map, the signal is complicated and composed

of several different frequencies. The strongest frequency is about 10 kHz, however other frequencies also have some notable lesser peaks. This could be a signal coming from a communication system, like a radio transmitter, or it could be a signal coming from a musical instrument, like a guitar or piano.

4.4 Summary

The first work provided the 3rd order $\Delta - \sum$ modulator design model. Changing your approach can help with this creating a new PLL architecture that is suitable for wireless applications and has low noise. The PLL overcomes several obstacles by reducing power, taking up less space, and increasing frequency. This comparison includes a diagram that illustrates various PLL. The fundamental loop transfer function, noise sources dividers, phase detectors, and fractional-N operation are all covered in this study. A local oscillator is required to generate the clock & synchronize with both of the schedule frequency in the circuit for an additional-order delta Sigma modulator that uses a lock frequency of 3.5 GHz & an internal reference rate of 26 MHz. This modulator is designed for usage in embedded systems and wireless communication. The frequency spurs may be ignored when charting the phase noise at different offset numbers, the frequency spectrum, or unwanted spurs produced at the references because no RF transceivers that could pick up so low frequencies. The most widely used multichannel wireless transceivers in wireless communication use the frequency produced by fractional N phases locked loops to reduce spurs. Using phase-locked loops, they are generally employed as local oscillations in receiver to convert a frequency used by the carrier to a lower, wireless frequency range. They are also employed in clock synthesis, where the accuracy is poor in easier-to-build crystal resonators but fixed at high frequencies, and the frequency can be created accurately by adding a fractional-N PLL.

A resolution multielement divider (fractional) is available and utilized to reduce noise that occurs in FNPLL and is known as quantization noise. Frequencies that make up a portion of the reference can be grouped using FNPLL. It can be utilized by analog and digital PLLs. The higher frequency and wider band width it offers hasten the settling process. Quantization error noise is an additional form of noise that is introduced by the modulator that creates the divided ratio in the FNPLL. With this suggested method, noise is systematically decreased across the full frequency range. It is difficult to simulate an f-NPLL frequency synthesis. In order to create a quick simulation environment, MATLAB is used for based FNPLL frequency synthesis. In the second study, a FNPLL with a modulation is developed in order to achieve enhanced noise

reduction, a rapid simulation environment, and several approaches to reduce the phase noise in FNPLL. A third order delta Sigma transmission has been developed using a fixed bandwidth of 3.5 GHz using a benchmark reference of 26 MHz. It uses system on chips and is intended for usage in wireless communication transceivers. It can also be used in embedded system technologies. The clock must be produced and synchronized with other clock frequencies in the circuit using a local oscillator. A local oscillator must be used to create the clock and synchronize it with other clocking frequencies in the circuit. Since no RF transceivers that could pick up these low frequencies, the frequency spurs may be disregarded when displaying phase noise at various offset numbers, the spectrum of frequencies and undesirable spurs created at the references.

CHAPTER 5

FAST-SETTLING FNDPLL SYNTHESIZER

5.1 Overview

Circumstances like severe and dark weather, radar systems based on frequency-modulated continuous-wave (FMCW) transmissions can outrun optical and ultrasonic sensors. To shorten the inactivity and modulation times of the chirp signal, FMCW radar systems require rapid settling frequency synthesizer. This chapter describes a new Fast Settling Fractional-N DPLL (FS-FNDPLL) for C-Band FMCW transmitter. By including automatic controller-depended TDC switching (AC-TDCSw) strategy in FNDPLL forward loop, the suggested FS-FNDPLL provides an ultra-fast low-noise smooth chirp with narrowband. FS-FNDPLL with new background gain calibrated digital-to-time converter (BGC-DTC) as fractional divider in the feedback loop for quantization noise cancellation (QNC). When compared to the fractional-N analog PLL, FNDPLL generate chirp having a configurable chirp rate and strong linearity. The reason for this is that the FNDPLL has a changeable loop configuration that can be controlled digitally [108].

5.2 FS-FNDPLL synthesizers with AC-TDCSw scheme

To reduce settling time, the suggested FS-FNDPLL adopts an AC-TDCSw system with hybrid phase detectors and variable TDCs. Because of non-linearity of DTC in FNDPLL structure, quantization error is created, which degrades noise performance. As a result, DTC gain must be set to match input clock period. Generally, curved quantization with low-noise pass filtered using a PLL having small bandwidth. This technique, however, has limitations because to the restricted modulation bandwidth, slower settling time, and insufficient phase noise filtering. Output of TDC and a reference clock are used in existing FNDPLL to detect residual quantization noise. The calibration gain of DTC was then set using the least mean square (LMS) correlation technique. To reduce noise of quantization at the output, the proposed FS-FNDPLL leverages novel BGC-DTC as a fractional divider in the feedback channel. It negates the quantization error without the use of a reference clock, resulting in superior performance as compared to previous approaches. Implemented FS-FNDPLL determines best trade-off among bandwidth supplies.

Figure 5.1 depicts the detailed design of the suggested FS-FNDPLL synthesizers with AC-TDCSw scheme. This method analyzes various Phase Error Detector units (both linear and

nonlinear) and TDC units (Counter-oriented TDC and delay line interpolation-oriented TDC) to increase the settling response of a FNDPLL without consuming additional power. The switching between these units is done here by taking into account the extent of phase inaccuracy.

Suggested structure leverages a variable TDC to digitize phase signals. In the literature, several methods for TDC-based digitization have been presented, the bulk of which use identical successive delay components with constant propagation delays. However, due to gate delay, this approach restricts the resolution. As a result, a high-resolution digitization architecture is required to reduce quantization error. The reference clock edges between two signals can be tallied simply and cheaply using a counter. As a result, a counter is utilized as a coarse TDC. Furthermore, the interval among signal and the following/preceding reference clock edge can be digitized using an interpolator to obtain sub-clock period resolution. As a result, the Fine TDC is a TDC that utilizes delay line interpolation. To compensate for measurement errors, the suggested delay line interpolation-based TDC employs internal averaging.

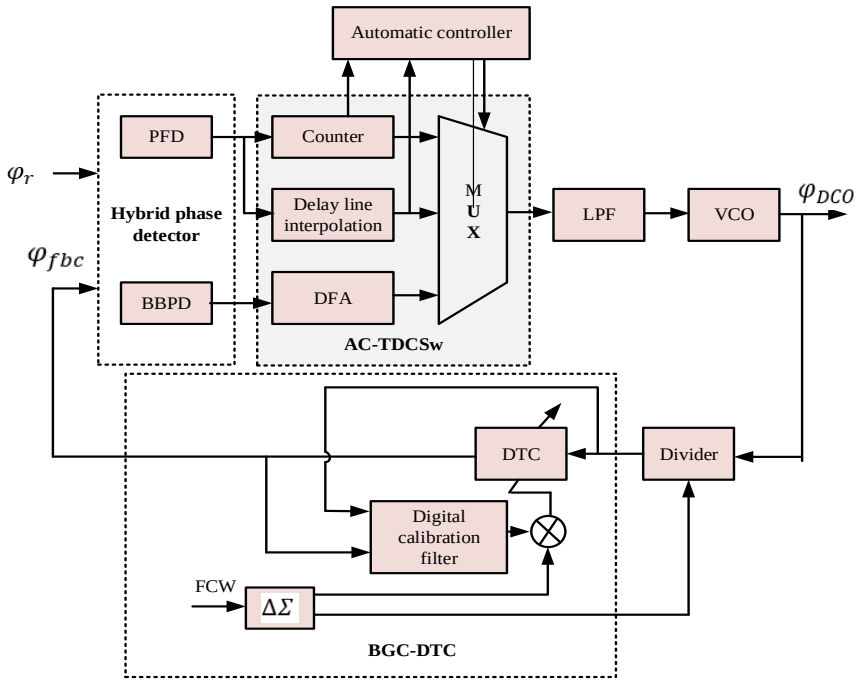

Figure 5.1: Architecture of the proposed FS-FNDPLL synthesizer

Automatic controller employed to monitor the outcomes of both the Counter-oriented TDC and the delay line interpolation-oriented TDC in order to estimate phase inaccuracy while nonlinear PED is on. In addition, the gain of the loop filter is modified on the basis of Phase Error

Detector and TDC units specified. This automatic adjustment and switching approach improves the loop filter bandwidth based on phase faults, allowing for faster fault tracking while reducing phase noise and spurs.

5.2.1 Counter and delay line interpolation-based TDC

Suggested variable TDC employs Counter in conjunction with interpolators to digitize phase signals. Counter calculates duration of a known frequency reference clock among two signals. The timing difference among the signals and the neighboring reference clock edges is determined by the interpolators. The variable TDC combines output of Counter T_a and interpolator O_{srt}, O_{stp} to produce output $T_{\upsilon TDC}$ as given below;

$$T_{\upsilon TDC} = T_a \times t_p + (O_{srt} - O_{stp}) \times t_{dpd} \tag{5.1}$$

Where, t_p indicate reference clock's time cycle and t_{dpd} indicate propagation delay of the delay components. Figure 3 illustrates the architecture of the suggested variable TDC.

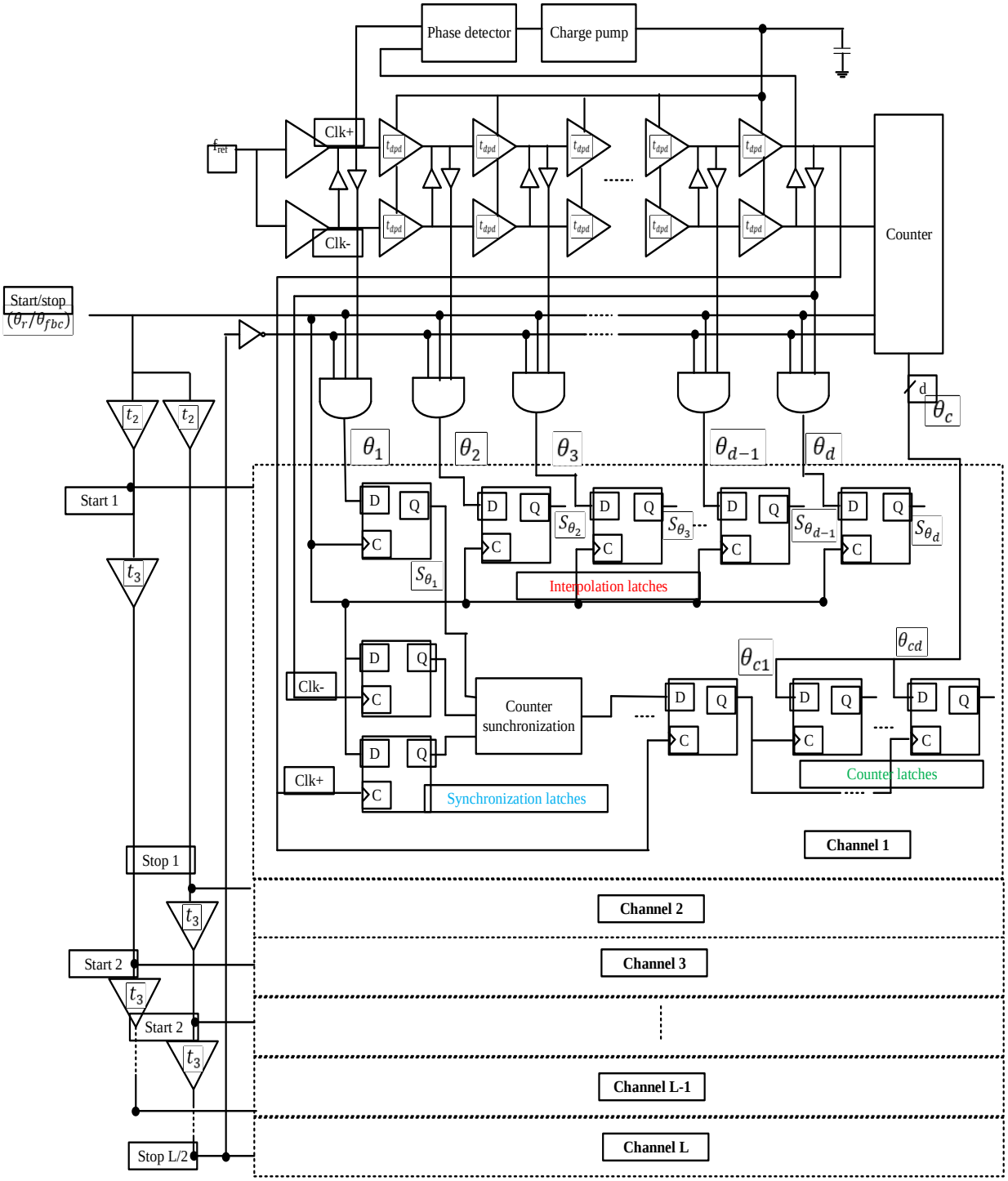

Figure 5.2: Structure of proposed variable TDC

Reference clock signal is propagated through delay lines, and rising edges of reference signal generate time samples $\theta_1, \theta_2, ...\theta_d$ to interpolators. Reference signal's edge enters delay line's input port, while earlier edge exits the chain. These two signals are detected by a phase detector, which controls a charge pump to change delay line control voltage V_a. This adjustment takes place up to the signals at start and end of delay line $C_{lk}+$ are synchronized. Hence, the delay

line is stabilized in contrary to PVT changes. In Figure 5.2, delay components contain two parallel delay-adaptable inverters, and their outputs are connected with shorter inverters functioning in the opposite direction. This arrangement is utilized to provide high resolution for the interpolators. The differential reference signal's passage through opposite phases parallel inverters increases nonlinearity of a single-ended configuration.

The delay line delay is locked to reference clock cycle time t_p in this case to force resolution of interpolation t_{dpd} to a recognized fraction of t_p . Among the input signals, a counter counts the amount of full reference clock cycles. However, synchronization among the counter output and the interpolator output is required.

While computing interval among the same signals multiple times, output of variable TDC T_{vTDC} changes throughout the average value. As a result, the interval among the same signals is measured R times in order to get the mean value T^m_{vTDC} . Because the differences between the mean outputs are lower, the averaging method improves measurement precision. In this case, on-chip averaging is assumed to replace the sequential measurements made utilizing several parallel measurement channels. This method was designed to reduce interpolation error by sampling independent errors numerous times.

Whole channels in this case use the same delay line and Counter. The counter and interpolators generate θ_a and time phases, $\theta_1, \theta_2, ...\theta_d$, respectively. These time phases are linked to a series of L parallel and indistinguishable measurement channels (interpolation latches). The start as well as stop signals enable the latches' clock inputs for storing the status of the delay line as it arrives at them, and latches provide interpolated results.

To reduce power consumption, AND-gates are employed between the channels and interruption line. Rising edge of the start signal comes, d bit Counter begins to count. AND gates deliver the interpolation stages to the measurement latches at the same time. Input start and stop signals are delayed by t_2 to settle the interpolation phases at the latches' inputs. . When the final channel latches the delay line status, the Counter stops ticking and the interpolation phases return to zero. On-chip averaging is achieved here by providing $L/2$ samples of the interval among the single start as well as stop input pair. If the start signal is received, half of the channels, $L/2$, are used to store the timing core's status, while the other

half is used for the stop signal. When all $L/2$ channels concurrently register the timing status, the precision is not improved by the averaging procedure. As a result, the channels are separated by a buffer with a delay of t_3.

5.2.1.1 AC-TDCSw scheme

Phase error status is employed in this study to permit switching between various phase error detectors and TDC units. AC-TDCSw scheme is used as a controller in FS-FNDPLL system to activate a pair of phase detectors and TDC units in the loop until the equivalent TDC output is zero. Switching rule of AC-TDCSw scheme for demonstrating the active subsystem in FS-FNDPLL is depicted in Figure 5.3. If the phase error ψ_e value is very high, the AC-TDCSw scheme engages the PFD and counters as a phase detector and coarse TDC. Figure 5.2 shows how a multiplexer is utilized to ensure that the loop filter's input is acquired from coarse TDC result. The loop filter receives a zero input if the phase error is less than quantization step of the active TDC.

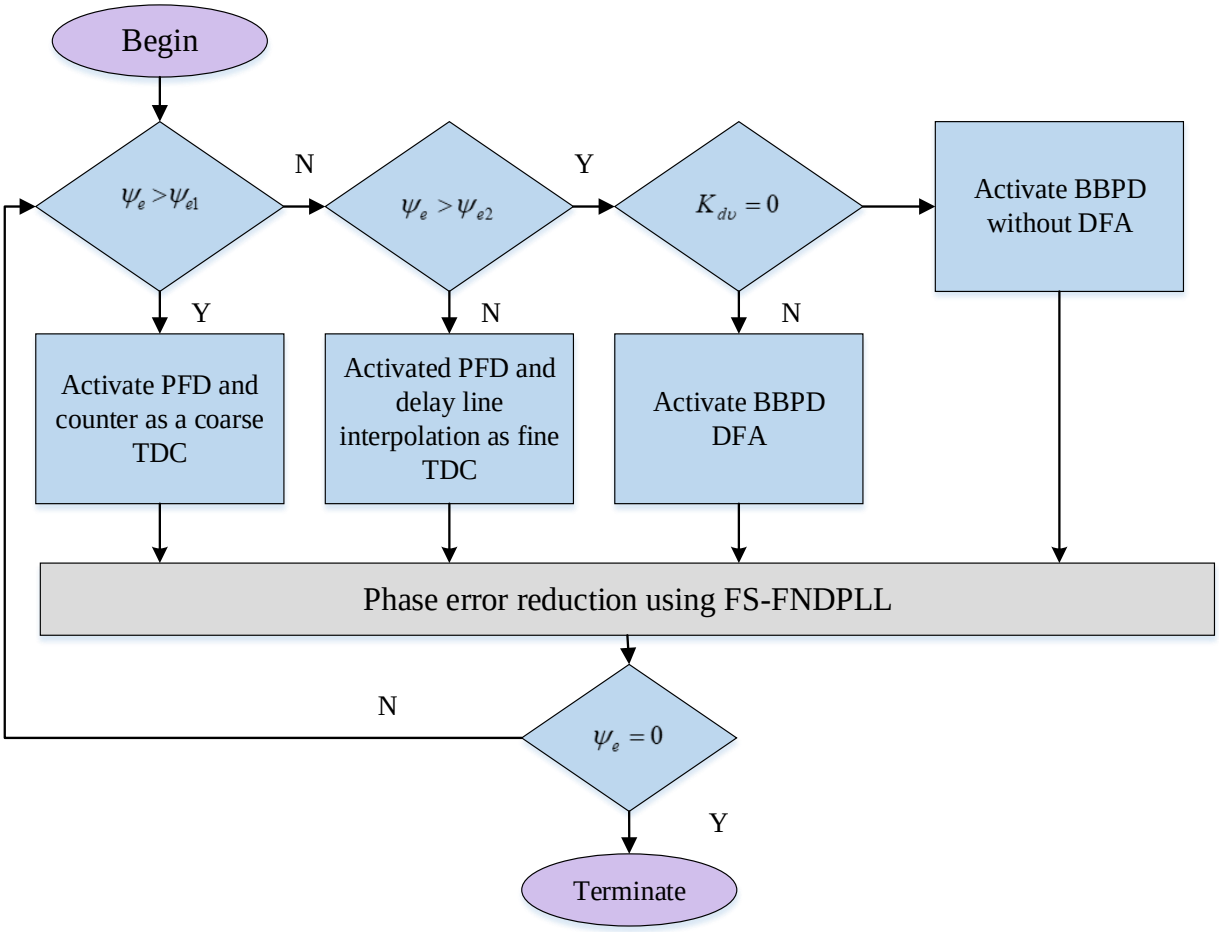

Figure 5.3: Switching rule of AC-TDCSw scheme

If the phase error value was less than threshold with regard to single VCO clock period ψ_{e1}, the AC-TDCSw method activates delay line interpolation-based TDC as a fine TDC. Alternatively, the AC-TDCSw approach activates BBPD if the phase error is less than delay value of single inverter ψ_{e2}, hence removing result jitter's dependence on the TDC resolution. The automatic controller monitors the results of the Counter and a delay line interpolation-based TDC to assess the magnitude of the phase inaccuracy. TDC findings from the current clock cycle are utilized to determine TDC activation and filter gain in the next clock cycle. The AC-TDCSw method begins by activating BBPD with a Deterministic Finite Automata (DFA) to progress the settling response. In the loop, this DFA simulates an additional integral as well as derivative controller. Derivative controller's gain recognizes the state for eliminating the DFA from loop. In the settled state, this method is utilized to avoid gossiping.

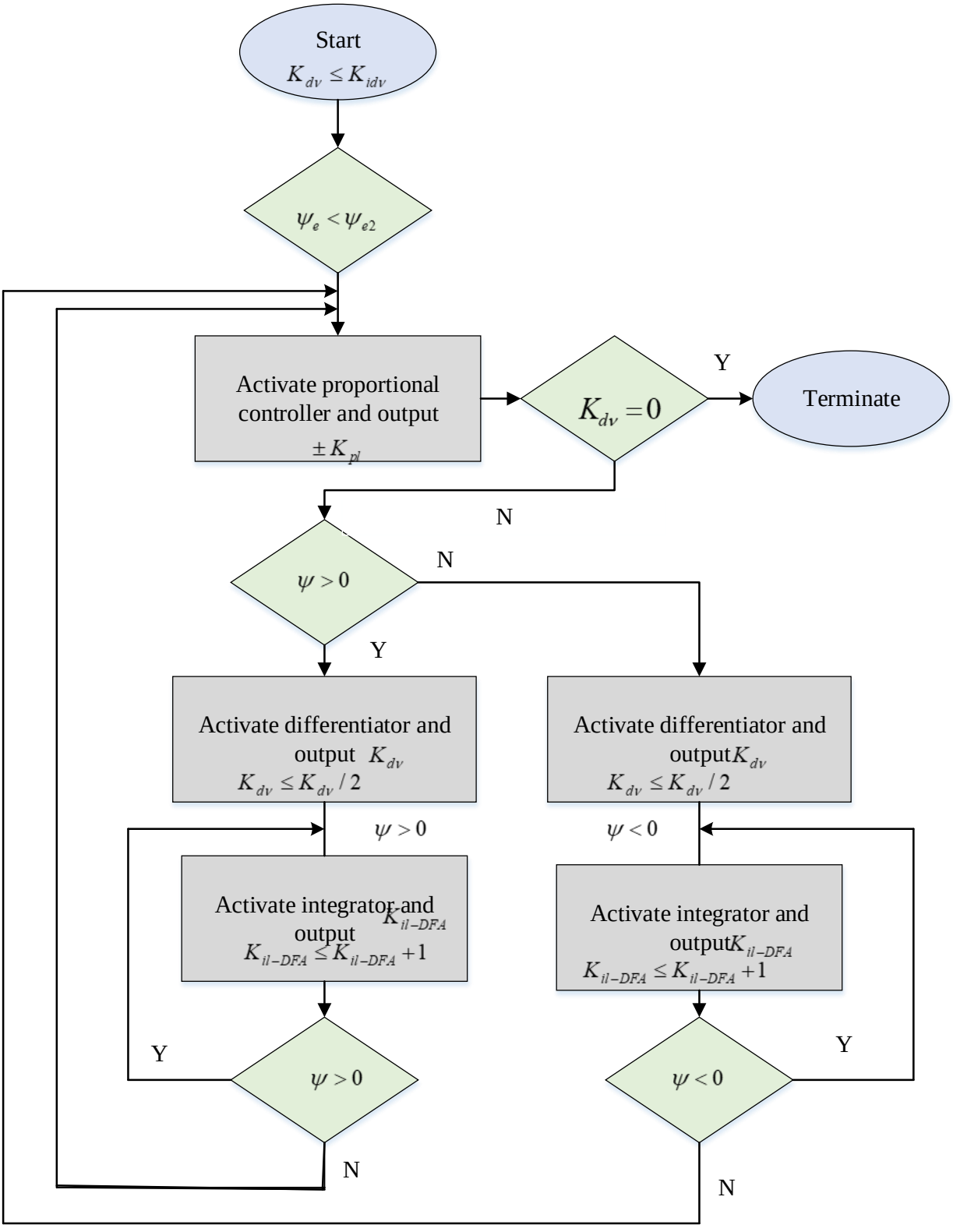

Figure 5.4: Process flow of DFA algorithm activated with a BBPD mode

The DFA in this case uses time-division multiplexer to add an extra proportional, integral, and derivative controller to system. The derivative as well as proportional gain are employed using a shift register. Simultaneously, an extra accumulator in the forward channel can be added to implement the integrator. DFA provides a high initial derivative gain K_{idv} to counteract the phase-error sign reversal when BBPD is enabled. The value of K_{idv} must be as high as possible for reducing phase error below the inverter delay ψ_{e2} as shown below:

$$K_{idv} = \frac{\nabla fr_{VCO}}{K_{VCO}} \tag{5.2}$$

Where, $\nabla fr_{VCO} \propto \nabla fr^2{}_{VCO} \frac{\psi_{e2}}{Z_{div}}$, fr_{DCO} indicate output frequency and Z_{div} indicate feedback division factor of FS-FNDPLL. When the BBPD states the same sign for the phase error in the successive cycles, the DFA enables integrator (K_{il-AC}) in loop for tracking frequency quickly until it reverses the phase error sign. Hence, gain of the integrator (K_{il-AC}) is maintained with the smallest value of "one". The K_{idv} reduced based on every sign reversal of the phase error, indicating the ongoing settling process in the loop. If the derivative gain reaches zero, the AC-TDCSw scheme removes DFA for avoiding the high peak during a settled state. Hence, phase and frequency errors are corrected quickly using the derivative and integral states of DFA.

The AC-TDCSw scheme used to switch the loop among different phase-detection and TDC models and to change the proportional (K_{Pl}) and integral (K_{il}) gain of loop filter at time of the settling process. If the AC-TDCSw scheme activates PFD, then the loop filter's proportional (K_{Pl}) and integral (K_{il}) gain can be calculated using the following formula [109]:

$$K_{pl} = \frac{Z_{div}}{K_{PFD}.K_{VCO}} \times \frac{\beta g}{\sqrt{1+\tan^{-2}(phZ)}} (1 - \frac{T_r}{2}.\beta M) \tag{5.3}$$

$$K_{il} = T_r . \frac{Z_{div}}{K_{PFD}.K_{VCO}} \times \frac{\beta^2 g}{\sqrt{1+\tan^{2}(phZ)}} \tag{5.4}$$

Where T_r represents period of reference clock, Z_{div} indicates divider on feedback and K_{VCO} denotes the gain of VCO. Also, the unity-gain bandwidth and the loop's phase margin are

denoteDd as $\beta_g$and PhM respectively. Similarly, if the AC-TDCSw scheme activates BBPD, the proportional gain (K_{Pl}) and integral gain ($K_{il}0$) are computed as;

$$K_{il} \leq \frac{\beta_u T_r K_{pl}}{\tan(\beta_u T_r L_D + phz)} \tag{5.5}$$

Where $L_D$represents the delay of the loop.

5.2.1.2 Background gain calibrated digital-to-time converter (BGC-DTC)

BGC-DTC is used in feedback path of the FS-FNPLL to efficiently cancel quantization noise. However, non-linearity in DTC is caused by misalignment between delay cells and routing pathways, which impairs phase noise performance of FS-FNDPLL. In this paper, a novel Background gain calibration (BGC) approach is developed to address nonlinearity difficulties. The existing ways set the calibration factor of DTC utilizing a least mean square (LMS) correlation algorithm. Proposed method, on the other hand, computes the residual quantization noise without the use of a reference clock.

A DTC is typically built with phase interpolator (PI) or a digitally controlled delay line (DCDL). Because of their weak linearity, PI-based designs are constrained. As a result, they required expensive digital calibration circuitry to correct the PI non-linearity, using a huge area and power. Alternatively, fine resolution can be accomplished using DCDL-based DTC, however the gain of this design is not properly specified. A DCDL-based DTC is employed in the proposed FS-FNDPLL structure due to its scaling-friendly properties. In addition, a background calibration is provided to properly calibrate DTC gain.

The suggested BGC scheme in the FS-FNDPLL structure is depicted in Figure 5.5. On this case, the VCO output on feedback path is divided utilizing a fractional divider. To save electricity, here divider have a multi-modulus divider (MMD) and D flip flops (DFFs). Then, for expressing the DTC range, a DCDL-based DTC is constructed with a BGC scheme that includes a digital calibration filter. This range is scaled by $\Delta\Sigma$ error signal ε_q to act as the calibrated gain of DTC $K_{gcf}.\varepsilon_q$ The foreground DTC gain calibration approach is vulnerable to PVT variations.

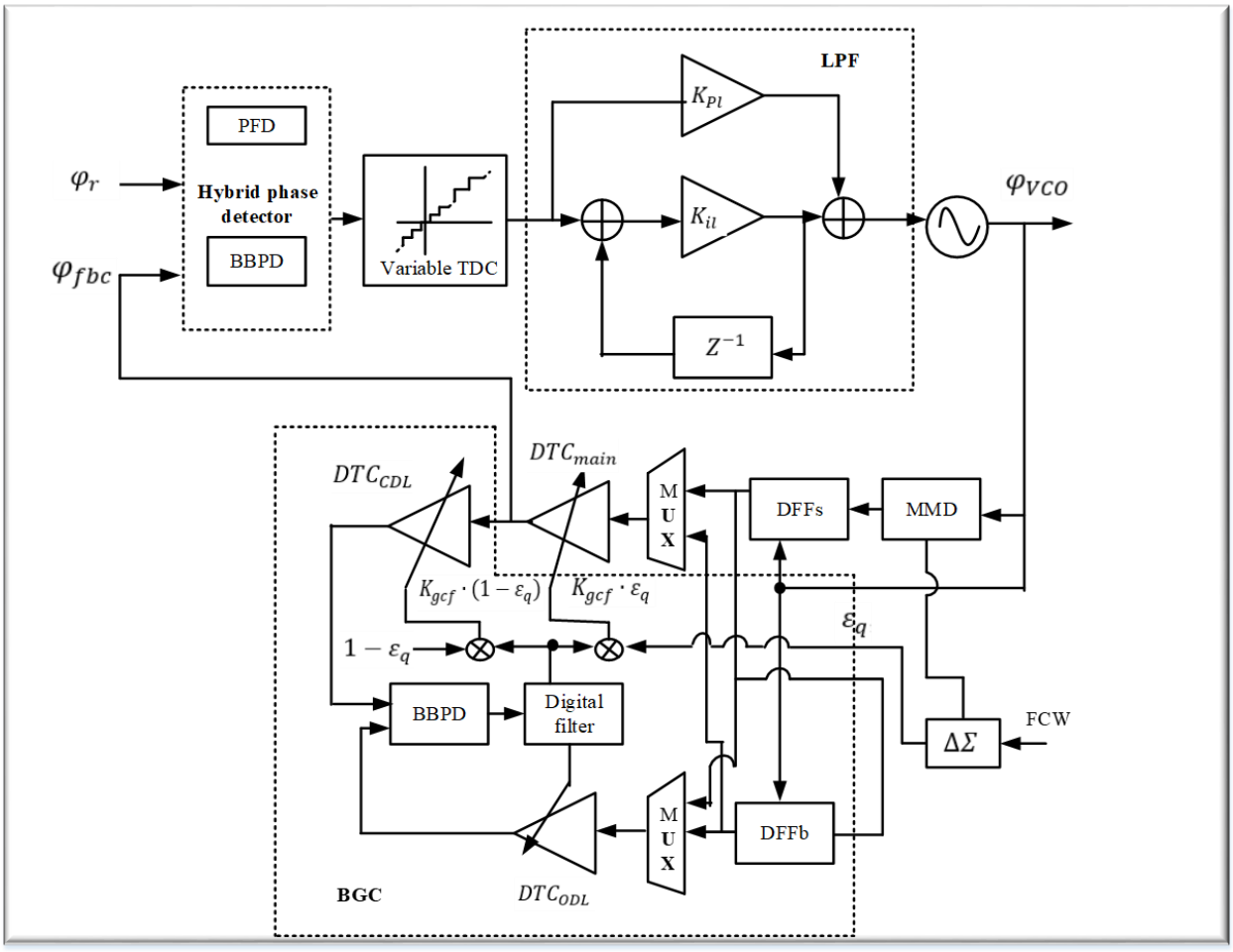

Figure 5.5: Architecture of FS-FNDPLL with BGC-DTC

Standardization must be done in the background utilizing complementary delay line, DTC_{CDL} in the feedback path. Here delay control words $DCW_{main} = K_{gcf} \times \varepsilon_q$ and $DCW_{main} = K_{gcf} \times (1-\varepsilon_q)$ are used to control DTC_{main} and DTC_{CDL} respectively. This locked loop equalizes addition of DTC_{main} and DTC_{CDL} delays to τ_{in} as given below;

$$T_{in} = \varepsilon_q . \tau_{DTC,main} + K_{gcf} . (1-\varepsilon_q) . T_{DTC,CDl} \tag{5.6}$$

Where $\tau_{DTC,main}$ and $\tau_{DTC,main} = T_{DTC,CDl}$ denotes full-scale delays of DTC_{main} and DTC_{CDL}, respectively. Here, the DTC $\tau_{DTC,main} = T_{DTC,CDl}$ are matched to reduce the sensitiveness of the gain calibration factor K_{gcf} to PVT changes. As a result of this,

$$K_{gcf} . \tau_{DTC,main} = \tau_{in} \tag{5.7}$$

DTC results least nonzero DTC delay, τ_{min} for a zero-input code, and this delay has appeared as an offset that worsens the calibration accuracy. Overcome this issue, reference time path uses an offset delay line, DTC_{ODL} to introduce an equal delay so that the delay of DTC_{main} and DTC_{CDL} are cancelled. Initially, the offset calibration step bypasses DFF_b utilizing a multiplexor MUX_{BG} and set $K_{gcf} = 0$. As a result of this, DTC_{main} and DTC_{CDL} receive zero input. When the loop is locked, the offset delays of DTC_{main} and DTC_{CDL} are matched by the DTC_{ODL} delay along with the offset of any input-referred BBPD. The current drained from DTC_{main} varies depending on its input code DCW_{main}. Because of the presence of DTC_{CDL}, the total current drained from the DTC is independent of the input code. This configuration is utilized to improve linearity and reduce deterministic jitter.

5.3. Results And Discussion

The suggested FS-FNDPLL, variable TDC, and BGC-DTC are realized in Cadence Virtuoso tool utilizing CMOS 45-nm technology. A 100 MHz reference clock is generated using an off-chip crystal oscillator and fed into the synthesizer.

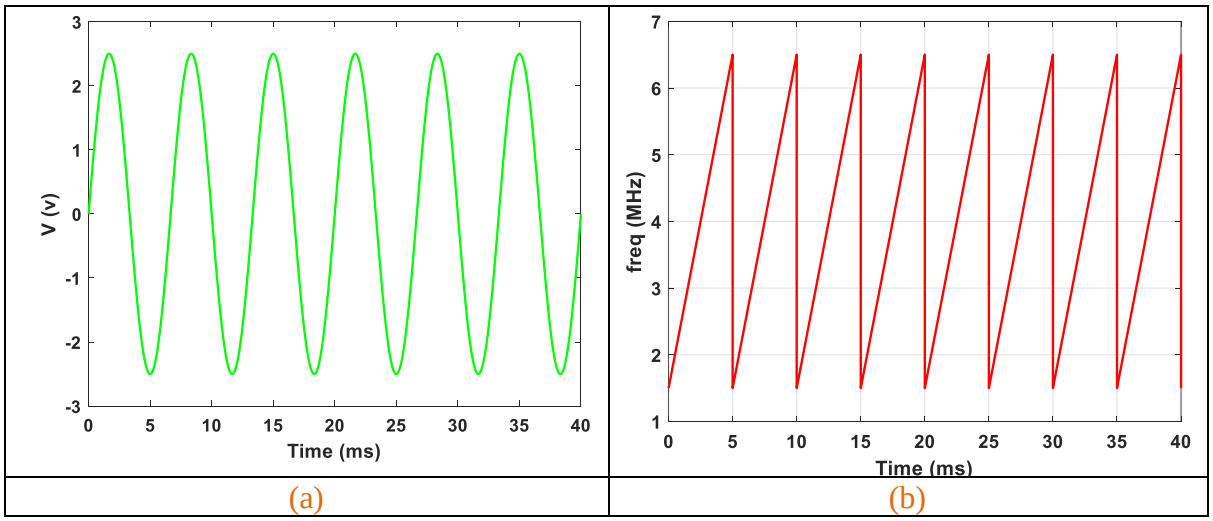

Figure 5.6 : (a) Input sinsoidal signal of 100MHz and (b) time-frequency plot of input signal for FS-FNDPLL

This part begins by evaluating the spectrum in order to characterize the created synthetic bandwidth chirp. Figure 5.6 displays a flat depiction of the spectrum at the relevant frequencies. The C-band FMCW chirp produces a 2-GHz chirp signal and covers the frequency span from 6 to 8 GHz. Output power is calculated to be 9 dBm. Figure 5.7 shows output spectrum of the FS-FNDPLL.

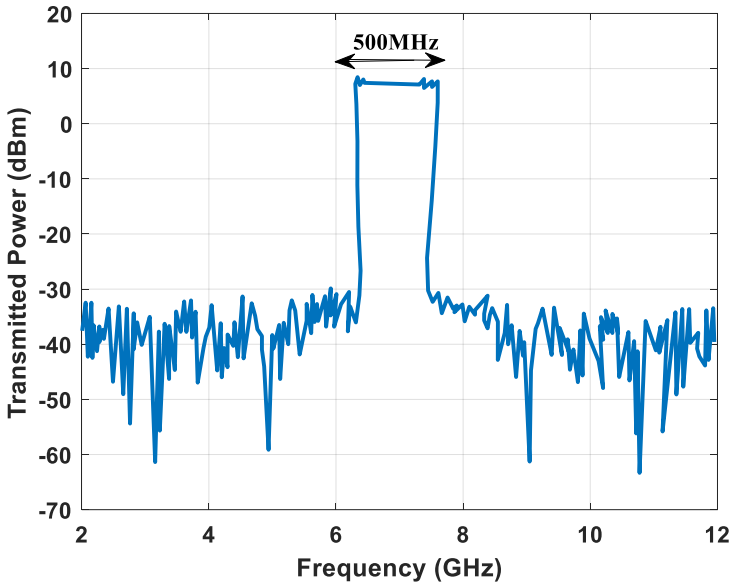

Figure 5.7: Transmitted output power

5.3.1 Evaluation of FS-FNDPLL

The FS-FNDPLL is crucial in implemented FMCW radar systems because of its capacity to decrease the inactive time as well as modulation duration of the chirp signal. The planned FS-FNDPLL uses a 100-MHz reference clock.

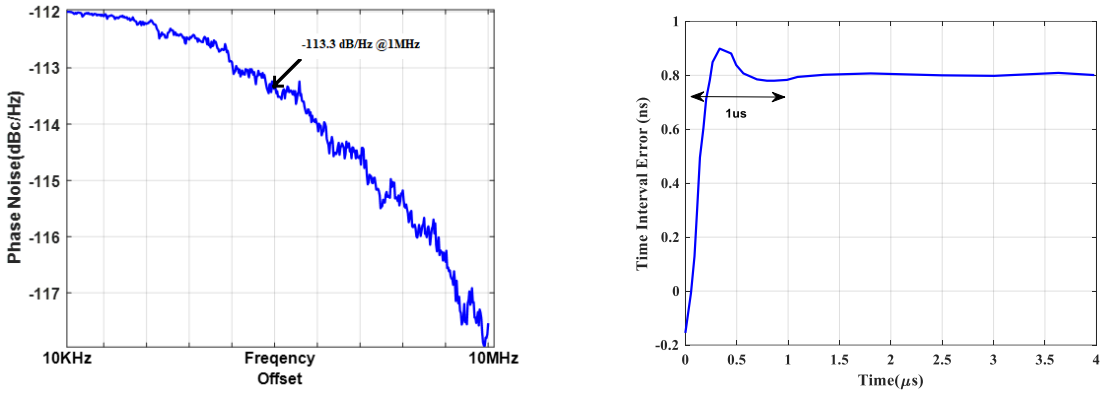

(a) (b)

Figure 5.8: Evaluation of FS-FNDPLL (a) phase noise (b) settling time

Figure 5.8 (a) illustrate that FS-FNDPLL reduces phase noise to 113 dBc/Hz at 1MHz. Furthermore, as presented in Figure 5. 8 (b), the proposed FS-FNDPLL shifts from stop frequency to the start frequency at the conclusion of every narrowband chirp period with a 1 μs settling time. This settling time is less than 1% of the chirp period. The phase detectors and

TDC in the proposed FS-FNDPLL are swapped automatically utilizing the AC-TDCSw technique to provide a short PLL settling period.

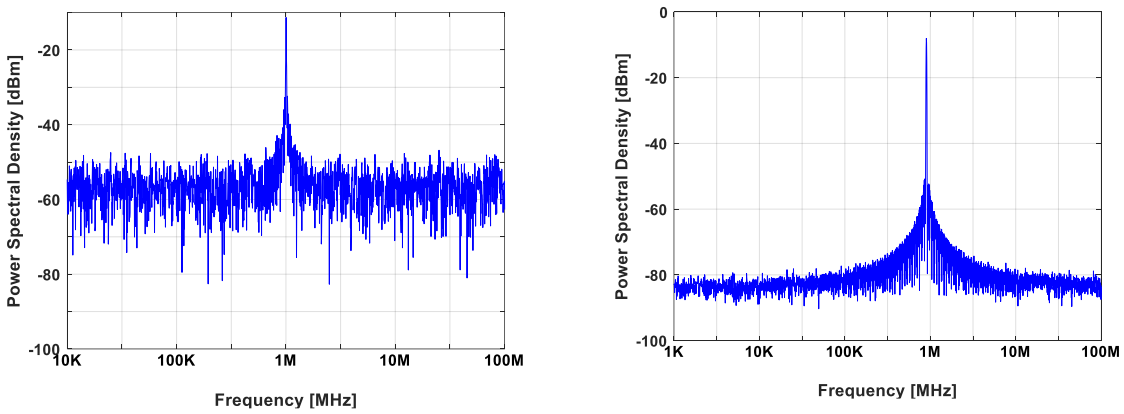

(a) (b)

Figure 5.9: Output spectrum of FS-FNDPLL (a) without BGC in DTC (b) with BGC in DTC

Figure 5.9 depicts measured spectrum of the FS-FNDPLL output in the DTC with and without background calibration. Figure 5.9 (a) depicts presence of spurious tones at fractional frequency multiples in the absence of background calibration in the DTC. DTC non-linearities typically degrade the FNPLL's output jitter performance. To increase DTC linearity, the sinusoidal fluctuations caused by spur generation at multiples of the fractional frequency offset should be decreased. As shown in Figure 5.9 (b), the suggested design includes a new background calibration mechanism to reduce periodic changes. This method is also utilized to improve the FS-FNDPLL's integrated jitter performance.

Table 5.1 compares the proposed system’s output FS-FNDPLL to that of other current FNDPLLs. The settling time is highlighted here to demonstrate the effectiveness of AC-TDCSw and BGC-DTC in the feed forward and feedback loops of FS-FNDPLL for minimizing lock time when compared to other structures. The proposed structure has a jitter performance of 0.47 ps. It also obtained a 4-dB greater FOM than Elkholy et al.'s [110] PLL design. Furthermore, the suggested FS-FNDPLL architecture employs BGC-DTC, which aids in achieving the highest linearity while consuming the least amount of power.

Table 5.1: Comparison table of the state-of-the-art FNDPLL

Specifications	Elkholy et al. [110]	Chen et al. [113]	Liu et al. [114]	Liu et al. [115]	Proposed	Proposed
Technology (nm)	65	65	65	65	45	65
Power (mW)	3.7	0.53	0.98	0.27	0.13	0.19
Integrated Jitter (ps_{rms})	0.55	0.87	0.53	12	0.47	0.50
Area (mm^2)	0.22	0.42	0.23	0.12	0.098	0.112
FOM (dB)	-293.4	-244	-246	-215	-297	-295
Phase noise (dBc/Hz)	-108	-95.6	-108	-105	-113	-110
Setting time (μs)	**38**	**-**	**16**	**8**	**1**	**2**

5.4 Summary

In dark and severe weather circumstances, radar systems based on frequency-modulated continuous-wave (FMCW) transmissions can outrun optical and ultrasonic sensors. To shorten the inactivity and modulation times of the chirp signal, FMCW radar systems need a rapid settling frequency synthesizer. This chapter describes a new Fast Settling Fractional-N DPLL (FS-FNDPLL). According to the suggested rsearch, FS-FNDPLL provides an ultra-fast low-noise smooth narrowband chirp by presenting an AC-TDCSw technique in the FNDPLL forward loop. Furthermore, the suggested FS-FNDPLL makes use of a new BGC-DTC as a fractional divider in feedback loop for QNC. Suggested transmitter up converts a 500-MHz narrowband chirp signal onto four adjacent carriers to produce a 2-GHz C-band chirp. According to simulation results, the suggested FMCW Transmitter consumes 79 mW of power. Additionally, suggested FS-FNDPLL has a phase noise of 113 dBc/Hz at 1-MHz. With the introduced AC-TDCSw system, this model FS-FNDPLL reduces settling time to μs 1 s.

CHAPTER 6

FMCW TRANSMITTER WITH THE UTILIZATION OF R-PILO TO PRODUCE FAST SWITCHING ADJACENT CARRIERS

6.1 Overview

Existing synthetic bandwidth-based FMCW SAR Transmitter is extremely complex due to many PLLs, RF switches of high-speed, and filter banks. Imaging radar, as opposed to traditional traffic detection radar, can offer more detailed target information to traffic management systems. FFT imaging method design for radar roadside imaging in urban traffic settings, allowing for the simultaneous imaging of static and dynamic goals [111]. For the vast range of applications, high-resolution photographs are required. SAR (synthetic aperture radar) acquires images at night and in bad weather using photographic and other optical image sensors. FMCW has recently become popular as a pulsed waveform for SAR to increase transmit power and sensing radius [112]. Furthermore, variable rate of chirp is necessary for optimize the range and Doppler resolution to satisfy requirements of varied applications. Various ways can used to generate the FMCW signal. One of the simplest approaches is to regulate a voltage-controlled oscillator (VCO) using a saw-tooth or triangular voltage waveform to generate a frequency chirp. Though, this method suffers from non-linearity in open-loop operation.

6.2 Proposed C-BAND FMCW SAR Transmitter

Radars (FMCW) use saw-tooth waveform for generating modulated CW (continuous-wave) signal, which is commonly referred to as a Chirp. Before transmission, the produced chirp signals are amplified. At the receiver side, signal is amplified, filtered then converted to zero-IF utilizing mixers and sent signal. Figure 6.1 depicts the planned FMCW transmitter's construction. An autonomous controller-based FS-FNDPLL, a ring-based pulse injection locking oscillator (R-PILO), a single sideband (SSB) mixer, a saturated driver-amplifier-power-amplifier (DA-PA), a bandpass filter (BPF), and a programmable gain amplifier (PGA) are all part of this architecture. Due to their ability to minimize the chirp signal's inactive period and modulation time, quick settling frequency synthesizers are required for FMCW radar systems. To shorten settling time in FS-FNDPLL synthesizers, a novel AC-TDCSw scheme is introduced here. A narrowband chirp is produced by this FS-FNDPLL with AC-TDCSw scheme.

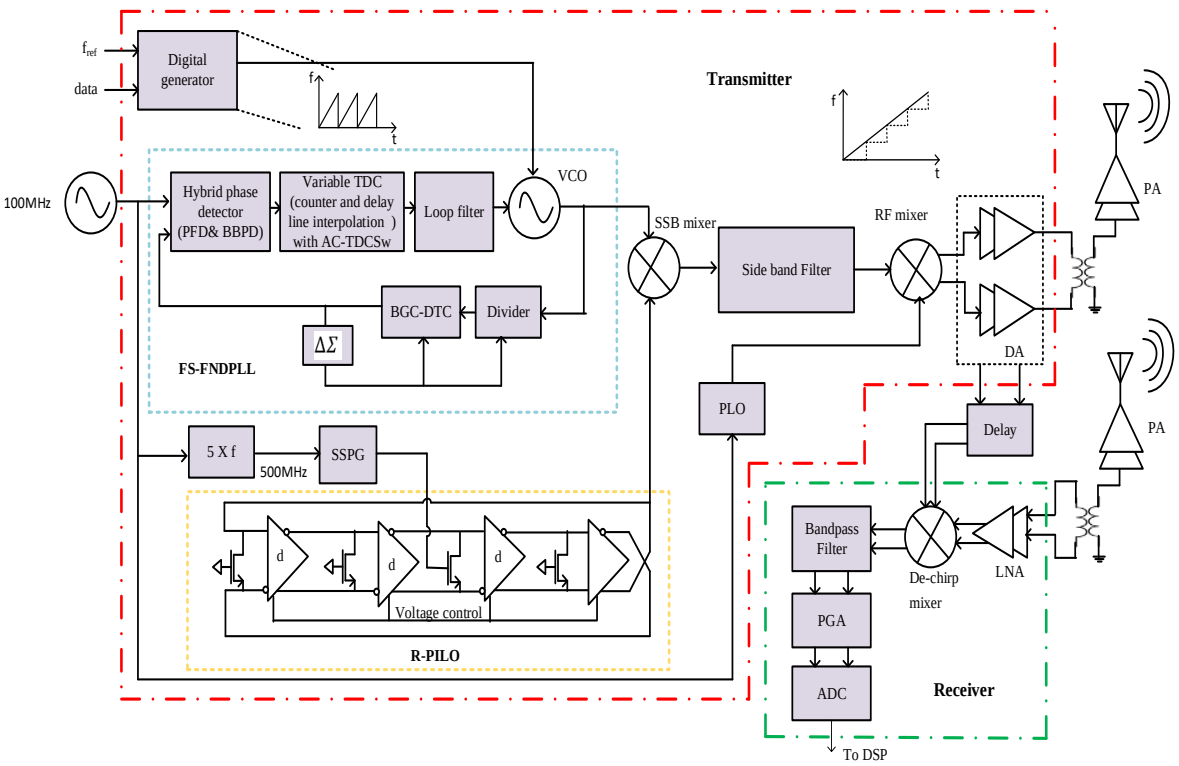

Figure 6.1: Diagram of the proposed FMCW transmitter

R-PILO incorporates spur suppressing pulse generator to eliminate unwanted harmonics before injecting the pulse into oscillator. This R-PILO takes up less space, improves power efficiency, and is immune to crosstalk. Outputs of FS-FNDPLL and R-PILO are then mixed by the SSB mixer to produce a wideband chirp. When Ka-band criterion is met, the resulting chirps can be up-converted using a local oscillator of high-frequency, as shown in Figure 6.1. Finally, suggested FMCW Transmitter employs saturated DA-PA (driver-amplifier-power-amplifier) to reduce the ripples in broadcast chirp.

6.2.2 Ring-based pulse injection locking oscillator (R-PILO)

Suggested FMCW transmitter employed R-PILO to achieve wideband chirp while maintaining energy economy and phase noise performance. Figure 6.1 depicts the R-PILO architecture, which includes a four-stage VCO and a pulse generator. This R-PILO incorporates a spur suppressing pulse generator (SSPG) to reduce unwanted harmonics before delivering pulse into the oscillator. Injection signal from the SSPG is received by the oscillator here. Figure 6.2 (a) depicts the fundamental ideas of pulse generation.

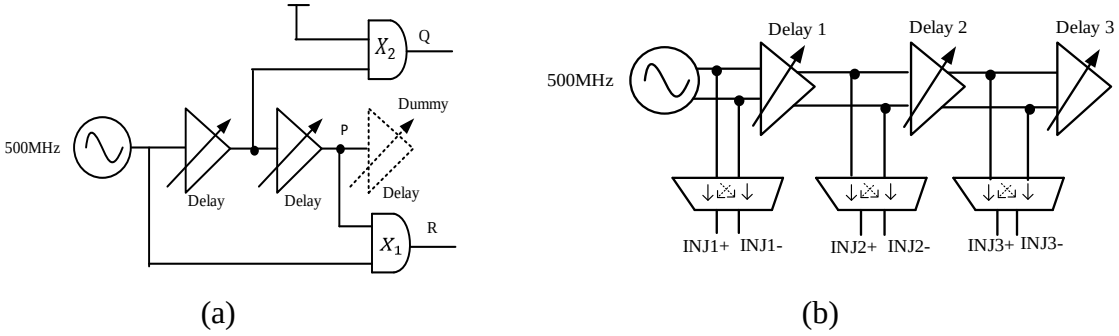

(a) (b)

Figure 6.2: Injection pulse generator (a) conceptional diagram for pulse generator (b) SSPG

After delaying by $2\times delay(p)$, an AND gate is used among the input references to generate a narrow pulse (R) with $2p = 2p/2 - 2d$, where T specifies the pulse's period. The pulse width can be adjusted by changing the delay value. In this case, a broader pulse (Q) is created by delaying the input reference by (1delay). The two pulses are aligned when the delay cells are matched. A fake delay cell is included in this case to ensure equal load for all cells and proper matching among delay cells. In addition, X_2 used to replicate the delay associated with X_1 and to avoid delay mismatches. Figure 6.2 (b) displays the precise design of the SSCG. The delay line is generated here by delay $-delay_3$. In this case, a pseudo-differential operation is used to suppress the even harmonics while using less power. It performed band hopping by switching between two separate control words using a multiplexer. The selected input of the multiplexer unit is saved on-chip to ensure a short rise/fall time and to limit its influence on frequency hop time. . In this case, resulting signals $INJ_1, INJ_2 \; and \; INJ_3$ should be added or subtracted to reduce the neighboring harmonics. This injection pulse is fed into one of the R-PILO structure's transistors through differential to single-ended converter. To avoid unsettling injection, the remaining transistors are grounded, as indicated in Figure 6.1.

6.3 Result and discussion

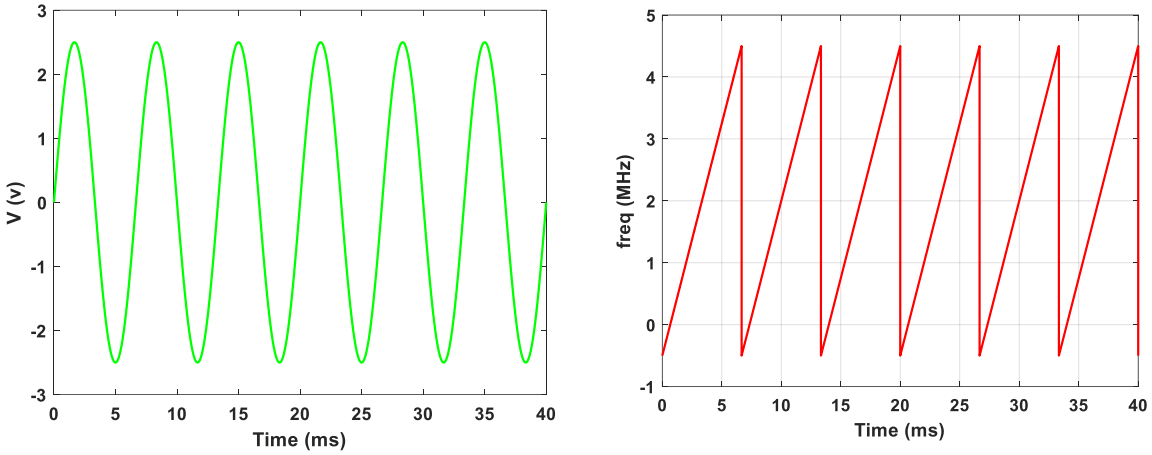

Figure 6.3 : (a) Input sinsoidal signal of 100MHz and (b) time-frequency plot of input signal for FMCW transmitter

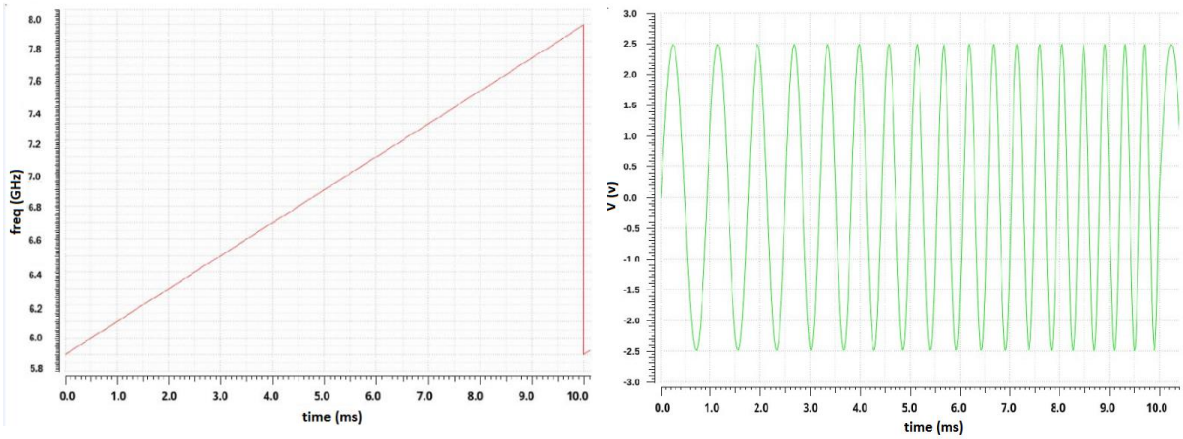

Figure 6.4: Time-frequency plot of FMCW signal for one sweep period and Time-amplitude plot of FMCW signal for one sweep period

Figure 6.3 (a) depicts the input frquency of 100MHz and Figure 6.3 (b) illustrate the time frequency plot of FMCW transmitter. Chirp, frequency sweep, or frequency ramp is used to describe the linear variations in frequency over time. FMCW waveform's time-frequency spectrum features numerous chirps/sweeps. The FMCW frequency changes linearly with respect to time during one sweep period, as in Figure 6.4 depicts a time-amplitude plot of the FMCW signal for one sweep interval. It has a chirp and begins as a sine wave with a frequency that grows linearly with time. Figure 6.5 shows the corresponding output specturm.

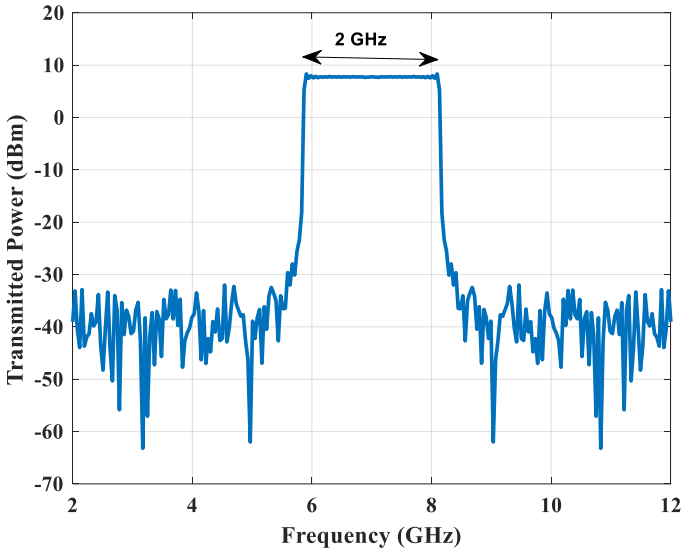

Figure 6.5: Measured output spectrum

The output graphs of SSB mixer output for 1GHz and RF mixer output for 2GHz are presented in Figure 6.6.

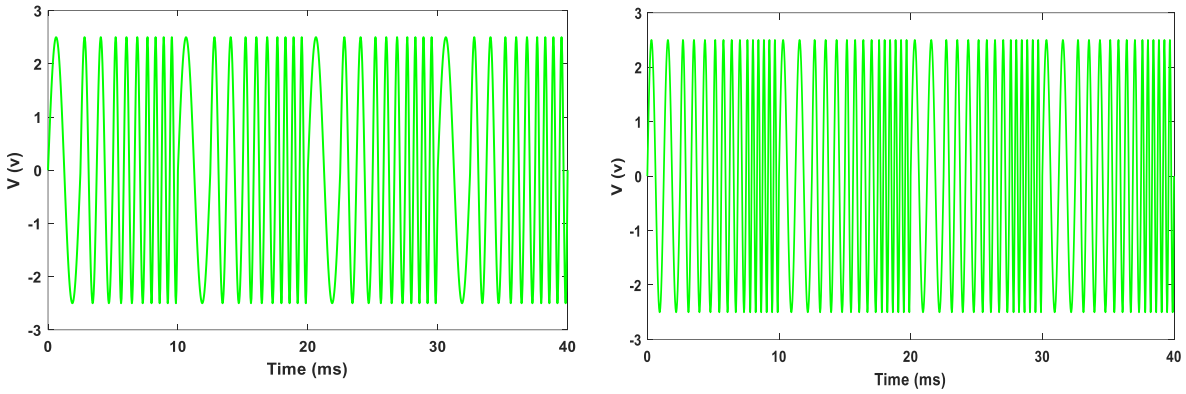

(a) (b)

Figure 6.6: (a) SSB mixer output for 1GHzand (b) RF mixer output for 2GHz

If we want output of 4 GHz: then it became as, Ka-band is wanted, so for getting the 4GHz, resulting 2-GHz chirp can be further up-converted with another local oscillator (LO) of high-frequency. Output signal with 4 GHz have signal and the spectrum as Figure 6.7 and Figure 6.8.

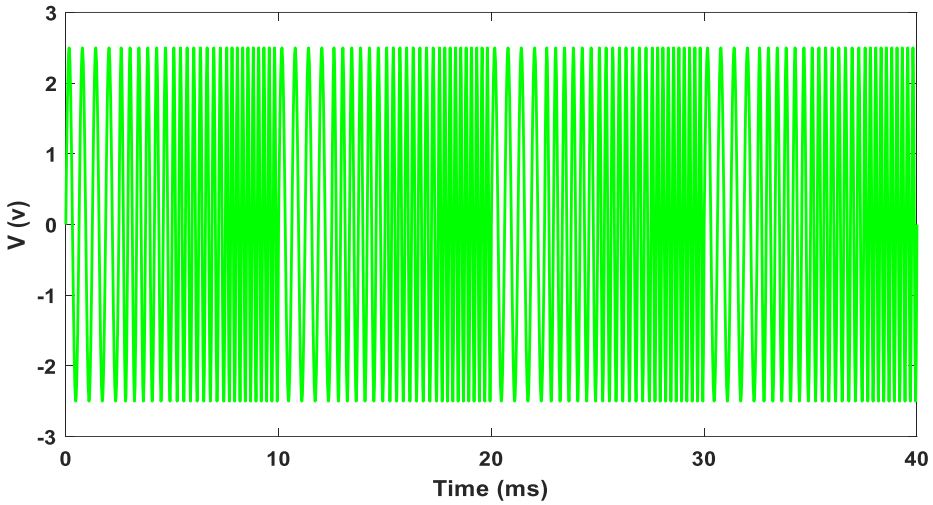

Figure 6.7: Output signal with 4 GHz have signal

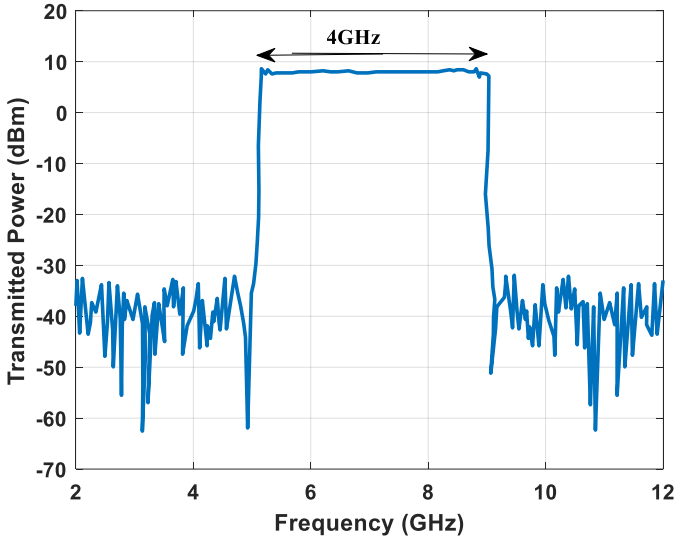

Figure 6.8: Output signal with 4 GHz have spectrum

6.3.1 Evaluation of FMCW Transmitter

By combining the up-converted narrowband chirp with adjacent carrier frequencies, the suggested FMCW transmitter generated a wideband chirp using a synthetic bandwidth technique. It is accomplished by combining output of a fast-switching R-PILO with a narrow band chirp created by FS-FNDPLL. In order to generate a smooth saw-tooth wideband chirp, an FMCW transmitter requires a rapid switching FNDPLL. The previous subsection's examination of the proposed FS-FNDPLL demonstrates the efficiency of quick switching with a lock time of μs 1 s. A rapid switching FNDPLL alone is insufficient for generating a smooth saw-tooth wideband chirp, and a fast switching ILO is required to

move from one carrier frequency to another. Figure 6.9 shows how proposed R-PILO with SSPG improves switching time. Measured settling time from 8.5 to 9.5 GHz is around 4 ns.

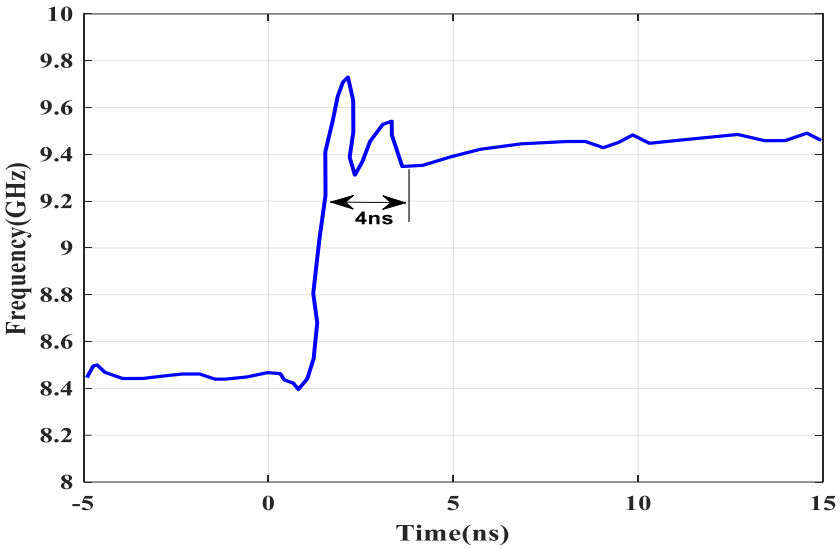

Figure 6.9 : Switching time analysis of R-PILO

Phase noise refers to the random fluctuations or variations in the phase of an oscillation signal.

$$L(f)=10\cdot\log_{10}(L_{osc})+10.\log_{10}(f) \tag{6.1}$$

Here, L_{osc} denotes the phase noise level of the oscillator at a 1 Hz offset frequency and is equivalent to −52dBc/Hz. f denotes offset frequency. Figure 6.9 depicts the proposed FMCW transmitter's phase noise performance for both narrowband and wideband chirps. BGC-DTC is used in the proposed transmitter to reduce nonlinearity in FS-FNDPLL and SSPG to suppress adjacent spurs in R-PILO. As a result, the planned FMCW transmitter's phase noise is improved to 112.6 dBc/Hz at a 1-MHz offset. Furthermore, because of its fast settling properties, FS-FNDPLL with the AC-TDCsw scheme decreased frequency inaccuracy.

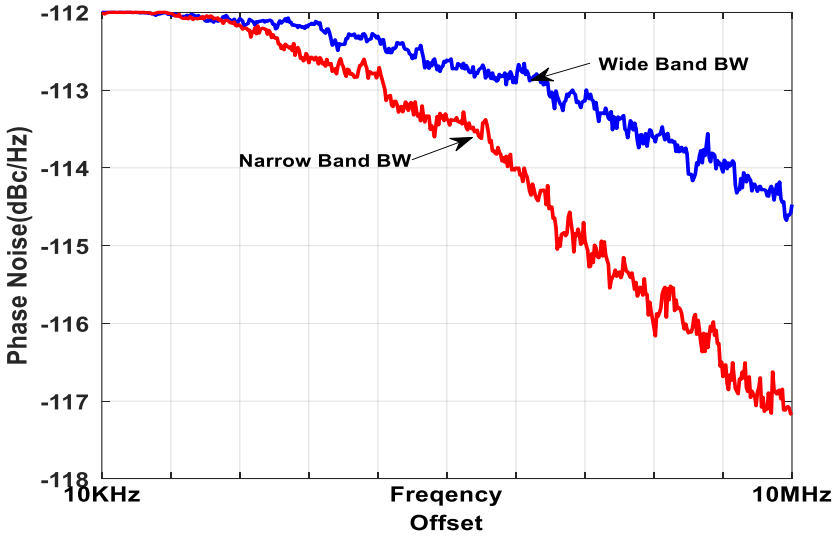

Figure 6.10: Phase analysis of the proposed FMCW transmitter

Table 6.1 summarizes and compares the suggested FMCW transmitter's effectiveness with other state-of-the-art FMCW transceivers. The chirp rate is a parameter used in radar signal processing, particularly in context of radar systems employing FMCW signals. Chirp rate (CR) is calculated as the ratio of the system's bandwidth (BW) to the pulse period.

$$Chirp\ rate = BW/pulse\ period \tag{6.2}$$

$$= 2G/10ms = 0.2\ GHz/ms$$

Table 6.1: Comparison table of the state-of-the-art FMCW transmitter

Specifications	**Wang et al. [123]**	**Balon et al. [124]**	**Su et al. [126]**	**Ding et al. [125]**	**Proposed**	Proposed
Technology (nm)	65	-	55	65	45	65
Chirp type	Sawtooth	Sawtooth	Sawtooth	-	Sawtooth	Sawtooth
Central frequency	15 GHZ	3.85 GHZ	7 GHZ	4.675GHZ	7 GHZ	4 GHZ
Chirp period (ms)	Tunable 1.18~10	2	Tunable 0.3~6.3	-	Tunable 0.3~10	.50
Chirp period rate	1.5 GHz/ms	1.925	0.15 GHz/ms	-	0.2 GHz/ms	0.112

Bandwidth	1.48 GHz	607.6 MHz	0.5-1GHZ	2GHZ	2GHz	2GHz
Phase noise (dBc/Hz)	-90	-	-105	-98	-112	-110
Area (mm^2)	4.06	-	2.24	2.16	1.12	2
TX power (mW)	211	-	84	132	79	120

According to Table 6.1, the suggested FMCW transmitter delivers best fractional bandwidth while consuming less power than previously published FMCW transmitters. Furthermore, FS-FNDPLL with AC-TDCsw and Ring-PILO outperformed previous FNPLL- and SHILO-based systems in terms of nonlinearity and switching time. As a result, it produced a smooth saw-tooth wideband chirp with best phase noise, power consumption, and chirp bandwidth performance.

6.3 Summary

By using Ring-PILO to get the necessary synthetic bandwidth-based FMCW chirp and incorporating a switching mechanism in FNDPLL design, this article suggests a novel FMCW transmitter. The proposed transmitter, capable of high GHz bandwidth chirps, utilizes a high-frequency local oscillator (LO) to achieve this expansion. With reduced phase noise of -112 dBc/Hz at 1 MHz and power consumption of only 79 mW, the demonstrated FMCW transceiver offers a promising solution for future UAV SAR applications. Its attributes include low-cost, high-integration, and high-performance capabilities, positioning it as an advantageous option in the realm of UAV SAR technology.

CHAPTER 7

CONCLUSION AND FUTURE SCOPE

7.1 Conclusion

First work establishes requirement for a local oscillator to produce clock and synchronize it's frequency via the other clock for a third order delta Sigma modulation with a starting frequency of 26 MHz as well as a locked frequency for 3.5 GHz within the fractional-NPLL for Small Phase Noise. With a circuit that has higher frequencies. This modulator is designed for usage in embedded systems and wireless communication. Frequency spikes can be disregarded when charting phase noise at different offsets values, the frequency range, and unwanted spurs produced at the references because no RF transceivers that could pick up these low frequencies. The most widely used multichannel wireless transceivers in wireless communication use the frequency produced by fractional N phases locked loops to reduce spurs. Using phase-locked loops, they are generally employed to act as local oscillator in detectors to convert carrier's frequency to a lower, wireless frequency range. They are also employed in clock synthesis, where the accuracy is poor in easier-to-build crystal resonators but fixed at high frequencies, and the frequency can be created accurately by adding a fractional-N PLL. For increasing Fractional-NPLL for Deepened short Phase Noise, a 3rd order delta Sigma modulation that has a locking frequency of 3.5 GHz & a starting frequency of 26 MHz has been developed. It is designed for use in communication via wireless transceivers and makes use of system on chips. It may additionally be utilized in technologies for embedded systems. A local oscillator must be used to create the clock and synchronize it with other clock frequency in the circuit. Since no RF transceivers that could pick up these low frequencies, these frequency spurs will be disregarded when displaying the phase distortion at various offset numbers, the spectrum of frequencies and undesirable spurs created at the references.

This article suggests a new FMCW transmitter with a mechanism for switching in FNDPLL architecture and Ring-PILO for obtaining the required synthetic bandwidth-based FMCW chirp. Second investigation shows that FS-FNDPLL can achieve 113 dBc/Hz in-band phase noise while reducing settling intervals to 1 s. The proposed FS-FNDPLL shifts from stop frequency to the start frequency at the conclusion of every narrowband chirp period with a 1 μs settling time. This settling time is less than 1% of the chirp period. The proposed FS-FNDPLL's phase noise & quantization error characteristics have been improved by applying background amplitude adjustment with a reference clock to increase the linearity associated

with the DTC in the feedback route. Additionally, to lessen neighboring spurs without complicating ILOs, a pulse shaping approach is applied. The proposed emitter can be readily extended to generate a chirp with a wide GHz bandwidth by using a high-frequency local oscillator (LO). Phase noise of the transmitter is lessened by approximately112 dBc/Hz over a single MHz by using just 79 mW of power and 40% reduction in power consumption along area reduced by 51%. This developed Transmitter by optimizing the structures of FNDPLL and ILO to improve the overall performance of the transmitter, power consumption and area requirement .

7.2 Future Scope

- In order to minimize spurs, the most popular multiple wireless transceivers in transmission use the frequency generated by fraction N phase locked loops. They are utilized in clock synthesizing, where frequency can be produced correctly by adding fractional frequencies to an N phase locked loop, but the accuracy is restricted due to a preset high q the frequency and the simplicity of building crystal resonators
- They are primarily used as local oscillations in phase-locked looping process wireless receivers that convert a frequency used as a carrier into a smaller frequency intermediate.
- Future UAV SAR applications may benefit from the shown FMCW transceiver's cheap cost, high integration, and high performance capabilities. FMCW transceivers can produce high-resolution SAR imaging despite their small dimensions and lower cost. Because they transmit a modulated signal continuously, providing a large bandwidth over time, they give great range resolution.

References:

[1] Gaidioz, David. "Ultra-Low Power Frequency Synthesizer For Internet-of-Things applications In 28nm FD-SOI technology." PhD diss., Université de Bordeaux, 2021.

[2] He, Ruixing. "Scalable LO Distribution Schemes For Building Large-scale Phased Arrays." PhD diss., University of Minnesota, 2022.

[3] Xu, Jinming, Hao Qian, Yuan Hu, Shenyiyang Bian, and Shaojun Xie. "Overview of SOGI-based single-phase phase-locked loops for grid synchronization under complex grid conditions." *IEEE Access* 9 (2021): 39275-39291.

[4] Álvarez-Fontecilla, Cristián Enrique. *Digital Enhancement Techniques for Digital Fractional-N Phase-Locked Loops*. University of California, San Diego, 2021.

[5] D. Cherniak, L. Grimaldi, L. Bertulessi, C. Samori, R. Nonis, and S. Levantino, "A 23GHz low-phase-noise digital bang-bang PLL for fast triangular and saw-tooth chirp modulation," in IEEE ISSCC Dig. Tech. Papers, Feb. 2018, pp. 248–250.

[6] Q. Shi, K. Bunsen, N. Markulic, and J. Craninckx, "A self-calibrated 16 GHz subsampling-PLL-based 30s fast chirp FMCW modulator with 1.5 GHz Bandwidth and 100 kHz rms error," in IEEE ISSCC Dig. Tech. Papers, Feb. 2019, pp. 408–410.

[7] D. Weyer, M. B. Dayanik, S. Jang, and M. P. Flynn, "A 36.3-to-38.2 GHz −216dBc/Hz2 40 nm CMOS fractional-N FMCW chirp synthesizer PLL with a continuous-time bandpass delta-sigma time-to-digital converter," in IEEE ISSCC Dig. Tech. Papers, Feb. 2018, pp. 250–252.

[8] F. Ahmad et al., "A 0.5-to-9.5 GHz 1.2 μs-lock-time fractional-N DPLL with ±1.25% UI period jitter in 16 nm CMOS for dynamic frequency and core-count scaling in SoC," in IEEE ISSCC Dig. Tech. Papers, Jan. 2016, pp. 324–325.

[9] P. Paliwal, J. Fadadu, A. Chawda, and S. Gupta, "A fast settling 4.7-5 GHz fractional-N digital phase locked loop," in Proc. 29th Int. Conf. VLSI Design 15th Int. Conf. Embedded Syst. (VLSID), Jan. 2016, pp. 553–554

[10] Wang, Bowen, Haixin Song, Woogeun Rhee, and Zhihua Wang. "Overview of ultra-wideband transceivers—System architectures and applications." *Tsinghua Science and Technology* 27, no. 3 (2021): 481-494.

[11] Moustakas, K., P. Rymaszewski, T. Hemperek, H. Krüger, M. Vogt, T. Wang, and N. Wermes. "A Clock and Data Recovery Circuit for the ATLAS/CMS HL-LHC Pixel Front End Chip in 65 nm CMOS Technology." In *Topical Workshop on Electronics for Particle Physics TWEPP2019*, vol. 2, p. 6. 2019.

[12] Bertulessi, Luca, Saleh Karman, Dmytro Cherniak, Alessandro Garghetti, Carlo Samori, Andrea L. Lacaita, and Salvatore Levantino. "A 30-GHz Digital Sub-Sampling Fractional-$ N $ PLL With− 238.6-dB Jitter-Power Figure of Merit in 65-nm LP CMOS." *IEEE Journal of Solid-State Circuits* 54, no. 12 (2019): 3493-3502.

[13] Luo, Zhihong, Guoxing Wang, Khalil Yousef, Benjamin Lau, Yong Lian, and Chun-Huat Heng. "A 0.0129 mm 2 DPLL With 1.6~ 2.0 ps RMS Period Jitter and 0.25-to-2.7 GHz Tunable DCO Frequency Range in 55-nm CMOS." *IEEE Transactions on Circuits and Systems II: Express Briefs* 65, no. 12 (2018): 1844-1848.

[14] Yoo, Jerald, and Mahsa Shoaran. "Neural interface systems with on-device computing: Machine learning and neuromorphic architectures." *Current opinion in biotechnology* 72 (2021): 95-101.

[15] Céspedes-Deliyore, Randy Steven. "Design of a power-saving strategy for a collaborative wireless sensor network of multi-core embedded systems." (2022).

[16] Elkholy, Ahmed, Saurabh Saxena, Guanghua Shu, Amr Elshazly, and Pavan Kumar Hanumolu. "Low-jitter multi-output all-digital clock generator using DTC-based open loop fractional dividers." *IEEE Journal of Solid-State Circuits* 53, no. 6 (2018): 1806-1817.

[17] Ding, Ming, Peng Zhang, Yuming He, Stefano Traferro, Minyoung Song, Hannu Korpela, Kenichi Shibata, Keisuke Ueda, Yao-Hong Liu, and Christian Bachmann. "A Bluetooth 5 transceiver with a phase-tracking RX and its corresponding digital baseband in 40-nm CMOS." *IEEE Journal of Solid-State Circuits* 56, no. 1 (2020): 254-266.

[18] Lokin, Christiaan Egidius. *Active PWM Ripple Reduction in Class-D Amplifiers Using Digital Loop Filters*. University of Twente, 2023.

[19] Van Bockel, Bjorn, Jeffrey Prinzie, and Paul Leroux. "Radiation assessment of a 15.6 ps single-shot time-to-digital converter in terms of TID." *Electronics* 8, no. 5 (2019): 558.

[20] Zong, Zhirui, Peng Chen, and Robert Bogdan Staszewski. "A Low-Noise Fractional-${N}$ Digital Frequency Synthesizer With Implicit Frequency Tripling for mm-Wave Applications." *IEEE Journal of Solid-State Circuits* 54, no. 3 (2018): 755-767.

[21] Helal, Eslam, Amr I. Eissa, and Ian Galton. "DTC Linearization via Mismatch-Noise Cancellation for Digital Fractional-N PLLs." *IEEE Transactions on Circuits and Systems I: Regular Papers* 69, no. 12 (2022): 4993-5006.

[22] Markulic, Nereo, Kuba Raczkowski, Jan Craninckx, Piet Wambacq, Nereo Markulic, Kuba Raczkowski, Jan Craninckx, and Piet Wambacq. "A Background-Calibrated Subsampling PLL for Phase/Frequency Modulation." *Digital Subsampling Phase Lock Techniques for Frequency Synthesis and Polar Transmission* (2019): 57-83.

[23] Li, Shaolan, Bo Qiao, Miguel Gandara, David Z. Pan, and Nan Sun. "A 13-ENOB second-order noise-shaping SAR ADC realizing optimized NTF zeros using the error-feedback structure." *IEEE Journal of Solid-State Circuits* 53, no. 12 (2018): 3484-3496.

[24] Sun, Tiancheng, Zexiang Xu, Xiuming Zhang, Sean Fanello, Christoph Rhemann, Paul Debevec, Yun-Ta Tsai, Jonathan T. Barron, and Ravi Ramamoorthi. "Light stage super-resolution: continuous high-frequency relighting." *ACM Transactions on Graphics (TOG)* 39, no. 6 (2020): 1-12.

[25] Muqueem, Md Abdul, Shanky Saxena, and Govind Singh Patel. "An Intensified Fractional-NPLL for Deepened low Phase Noise." In *2023 2nd International Conference on Vision Towards Emerging Trends in Communication and Networking Technologies (ViTECoN)*, pp. 1-5. IEEE, 2023.

[26] Liao, Dongyi. "Design of High Performance Radio-Frequency Phase-Locked Loops." PhD diss., Auburn University, 2018.

[27] Lin, Tsung-Hsien, Ching-Lung Ti, and Yao-Hong Liu. "Dynamic current-matching charge pump and gated-offset linearization technique for delta-sigma fractional-$ N $ PLLs." *IEEE Transactions on Circuits and Systems I: Regular Papers* 56, no. 5 (2009): 877-885.

[28] Zhao, Jun. "A low power CMOS design of an all digital phase locked loop." (2011).

[29] Rhee, Woogeun, Bo Zhou, and Zhihua Wang. "Fractional-N frequency synthesis: overview and design perspectives." In *2011 IEEE International Symposium on Radio-Frequency Integration Technology*, pp. 125-128. IEEE, 2011.

[30] Milovanović, Vladimir. "On fundamental operating principles and range-doppler estimation in monolithic frequency-modulated continuous-wave radar sensors." *Facta Universitatis, Series: Electronics and Energetics* 31, no. 4 (2018): 547-570.

[31] Wang, Xiong, Linghe Kong, Fanxin Kong, Fudong Qiu, Mingyu Xia, Shlomi Arnon, and Guihai Chen. "Millimeter wave communication: A comprehensive survey." *IEEE Communications Surveys & Tutorials* 20, no. 3 (2018): 1616-1653.

[32] Xu, Min, Jingyu Hu, and Yinyin Gao. "FPGA-based design and implementation of arbitrary waveform generator." In *2011 International Conference on Control, Automation and Systems Engineering (CASE)*, pp. 1-4. IEEE, 2011.

[33] Mohanty, Saraju P. *Nanoelectronic mixed-signal system design*. McGraw-Hill Education, 2015.

[34] Elkholy, Ahmed, Saurabh Saxena, Guanghua Shu, Amr Elshazly, and Pavan Kumar Hanumolu. "Low-jitter multi-output all-digital clock generator using DTC-based open loop fractional dividers." *IEEE Journal of Solid-State Circuits* 53, no. 6 (2018): 1806-1817.

[35] Rena, Rakesh Verma, Raviteja Kammari, and Vijay Shankar Pasupureddi. "A 0.4-1.8 GHz Quarter-Rate Sub-Sampling Mixer-First Direct Down-Conversion RF Front-End." (2023).

[36] Kalkhoran, Ali Mohammadian, and Seyed Hassan Sedighy. "Affordable Satellite on the Move Antenna Based on Delay-Line-PLL Phase Shifting." *Progress In Electromagnetics Research C* 131 (2023): 59-72.

[37] Meenakshi Vidya, P., and S. Sudha. "Open-loop digital clock generator based VLSI architecture for electromagnetic interference reduction." *Analog Integrated Circuits and Signal Processing* 105 (2020): 21-32.

[38] Yoo, Seyeon, Seojin Choi, Yongsun Lee, Taeho Seong, Younghyun Lim, and Jaehyouk Choi. "A low-jitter and low-reference-spur ring-VCO-based injection-locked clock multiplier using a triple-point background calibrator." *IEEE Journal of Solid-State Circuits* 56, no. 1 (2020): 298-309.

[39] Santiccioli, Alessio, Mario Mercandelli, Luca Bertulessi, Angelo Parisi, Dmytro Cherniak, Andrea L. Lacaita, Carlo Samori, and Salvatore Levantino. "A 66-fs-rms jitter 12.8-to-15.2-GHz fractional-N bang–bang PLL with digital frequency-error recovery for fast locking." *IEEE Journal of Solid-State Circuits* 55, no. 12 (2020): 3349-3361.

[40] De Caro, Davide, Gennaro Di Meo, Ettore Napoli, Nicola Petra, and Antonio Giuseppe Maria Strollo. "A 1.45 GHz all-digital spread spectrum clock generator in 65nm CMOS for synchronization-free SoC applications." *IEEE Transactions on Circuits and Systems I: Regular Papers* 67, no. 11 (2020): 3839-3852.

[41] Peng, Kang-Chun, Wei-Lung Wu, and Jiang-Hong Lin. "Reduction of phase noise in fractional-N frequency synthesizer using self-injection locking loop." *IEEE Transactions on Microwave Theory and Techniques* 68, no. 9 (2020): 3724-3731.

[42] Reddy, Gujjula Ramana, Chitra Perumal, and Bodapati Venkata Rajanna. "Design and Memory Optimization of Hybrid M-GDI Numerical Controlled Oscillator." (2022).

[43] Lo, Yu-Lung, Fang-Yu Fan, Hsi-Hua Wang, Yu-Hsin Li, Zi-Yi Chen, and Jen-Chieh Liu. "A fast-lock low-power all-digital DLL-based clock generator with fractional multiple technique." *Microsystem Technologies* 27 (2021): 1335-1346.

[44] Reddy, Gujjula Ramana, Chitra Perumal, Prakash Kodali, and Venkata Rajanna Bodapati. "Design and memory optimization of hybrid gate diffusion input numerical controlled oscillator." *International Journal of Reconfigurable and Embedded Systems* 12, no. 1 (2023): 78.

[45] Liu, Yushan, Runchuan Ye, Qidi Hu, Bao Chen, Wenchao Zhang, Feifei Zhou, and Nanyang Xu. "A DDS-based integrated microwave source for fast frequency sweeping in quantum magnetic-resonance systems." *AIP Advances* 13, no. 1 (2023).

[46] Alvarez-Fontecilla, Enrique, Amr I. Eissa, Eslam Helal, Colin Weltin-Wu, and Ian Galton. "Delta-sigma FDC enhancements for FDC-based digital fractional-N PLLs." *IEEE Transactions on Circuits and Systems I: Regular Papers* 68, no. 3 (2020): 965-974.

[47] Choo, Min-Seong, Sungwoo Kim, Han-Gon Ko, Sung-Yong Cho, Kwanseo Park, Jinhyung Lee, Soyeong Shin, Hankyu Chi, and Deog-Kyoon Jeong. "A PVT variation-robust all-digital injection-locked clock multiplier with real-time offset tracking using time-division dual calibration." *IEEE Journal of Solid-State Circuits* 56, no. 8 (2021): 2525-2538.

[48] Ibro, Marsida, and Gentiana Blakaj. "Direct Digital Synthesis Optimization Based on VHDL Code." (2021).

[49] Jin, Junting, Yuhua Jin, and Yebing Gan. "A 500 kHz to 150 MHz Multi-Output Clock Generator Using Analog PLL and Open-Loop Fractional Divider with 0.13 μm CMOS." *Electronics* 11, no. 15 (2022): 2347.

[50] Helal, Eslam, Enrique Alvarez-Fontecilla, Amr I. Eissa, and Ian Galton. "A time amplifier assisted frequency-to-digital converter based digital fractional-N PLL." *IEEE Journal of Solid-State Circuits* 56, no. 9 (2021): 2711-2723.

[51] Jordan, Darryn Anton, Michael Raymond Inggs, and Mohammed Yunus Abdul Gaffar. "Suppression of spur chirps for fractional-N PLL-based heterodyne FMCW SAR." *IEEE Transactions on Microwave Theory and Techniques* 69, no. 1 (2020): 409-417.

[52] Li, Zhijun, Lijuan Wang, Yanan Wang, and Gege Li. "Harmonic detection method based on adaptive noise cancellation and its application in photovoltaic-active power filter system." *Electric Power Systems Research* 184 (2020): 106308.

[53] Liao, Dongyi, and Fa Foster Dai. "A fractional-N reference sampling PLL with linear sampler and CDAC based fractional spur cancellation." *IEEE Journal of Solid-State Circuits* 56, no. 3 (2020): 694-704.

[54] Liu, Bangan, Yuncheng Zhang, Junjun Qiu, Huy Cu Ngo, Wei Deng, Kengo Nakata, Toru Yoshioka et al. "A fully synthesizable fractional-N MDLL with zero-order interpolation-based DTC nonlinearity calibration and two-step hybrid phase offset calibration." *IEEE Transactions on Circuits and Systems I: Regular Papers* 68, no. 2 (2020): 603-616.

[55] Prinzie, Jeffrey, Shuja Andrabi, Christophe Beghein, Changhua Cao, Hsinhua Chen, Xiaochuan Guo, Jon Strange, and Bernard Tenbroek. "A fast locking 5.8–7.2-GHz fractional-N synthesizer with sub-2-us settling in 22-nm FDSOI." *IEEE Solid-State Circuits Letters* 3 (2020): 546-549.

[56] Shansho, A., G. E. Dunaevsky, I. O. Dorofeev, A. V. Badin, and E. V. Emelyanov. "Stabilization of the backward wave oscillator frequency for operation with high quality resonators." In *Journal of Physics: Conference Series*, vol. 2140, no. 1, p. 012011. IOP Publishing, 2021.

[57] Shen, Zhengkun, Haoyun Jiang, Heyi Li, Zherui Zhang, Fan Yang, Junhua Liu, and Huailin Liao. "A 12-GHz calibration-free all-digital PLL for FMCW signal generation with 78 MHz/μs chirp slope and high chirp linearity." *IEEE Transactions on Circuits and Systems I: Regular Papers* 67, no. 12 (2020): 4445-4456.

[58] An, Hongyang, Junjie Wu, Kah Chan Teh, Zhichao Sun, and Jianyu Yang. "Geosynchronous spaceborne–airborne bistatic SAR imaging based on fast low-rank and sparse matrices recovery." *IEEE Transactions on Geoscience and Remote Sensing* 60 (2021): 1-14.

[59] Chen, Zhe, Debin Hou, Ji-Xin Chen, Pinpin Yan, Lei Bao, Zheying Hong, and Yuanye Zheng. "A K-Band FMCW Frequency Synthesizer Using Q-Boosted Switched Inductor VCO in SiGe BiCMOS for 77 GHz Radar Applications." *Electronics* 9, no. 11 (2020): 1933.

[60] Lee, Jun-Hee, Mun-Kyo Lee, and Jung-Dong Park. "A Direct Feedback FVF LDO for High Precision FMCW Radar Sensors in 65-nm CMOS Technology." *Sensors* 22, no. 24 (2022): 9672.

[61] Wu, Jianxi, Wei Deng, Zipeng Chen, Wei Zheng, Yibo Liu, Shufu Wang, Nan Qi, and Baoyong Chi. "A 77-GHz mixed-mode FMCW generator based on a Vernier TDC with dual rising-edge fractional-phase detector." *IEEE Transactions on Circuits and Systems I: Regular Papers* 67, no. 1 (2019): 60-73.

[62] Zhang, Ying, Wei Xiong, Xichao Dong, and Cheng Hu. "A novel azimuth spectrum reconstruction and imaging method for moving targets in geosynchronous spaceborne–airborne bistatic multichannel SAR." *IEEE Transactions on Geoscience and Remote Sensing* 58, no. 8 (2020): 5976-5991.

[63] Zhou, Fang, Jun Yang, Lu Jia, Xingming Yang, and Mengdao Xing. "Ultra-high resolution imaging method for distributed small satellite spotlight MIMO-SAR based on sub-aperture image fusion." *Sensors* 21, no. 5 (2021): 1609.

[64] Saravanan, Darshana, Naresh Manwani, and Vineet Gandhi. "SARI: Simplistic Average and Robust Identification based Noisy Partial Label Learning." *arXiv preprint arXiv:2402.04835* (2024).

[65] Kuznetsov, Nikolay V., Mikhail Y. Lobachev, Marat V. Yuldashev, Renat V. Yuldashev, and Mohammad S. Tavazoei. "The Gardner problem on the lock-in range of second-order type 2 phase-locked loops." *IEEE Transactions on Automatic Control* (2023).

[66] Kasilingam, Kalpana, Paulchamy Balaiyah, Stephen Jeswinde Nuagah, and Piyush Kumar Shukla. "Design of a high-performance advanced phase locked loop with high stability external loop filter." *IET Circuits, Devices & Systems* 17, no. 1 (2023): 1-12.

[67] Lei, Jiaxing, ZhiChao Yang, Shuang Feng, Jianfeng Zhao, Wu Chen, and Bingtuan Gao. "Straightforward high-order design of frequency-adaptive advanced phase-locked loop with improved dynamic performance." *Electric Power Systems Research* 217 (2023): 109098.

[68] Zhang, Ziqian, and Robert Schuerhuber. "Impact of Reactive Current and Phase-Locked Loop on Converters in Grid Faults." *Energies* 16, no. 7 (2023): 3122.

[69] Zhou, Tong, and Gaëtan Kerschen. "Identification of Secondary Resonances of Nonlinear Systems using Phase-Locked Loop Testing." *arXiv preprint arXiv:2401.01151* (2024).

[70] Arya, Rachana, Bijay Kumar Singh, Khalaf Ibrahim Osamah, Satheeshkumar Palanisamy, Sameer Algburi, and Habib Hamam. "Approximation of Digital PLL using CMOS Technology." *International Journal of Computing and Digital Systems* 16, no. 1 (2024): 1-14.

[71] Hemel, Md Shahriar Khan, Mamun Bin Ibne Reaz, Sawal Hamid Bin Md Ali, Mohammad Arif Sobhan Bhuiyan, and Mahdi H. Miraz. "Optimisation and Performance Computation of a Phase Frequency Detector Module for IoT Devices." *arXiv preprint arXiv:2401.03389* (2024).

[72] Lu, Hongyu, and Patrick P. Mercier. "Computationally-Efficient Linear Periodically Time-Variant Digital PLL Modeling Using Conversion Matrices and Uncorrelated Upsampling." *arXiv preprint arXiv:2401.13897* (2024).

[73] Mao, Yuqing, Yoann Charlon, Yves Leduc, and Gilles Jacquemod. "A low power injection-locked CDR using 28 nm FDSOI technology for burst-mode applications." (2024).

[74] H. Afzal, C. Li, and O. Momeni, ‘‘A 17 Gb/s 10.7 pJ/b 4FSK transceiver system for point to point communication in 65 nm CMOS,’’ in Proc. IEEE Radio Freq. Integr. Circuits Symp. (RFIC), Jun. 2022, pp. 71–74.

[75] H. Kim, Y. Kim, T. Kim, H.-J. Ko, and S. Cho, ‘‘A 2.4-GHz 1.5-mW digital multiplying delay-locked loop using pulsewidth comparator and double injection technique,’’ IEEE J. Solid-State Circuits, vol. 52, no. 11, pp. 2934–2946, Nov. 2017.

[76] Z. Yang, Y. Chen, S. Yang, P.-I. Mak, and R. P. Martins, ‘‘A 25.4-to29.5 GHz 10.2 mW isolated sub-sampling PLL achieving −252.9 dB jitterpower FoM and −63 dBc reference spur,’’ in IEEE Int. Solid-State Circuits Conf. (ISSCC) Dig. Tech. Papers, Feb. 2019, pp. 270–272.

[77] Z. Liang, X. Yi, K. Yang, and C. C. Boon, ‘‘A 2.6–3.4 GHz fractional-N sub-sampling phase-locked loop using a calibration-free phase-switchingsub-sampling technique,’’ IEEE Microw. Wireless Compon. Lett., vol. 28, no. 2, pp. 147–149, Feb. 2018.

[78] Z. Huang, B. Jiang, and H. C. Luong, ‘‘A 2.1-GHz third-order cascaded PLL with sub-sampling DLL and clock-skew-sampling phase detector,’’ IEEE Trans. Circuits Syst. I, Reg. Papers, vol. 65, no. 7, pp. 2118–2126, Jul. 2018.

[79] Y. Huang, Y. Chen, H. Jiao, P.-I. Mak, and R. P. Martins, ‘‘A 3.36-GHz locking-tuned type-I sampling PLL with −78.6-dBc reference spurmerging single-path reference-feedthrough-suppression and narrow-pulseshielding techniques,’’ IEEE Trans. Circuits Syst. II, Exp. Briefs, vol. 68, no. 9, pp. 3093–3097, Sep. 2021.

[80] S. Kazeminia and A. Soltani, ‘‘A low-jitter leakage-free digitally calibrated phase locked loop,’’ Comput. Electr. Eng., vol. 88, Dec. 2020, Art. no. 106865.

[81] N. T. Abou-El-Kheir, R. D. Mason, M. Li, and M. C. E. Yagoub, ‘‘A subharmonic injection locking clock multiplier with FLL PVT calibrator,’’ Microelectron. J., vol. 98, Apr. 2020, Art. no. 104729.

[82] C.-Y. Lin, Y.-T. Hung, and T.-H. Lin, ‘‘A 2.4-GHz 500-µW 370-fsrms integrated jitter sub-sampling sub-harmonically injection-locked PLL in 90-nm CMOS,’’ in Proc. IEEE Asian Solid-State Circuits Conf. (A-SSCC), Nov. 2019, pp. 91–94.

[83] M.-H. Chou and S.-I. Liu, ‘‘A 2.4-GHz area-efficient and fast-locking subharmonically injection-locked type-I PLL,’’ IEEE Trans. Very Large Scale Integr. (VLSI) Syst., vol. 28, no. 11, pp. 2474–2478, Nov. 2020.

[84] Z. Zhang, L. Liu, P. Feng, and N. Wu, ‘‘A 2.4–3.6-GHz wideband subharmonically injection-locked PLL with adaptive injection timing alignment technique,’’ IEEE Trans. Very Large Scale Integr. (VLSI) Syst., vol. 25, no. 3, pp. 929–941, Mar. 2017.

[85] A. Li, Y. Chao, X. Chen, L. Wu, and H. C. Luong, ‘‘A spur-and-phasenoise-filtering technique for inductor-less fractional-N injection-locked PLLs,’’ IEEE J. Solid-State Circuits, vol. 52, no. 8, pp. 2128–2140, Aug. 2017

[86] Ma, Jing, Yang Qiu, Yinan Li, Weibo Zhang, Zhanxiang Song, and James S. Thorp. "Research on the impact of DFIG virtual inertia control on power system small-signal stability considering the phase-locked loop." IEEE Transactions on Power Systems 32, no. 3 (2016): 2094-2105.

[87] Kavyashree, Prathibha, and Venkata Siva Reddy. "Implementation of all digital phase locked loop." International Journal of Research and Analytical Reviews, Reva University 5, no. 2 (2018): 1386-1389.

[88] Yadav, Lalita, and Manoj Duhan. "Design of All Digital Phase Locked Loop with Digitally Controlled Oscillator Using 45nm for Low Power Consumption." (2023).

[89] Lad Kirankumar, H., S. Rekha, and Tonse Laxminidhi. "A dead-zone-free zero blind-zone high-speed phase frequency detector for charge-pump PLL." Circuits, Systems, and Signal Processing 39, no. 8 (2020): 3819-3832.

[90] M. Hekmat, F. Aryanfar, J. Wei, V. Gadde, and R. Navid, ‘‘A 25 GHz fast-lock digital LC PLL with multiphase output using a magneticallycoupled loop of oscillators,’’ IEEE J. Solid-State Circuits, vol. 50, no. 2, pp. 490–502, Feb. 2015.

[91] Costa, Israel DL, Danilo I. Brandao, Lourenço Matakas Junior, Marcelo G. Simões, and Lenin MF Morais. "Analysis of stationary-and synchronous-reference frames for three-phase three-wire grid-connected converter AC current regulators." Energies 14, no. 24 (2021): 8348.

[92] Kamil, H. Sardar, Dalila Mat Said, Mohd Wazir Mustafa, Mohammad Reza Miveh, and Nasarudin Ahmad. "Recent advances in phase-locked loop based synchronization methods for inverter-based renewable energy sources." Indonesian Journal of Electrical Engineering and Computer Science 18, no. 1 (2020): 1-8.

[93] Konwar, G., and T. Bezboruah. "Studies on Phase Noise Profiles of Proportional-Integral-Derivative Controlled PLL." International Journal of Electrical and Electronic Engineering and Telecommunications 10, no. 5 (2021): 369-376.

[94] Ali, Zunaib, Nicholas Christofides, Lenos Hadjidemetriou, Elias Kyriakides, Yongheng Yang, and Frede Blaabjerg. "Three-phase phase-locked loop synchronization algorithms for grid-connected renewable energy systems: A review." Renewable and Sustainable Energy Reviews 90 (2018): 434-452.

[95] Patel, Pranav R., and Richard K. Martin. "End-to-End Direct Digital Synthesis Simulation and Mathematical Model to Minimize Quantization Effects of Digital Signal Generation." IEEE Open Journal of the Communications Society 1 (2020): 1647-1657.

[96] S. Tang, C. Li, and Y. Hou, "A suppressing method for spur caused by amplitude quantization in DDS," IEEE Access, vol. 7, pp. 62344–62351, 2019.

[97] M. Ferriss, B. Sadhu, A. Rylyakov, H. Ainspan, and D. Friedman, ''A 13.1-to-28 GHz fractional-N PLL in 32 nm SOI CMOS with a 16 noise-cancellation scheme,'' in IEEE Int. Solid-State Circuits (ISSCC) Conf. Dig. Tech. Papers, Feb. 2015, pp. 1–3.

[98] X. Jin, W. Park, D.-S. Kang, Y. Ko, K.-W. Kwon, and J.-H. Chun, ''A 4-GHz sub-harmonically injection-locked phase-locked loop with selfcalibrated injection timing and pulsewidth,'' IEEE J. Solid-State Circuits, vol. 55, no. 10, pp. 2724–2733, Oct. 2020.

[99] Turner, Steven Eugene, and David E. Kotecki. "Direct digital synthesizer with sine-weighted DAC at 32-GHz clock frequency in InP DHBT technology." IEEE Journal of Solid-State Circuits 41, no. 10 (2006): 2284-2290.

[100] Gutierrez-Aitken, Augusto, Jim Matsui, Eric N. Kaneshiro, Bert K. Oyama, Donald Sawdai, Aaron K. Oki, and Dwight C. Streit. "Ultrahigh-speed direct digital synthesizer using InP DHBT technology." IEEE Journal of Solid-State Circuits 37, no. 9 (2002): 1115-1119.

[101] Elliott, Kenneth R. "Direct digital synthesis for enabling next generation RF systems." In IEEE Compound Semiconductor Integrated Circuit Symposium, 2005. CSIC'05., pp. 4-pp. IEEE, 2005.

[102] Zhang, Yi, Xiaopeng Li, Youtao Zhang, Min Zhang, Yufeng Guo, and Hao Gao. "A 17 GHz direct digital synthesizer in a InP DHBT technology." Sādhanā 46 (2021): 1-9.

[103] Zuo, Shi, Jianzhong Zhao, and Yumei Zhou. "A 0.8 V, 5.3–5.9 GHz Sub-Sampling PLL with 196.5 fs rms Integrated Jitter and− 251.6 dB FoM." *Sensors* 21, no. 22 (2021): 7648.

[104]Kasilingam, Kalpana, Paulchamy Balaiyah, Stephen Jeswinde Nuagah, and Piyush Kumar Shukla. "Design of a high-performance advanced phase locked loop with high stability external loop filter." *IET Circuits, Devices & Systems* 17, no. 1 (2023): 1-12.

[105]Mostafa Abedi (2018) "A Fast Locking Phase-Locked Loop with Low Reference Spur" 26th Iranian Conference on Electrical Engineering (ICEE2018).

[106]Ye Zhangn, Ralf Wunderlich, Stefan Heinen (2018) " A lowcomplexity low-spurs digital architecture for wideband PLL applications "Chair of Integrated Analog Circuits and RF Systems, RWTH Aachen University, D-52062

[107] Govind Singh Patel and Sanjay Sharma,"Parametric Analysis of a Novel Architecture of Phase Locked Loop for Communication System", Wireless Personal Communication, (2014).

[108] Paliwal, Pallavi, Vivek Yadav, Zeeshan Ali, and Shalabh Gupta. "A Fast Settling Fractional-$ N $ DPLL With Loop-Order Switching." *IEEE Transactions on Very Large Scale Integration (VLSI) Systems* 28, no. 3 (2019): 714-725.

[109] V. Kratyuk, P.K. Hanumolu, U.K. Moon, & K. Mayaram, A design procedure for all-digital phase-locked loops based on a charge-pump phase-locked-loop analogy, *IEEE Transactions on Circuits and Systems II: Express Briefs.* **54**(3) (2007) 247-251.

[110]A. Elkholy, T. Anand, W. S. Choi, A. Elshazly, & P.K. Hanumolu, A 3.7 mW low-noise wide-bandwidth 4.5 GHz digital fractional-N PLL using time amplifier-based TDC, *IEEE Journal of Solid-State Circuits.* **50**(4) (2015) 867-881.

[111]Yang, Bo, Hua Zhang, Yurong Chen, Yongjun Zhou, and Yu Peng. "Urban Traffic Imaging Using Millimeter-Wave Radar." *Remote Sensing* 14, no. 21 (2022): 5416.

[112]Johnson, Jessi E., Oliver Shay, Chris Kim, and Catherine Liao. "Wearable millimeter-wave device for contactless measurement of arterial pulses." *IEEE transactions on biomedical circuits and systems* 13, no. 6 (2019): 1525-1534.

[113] P. Chen, X. Meng, J. Yin, P.I. Mak, R.P. Martins, & R.B. Staszewski, A 529-μW Fractional-N All-Digital PLL Using TDC Gain Auto-Calibration and an Inverse-Class-F DCO in 65-nm CMOS, *IEEE Transactions on Circuits and Systems I: Regular Papers.* (2021).

[114] H. Liu, D. Tang, Z. Sun, W. Deng, H.C. Ngo, & K. Okada, A submW fractional-N ADPLL with FOM of −246 dB for IoT applications, *IEEE J. Solid-State Circuits*. **53**(12) (Dec. 2018) 3540–3552.

[115] H. Liu et al, A 265 μW fractional-N digital PLL with seamless automatic switching subsampling/sampling feedback path and dutycycled frequency-locked loop in 65nm CMOS, *IEEE J. Solid-State Circuits*. **54**(12) (Dec. 2019) 3478–3492.

[116] Hanumolu, Pavan Kumar, Gu-Yeon Wei, Un-Ku Moon, and Kartikeya Mayaram. "Digitally-enhanced phase-locking circuits." In *2007 IEEE Custom Integrated Circuits Conference*, pp. 361-368. IEEE, 2007.

[117] Abramovitch, Daniel. "Lyapunov redesign of classical digital phase-lock loops." In *Proceedings of the 2003 American Control Conference, 2003.*, vol. 3, pp. 2401-2406. IEEE, 2003.

[118] Ghai, Deepika, and Neelu Jain. "All-digital phase locked loop (adpll)-a review." *International Journal of Electronics and Computer Science Engineering* 2, no. 1 (2012): 94-101.

[119] Leoncini, Mauro, Andrea Bonfanti, Salvatore Levantino, and Andrea L. Lacaita. "Efficient behavioral simulation of charge-pump phase-locked loops." *IEEE Transactions on Circuits and Systems I: Regular Papers* 65, no. 6 (2017): 1968-1980.

[120] Lin, Tsung-Hsien, Ching-Lung Ti, and Yao-Hong Liu. "Dynamic current-matching charge pump and gated-offset linearization technique for delta-sigma fractional-$ N $ PLLs." *IEEE Transactions on Circuits and Systems I: Regular Papers* 56, no. 5 (2009): 877-885.

[121] Rezaeian, Adel, Gholamreza Ardeshir, and Mohammad Gholami. "A low-power and high-frequency phase frequency detector for a 3.33-GHz delay locked loop." *Circuits, Systems, and Signal Processing* 39 (2020): 1735-1750.

[122] Daniels, Brian, Gerard Baldwin, and Ronan Farrell. "Modeling and design of high-order phase locked loops." In *VLSI Circuits and Systems II*, vol. 5837, pp. 278-287. SPIE, 2005.

[123] Y. Wang, L. Lou, B. Chen, Y. Zhang, K. Tang, L. Qiu, & Y. Zheng, A 260-mW Ku-band FMCW transceiver for synthetic aperture radar sensor with 1.48-GHz bandwidth in 65-nm CMOS technology, *IEEE Transactions on Microwave Theory and Techniques* **65**(11) (2017) 4385-4399.

[124] S. Balon, K. Mouthaan, C.H. Heng, & Z.N. Chen, An injection-locked-based FMCW transmitter with synthetic bandwidth technique, *IEEE Microw. Wireless Compon. Lett. vol*. **28**(1) (Jan. 2018) 55–57.

[125] B. Ding, S. Yuan, C. Zhao, L. Tao, & T. Tian, A Ka band FMCW transceiver front-end with 2-GHz bandwidth in 65-nm CMOS, *IEEE Trans. Circuits Syst. II, Exp. Briefs*. **66**(2) (Feb. 2019) 212–216.

[126] H. Su, S.D. Balon, K. Cheong, & C.H. Heng, A C-Band FMCW SAR Transmitter Based on Synthetic Bandwidth Technique, *IEEE Microwave and Wireless Components Letters*. **31**(1) (2020) 92-95.

List of Publications

S.No	Type of Paper (Journal Paper/Conference proceeding/ Book Chapter)	Name of the Journal/Conference/Book	Jounal indexing (Scopus/UGC/Web of Science)	Title of the Paper	Authors	Published Date (Date/Month/Year)	DOI: Number,ISSN/ISBN Number
1	Journal	Journal of Circuits, Systems, and Computers	SCI	An Ultra-Low-Power C-Band FMCW Transmitter Using a Fast Settling Fractional-N DPLL and Ring-Based Pulse Injection Locking Oscillator	Abdul Muqueem, Shanky Saxena,Govind Singh Patel	16.09.2022	https://doi.org/10.1142/S0218126623500457
2	Conference	2nd IEEE International Conference on vision towards Emerging Trends in Communication and Networking Technologies 2023	IEEE Conferenceheld at VIT Chennai (Scopus)	An Intensified Fractional-NPLL for Deepened Low Phase Noise	Md Abdul Muqueem,Shanky Saxena,Govind Singh Patel,	06.05 2023	979-8-3503-4799-9, DOI: 10.1109/ViTECoN58111.2023.10157928
3	Conference	International Conference on Intelligent and smart Computation	Held at Chandigarh university Published in AIP Proceedings (Scopus)	Design of Fractional-NPLL For low phase Noise	Md Abdul Muqueem,Shanky Saxena,Govind Singh Patel,	08.07 2023	https://doi.org/10.1063/5.0198647

4	Conference	5th International Conference on Intelligent Circuits and Systems ICICS-2023	Held at Lovely Professional University, proceeding published in Taylor and Francis (Scopus)	Design of Fractional-NPLL Using Delta Sigma Modultion For low phase Noise	Md Abdul Muqueem,Shanky Saxena,Govind Singh Patel,	13.10 2023	9781003521716,https://www.taylorfrancis.com/chapters/edit/10.1201/9781003521716-82/design-fractional-npll-using-delta-sigma-modulation-low-phase-noise-abdul-muqueem-shanky-saxena-govind-singh-patel